An assessment of the skeletal morphology of the hand of *Theropithecus gelada*

By

Sarah Elizabeth Edlund

A dissertation submitted in partial fulfillment of

the requirements for the degree of

Doctor of Philosophy

(Anthropology)

at the

UNIVERSITY OF WISCONSIN-MADISON

2020

Date of final oral examination: 4/29/2020

The dissertation is approved by the following members of the Final Oral Committee:

John Hawks, Professor, Anthropology
Karen B. Strier, Professor, Anthropology
Richard McFarland, Assistant Professor, Anthropology
Sissel Schroeder, Professor, Anthropology
Meghan M. Cotter, Lecturer, Anatomy

Contents

Abstract

The primate hand is remarkably adept, allowing for complex manipulation of objects in some species and providing essential stability during locomotion. These dual demands, in tandem with diverse ecological niches, have led to important variation among extant and extinct primate species. The hands of *Theropithecus gelada* are a key component to understanding the evolutionary forces that gave rise to morphology present in modern humans and recently discovered fossil hominins alike. Broadly, geladas are of interest to our evaluation of human evolutionary history because of their phylogenetic proximity and similar geographic range to fossil hominins. More specifically, geladas have significance for analyses of hand function largely due to the similarities they share with humans in manual digit proportions. Both humans and geladas have relatively long thumbs and short index fingers, which has previously been interpreted as an indication of increased manipulative capabilities among these groups. For geladas, this trait is often thought to be essential for manual grazing though they also groom each other at particularly high rates, using their hands in postures which include similar pad-to-pad grips as those used during foraging.

This dissertation provides detailed descriptions of the skeletal morphology of *Theropithecus gelada* as well as functional analyses of the first and second proximal metacarpal bases as compared to baboons (*Papio* spp.). Overlapping geographic ranges, locomotor similarities, and phylogenetic closeness all contribute to broad similarities between baboon and gelada manual skeletal morphology with the noted exception of intrinsic digit proportions. Through these detailed analyses, it is apparent that additional differences exist and likely contribute to

functional disparities between geladas and baboons. I suggest that unequal levels of joint stability present for geladas and baboons and are linked to differences in locomotion and forceful precision gripping behaviors. Additionally, I investigate a possible link between grooming behaviors and hand morphology, offering an alternative explanation for the unique digit proportions geladas possess. While a multitude of factors contribute to rates of grooming across primate taxa, there is a positive correlation between grooming time investment and digit ratios, suggesting that hand morphology may drive or be driven by grooming behaviors.

Acknowledgements

I am forever grateful to many individuals and organizations for their support throughout my graduate studies. Firstly, I want to thank my committee members. Their guidance and constructive feedback has helped me become a better scholar and I am honored to have each of them on my committee. I would especially like to thank Dr. Sissel Schroeder for her timely contributions on the committee and dedication to student success.

I want to further acknowledge the support of my advisor, Dr. John Hawks. His advice and experience have been invaluable throughout the final stages of my degree and I cannot imagine where this project would be without his guidance. I am truly grateful for his leadership and expertise. I am also extremely appreciative of the fact that John has valued my perspective and treated me with respect as his graduate student.

There are several other members of the Department of Anthropology I wish to recognize. I am very grateful to Dr. Karen B. Strier and Dr. Richard McFarland for helping me become a more critical scientist and for showing me that living primates are almost as fascinating as their bones. Thank you to Dr. Travis Pickering for the opportunity to work and learn at Swartkrans. Thank you to Dr. Nam Kim for his commitment to improving the graduate student experience and eagerness to help. I also want to thank Dr. Claire Wendland for her enthusiasm, openness, and dedication. She is an impressive educator for whom I have the utmost respect. Thank you to the office staff who have all provided excellent support and willingly answered the many questions I sent their way.

Several other members of the UW-Madison campus community are also deserving of acknowledgement. I want to express my gratitude to Gale Oakes and the Integrative Biology Department for their continued support and mentorship. Gale's unequaled devotion to undergraduate education and support of graduate teaching assistants has been a source of comfort and inspiration. My teaching experiences through the Integrative Biology Department have further solidified my desire to continue teaching. My interactions with students as a teaching assistant and lecturer are some of my favorite from my time at UW-Madison. Thank you to Dr. Meghan Cotter and Dr. Elise Davis for allowing biological anthropology students to participate in their PT/OT anatomy course. I am very grateful for the opportunity to learn from such skilled anatomists. I am also indebted to Dr. Heidi-Lynn Ploeg and Dr. Roxann Engelstad for their guidance and patience. Their selfless commitment to interdisciplinary work is truly commendable.

This dissertation would not have been possible without funding from the UW-Madison graduate school, UW-Madison Department of Anthropology, the Buckingham Award for Interdisciplinary Anthropology, the John T. Hitchcock Prize for Anthropology, and the Research Triangle Nanotechnology Network Kickstarter Grant. I am also extremely grateful for the support of Boulder's Gym and the Madison rock climbing community for their willingness to engage in research and provide access to their facility. Additionally, I want to thank the curatorial staff and lab managers for the resources and specimens provided in Cleveland, New York, Washington, and Durham.

Graduate school is an arduous and often trying undertaking. I would not have succeeded without the support and generosity of many friends. I want to thank my fellow graduate students who have helped me navigate the challenges of completing my PhD. I specifically want to thank Dr. Sarah Traynor, Dr. Mary Dinsmore, and Dr. Jeanelle Uy for their camaraderie and encouragement in addition to their biological anthropology expertise. Thank you to Dr. Joe Quick, Caitlin Benedetto, and Jasmine Wyant for challenging me to become a more well-rounded anthropologist and educator. I am forever grateful to Kory Breuer for being a wonderful friend and lifetime supporter outside of graduate school and for our many kitchen counter discussions. Thank you to the game night crew and the theatre community for providing a creative and fun outlet outside of my research.

This dissertation is dedicated to my incredible family. Words cannot express the endless gratitude I feel to my parents and brothers. They have been the strongest supporters and unwavering cheerleaders at all stages of my life, helping me through every high and low. I additionally want to thank them for always making me feel worthy and capable. They have been inspiring role models and have always encouraged my curiosity and ambition. Finally, I want to thank Finn for his patience, love, and support. He is an incredible and inspiring partner and I am excited to share all of life's future adventures (and cats) with him. To Mom, Dad, Matt, Chris, Finn and the cats – I love you.

List of Figures

List of Tables

Chapter 1
Introduction

Geladas (*Theropithecus gelada*), and cercopithecines more broadly, have been of interest to anthropologists for many years. Aspects of their lives including dominance structure, dispersal patterns, kin relationships, and terrestrial locomotion have been viewed as indicators of their similarities with humans and suitability as inferential models of hominin evolution, despite marked diversity throughout primates (Strier, 1994). The morphological differences between geladas and other cercopithecines have been further cited as evidence for the utility of geladas in understanding our own evolutionary path (Jolly, 1970).

Hand functional morphology has been central to defining humanlike behaviors in the fossil record. The competing demands of locomotion and manipulation drive our questions about the function of recently discovered fossil hominin hands. Our interest in hand function within the context of human evolution extends to Darwin (1871), placing it is a driver of uniquely human obligate bipedal locomotion. To understand the evolution of human hands, inferential models are vital.

This dissertation examines the manual skeletal morphology of *Theropithecus gelada* and *Papio* spp., revisiting the seed-eaters model (Jolly, 1970) with special emphasis on hand morphology. Geladas exhibit some unique behaviors closely linked to hand function including grooming and manual grazing. They also possess hand morphology that shares important similarities with modern human hands related to manipulation. Geladas have relatively long thumbs and short index fingers, a pattern observed in exclusively in humans among the extant apes. This

proportion, the opposability index (Napier and Napier, 1967), has been interpreted as an indicator of the manipulative capabilities of living and fossil primates and is one way in which geladas and baboons differ morphologically (Etter, 1973).

Geladas and baboons share many behavioral and skeletal traits. Comparisons between gelada and baboon manual skeletal morphology can reveal the impact of relatively subtle differences in behavior, substrate use, and posture that can inform our interpretations of the past. In chapter 3, I have provided a detailed description of the manual skeletal elements of *Theropithecus gelada*. Previous descriptive work on the extant species of *Theropithecus* has largely neglected the skeletal morphology of the hand, instead focusing on the musculature or skeletal elements throughout other parts of the body (e.g., Maier, 1971). Studies of fossil *Theropithecus* manual elements are also available, though they do not include extant species in their descriptions (Guthrie, 2011; Jablonski et al., 2002). The opposability index of geladas has been the primary distinguishing element between baboon and gelada manual morphology, though a modern interpretation of the seed-eater model requires a more thorough understanding of additional aspects of gelada manual morphology. When comparing gelada hand morphology, there are many similarities, likely linked to their terrestrial digitigrade locomotion. Aside from the relative length of the phalanges of rays 1 and 2, the phalanges of baboons and geladas are very similar. The primary differences noted in chapter 3 are in the metacarpals. The descriptions provided in there are foundational to further analyses that quantify differences in manual morphology between geladas and baboons.

Chapter 4 examined 3-dimensional shape differences between gelada and baboon hand bones. Linear measurements are useful for understanding proportions, but other shape differences are difficult to quantify without 3D analyses. Geometric morphometrics allows us to do just that. The study described in this chapter assessed shape differences in the proximal articular surfaces of Mc1 and Mc2 for geladas and baboons using 3D geometric morphometric analyses. The very high opposability index of geladas, which has been assumed to be an adaptation to fine object manipulation during food gathering, involves the first and second metacarpals (Mc1 and Mc2, respectively). The act of opposition, as facilitated by high opposability, involves movement at the Mc1-trapezium joint. Pad-to-pad precision gripping between the distal first and second rays could also involve movement at the Mc2-trapezoid joint. As a result of the study described in chapter 4, I found that there are important shape differences between these two groups, largely in joint stability and flexion-extension range. Geladas show some increased stability at the Mc1-trapezium joint that could be related to forceful pulling of vegetation (Marzke, 2005). Baboons tend to show more stability at the Mc2-trapezoid joint, though both primate groups have relatively low stability across both joints investigated compared to apes (Marzke et al., 2010; Marchi et al., 2017). The differences highlighted in chapter 4 could indicate variations on the general terrestrial digitigrade locomotion geladas and baboons perform, with baboons potentially moving at higher speeds more often, and reinforce differences in manual foraging.

Chapter 5 examined primate allogrooming and the opposability index. Grooming is very important for primates both hygienically and socially. A correlation has been demonstrated between grooming time and group size for catarrhines and between grooming time and body

size in platyrrhines (Dunbar, 1991; Lehmann et al., 2007). Grooming is a complex behavior that varies across primate groups. A variety of hand postures, including pad-to-pad precision gripping between the first and second digits, are used during grooming. High opposability, as measured by the opposability index, could allow for greater efficiency or ease while performing this grooming posture. Geladas groom at high rates and are particularly skilled at this type of hand posture because of their high opposability index (Iwamoto and Dunbar, 1983). In this chapter, I assessed whether or not a relationship exists between grooming investment (characterized by percent of daily activity budget devoted to grooming) and opposabilitiy index in apes and Old World monkeys. I found that a strong positive correlation does exist. Primates with high opposability indices tend to groom for a larger proportion of the day than primates with lower opposability indices. Further work is essential to understanding how the hands are used during grooming across taxa. This is especially relevant for including other taxa with varying degrees of opposability by Napier and Napier's (1967) classification.

The findings throughout this dissertation have implications for studying links between behavior and skeletal morphology of the hand of primates. They support the need to reimagine the seed-eaters model with modern techniques and applications as a means of understanding the hominin fossil record and the evolutionary path of hominin hand morphology. Geladas represent an important inferential model for hominin hand evolution that deserves continued attention.

Works Cited

Darwin, C. (1871). The descent of man, and selection in relation to sex. *Princeton: Princeton UP*.

Dunbar, R.I.M. (1991). Functional significance of social grooming in primates. *Folia primatologica*, *57*(3), 121-131.

Etter, H.F. (1973). Terrestrial adaptations in the hands of Cercopithecinae. *Folia Primatologica*, *20*(5-6), 331-350.

Guthrie, E.H. (2011). *Functional morphology of the postcranium of Theropithecus brumpti (Primates: Cercopithecidae)* (Doctoral dissertation, University of Oregon).

Iwamoto, T., & Dunbar, R.I.M. (1983). Thermoregulation, habitat quality and the behavioural ecology of gelada baboons. *The Journal of animal ecology*, 357-366.

Jablonski, N.G., Leakey, M.G., Kiarie, C., & Antón, M. (2002). A new skeleton of Theropithecus brumpti (Primates: cercopithecidae) from Lomekwi, west turkana, Kenya. *Journal of Human Evolution*, *43*(6), 887-923.

Jolly, C.J. (1970). The seed-eaters: a new model of hominid differentiation based on a baboon analogy. In *Primate Evolution and Human Origins* (pp. 323-332). Routledge.

Lehmann, J., Korstjens, A.H., & Dunbar, R.I.M. (2007). Group size, grooming and social cohesion in primates. *Animal Behaviour*, *74*(6), 1617-1629.

Napier, J.R. & Napier, P.H. (1967): A handbook of living Primates. Academic Press, London.

Maier, W. (1971): Vergleichend- und funktionell-anatomische Untersuchungen an der Vorderextremität von *Theropithecus gelada* (Ruppell 1835). Abhdl. Senckenb. Naturf. Ges., No. 527, 1-284, Frankfurt a. M.

Marchi, D., Proctor, D.J., Huston, E., Nicholas, C.L., & Fischer, F. (2017). Morphological correlates of the first metacarpal proximal articular surface with manipulative capabilities in apes, humans and South African early hominins. *Comptes Rendus Palevol*, *16*(5-6), 645-654.

Marzke, M.W. (2005). Who made stone tools. *Stone knapping: the necessary conditions for a uniquely hominin behaviour. Cambridge: McDonald Institute for Archaeological Research*, 243-256.

Marzke, M.W., Tocheri, M.W., Steinberg, B., Femiani, J.D., Reece, S.P., Linscheid, R.L., ... & Marzke, R.F. (2010). Comparative 3D quantitative analyses of trapeziometacarpal joint surface curvatures among living catarrhines and fossil hominins. *American Journal of Physical Anthropology: The Official Publication of the American Association of Physical Anthropologists*, *141*(1), 38-51.

Strier, K.B. (1994). Myth of the typical primate. *American Journal of Physical Anthropology*, *37*(S19), 233-271.

Chapter 2
Geladas and baboons: inferential models, hand morphology, and behavior

This dissertation focuses on the manual morphology of *Theropithecus gelada*, an extant African cercopithecine. Geladas are member of tribe Papionini (Strasser and Delson, 1987). This successful group of primates includes several extant groups, including baboons (*Papio*), mandrills and drills (*Mandrillus*), mangabeys (*Cercocebus, Lophocebus,* and *Rungwecebus*), and macaques (*Macaca*). It also includes the extinct genera *Dinopithecus*, *Gorgopithecus*, *Paradolichopithecus*, *Procynocephalus*, and *Parapapio* (Fleagle, 1999). Papionins are abundant and widespread, inhabiting diverse landscapes throughout Asia and Africa.

Due to their evolutionary success, many have recognized the potential importance of papionins to understanding many aspects of the evolutionary history of humans (Jolly, 1970; 2001; Almécija et al., 2015; Elton, 2006) and these ideas have been formative in the study of human origins. This chapter reviews some of the ways that geladas and baboons have informed ideas about human evolution. It then looks more specifically at the hand morphology of geladas. I consider the foraging ecology of geladas in comparison to baboons and other cercopithecines, and how this influences overall gelada morphology as well as hand morphology specifically.

The role of geladas and baboons in inferential models about human evolution

In the 1970s, Clifford Jolly initiated a pulse of interest in the contrasts between baboons and geladas as a model for the origin of hominins. Though this was not the first time that baboon models were consider for hominin origins (e.g., Washburn and DeVore, 1961; DeVore and Washburn, 1963), Jolly's formulation was the first to highlight the adaptive complex of

Theropithecus and its purported similarities to the hominin adaptive complex. Jolly suggested that these two patterns represented evolutionary parallelism and that resulted in functional equivalences. *Theropithecus* may have differentiated from *Papio* in much the same way that early Pleistocene hominins differentiated from *Pan*. Shared morphologies in the hominin and *Theropithecus* lineages could serve a similar function and have arisen from parallel selective pressures. Termed the seed-eaters model, the initial basis for this inferential analogy was dietary, though the postcranial anatomy of *Theropithecus* and hominins was fundamental in facilitating a diet primarily composed of small, tough object.

Hand morphology played a central role in the seed-eaters model. Jolly stressed the high opposability index and the independent movement of the index finger as essential for fine object manipulation related to manual grazing of geladas. He interpreted these characters as significant shared traits within the *Theropithecus* and hominin evolutionary paths. Jolly further emphasized the importance of this opposability index in seed-eating by stating that, "the gelada (in contrast to, for instance *Papio)* uses a precision-grip for most of its food-collecting," (p. 12 Jolly, 1970). By Jolly's definition, an adept hand, like that of hominins, requires high opposability and precision grip capabilities. Jolly also pointed out that, though primarily used during feeding, the importance of the adept hand of geladas should not be ignored, arguing that, "it is significant that the precision-grip of the gelada, which like other Cercopithecinae has not been seen making or using artefacts in the wild, should far outclass that of the tool- and weapon-using chimpanzee," (p. 13, Jolly, 1970). By Jolly's estimation, the seed-eaters model surpassed chimpanzee-based inferential models, especially given these manual similarities,

namely the high opposability indices and precision grip capabilities of the *Theropithecus* and hominin lineages.

The seed-eaters model was a contrast to earlier ideas about hominin origins, which ultimately derived from Darwin. The hand played a central role in Darwin's conception of hominins. In his *Descent of Man* (1871), Darwin argued that freeing the hands of the constraints of locomotion drove hominins to adopt a bipedal stance and gait. He stated that, "Man alone has become a biped; and we can, I think, partly see how he has come to assume his erect attitude, which forms one of his most conspicuous characters. Man could not have attained his present dominant position in the world without the use of his hands, which are so admirably adapted to act in obedience to his will," (p. 51). Darwin continued by stating that "the hands and arms could hardly have become perfect enough" if they were used habitually for locomotion as in other primates (p. 51). The freedom granted by bipedal locomotion allowed the evolution of the "perfect hand" which, by Darwin's interpretation, was essential for complex manipulation and tool manufacture.

Later discoveries of early hominins, including *Australopithecus*, were accompanied by ideas about the importance of hand morphology. Raymond Dart's (1957) hypothesis of the Osteodontokeratic Culture of *Australopithecus* necessitated skilled hands to create the tools and weapons from bones, teeth, and horns he believed early hominin 'killer apes' used against each other. The importance of hand morphology and tool use also featured prominently in interpretations of *Homo habilis* skeletal material and behavior. The discovery of the OH 7 hand

in direct association with stone tools solidified the conceptual link between manual manipulative capabilities and tool manufacture and use (Leakey et al., 1964). Functional assessments of early hominin hands were tied to tool use and the precision grip that facilitates stone tool production.

All of these ideas implicitly contrasted hominin hand morphology from the morphology in living great apes like chimpanzees and humans. By the 1980s, it was clear that humans have a phylogenetic position amid the great apes, not separate from them. This prompted an increased interest in inferential models for hominin origins that assumed that the human-chimpanzee common ancestor was very much like living chimpanzees in morphology and behavior. This extended to the study of the functional morphology of hominin hands. The idea of a chimpanzee-like ancestor for hominins continues to influence the research on this portion of the body (e.g. Richmond et al., 2001; Young, 2003; Tocheri et al., 2008; Almécija et al., 2015).

New fossil analyses, assessments of chimpanzee behavior, and recent hominin discoveries have all challenged the assumption that hominins descend from a chimpanzee-like ancestor (e.g., Sayers and Lovejoy, 2008; Lovejoy et al., 2009; White et al., 2015; Almécija et al., 2015). Some authors have also questioned the importance of phylogenetic proximity in selecting a model for early hominin species variability, behavior, and diet asserting that cercopithecines might serve as more appropriate analogues for early hominins (e.g., Aiello et al., 2000; Lee-Thorp et al., 2003; Elton, 2006; Sayers and Lovejoy, 2008). Cercopithecines as a group occupy a much wider geographic range than any of the extant great apes (Elton, 2006). Some cercopithecines have a

similar dietary ecology to that proposed for many early African hominins (Lee-Thorp et al., 2003; Macho, 2014; Cerling et al., 2013; Fashing et al., 2014). Lee-Thorp and colleagues (2003) found stable isotope signatures of South African australopithecines were more closely aligned with the diets of hamadryas and chacma baboons than any extant ape. Likewise, Macho (2014) demonstrated *Paranthropus boisei* was probably a dietary generalist, much like *Papio,* based on dental microwear patterns and a strong C_4 signature in isotopic analyses. Other authors highlighted *Theropithecus* in their comparisons suggesting that *Paranthropus boisei* may have consumed both above and below ground food resources, shifting between the two sources in response to season variation in much the same way of extant *Theropithecus gelada* (Fashing et al., 2014). Additionally, though average *Pan troglodytes* body mass and estimated body mass for many African hominins is not statistically different (Grabowski et al., 2015), estimates of some fossil cercopithecoid body masses are comparable to those of African hominins (Wood and Collard, 1999; Delson et al., 2000). Body mass estimates for *Theropithecus oswaldi* range between 34 kg to in excess of 60 kg (Delson et al., 2000), well within the estimated range of African hominins including *Homo habilis* (34 kg), *Australopithecus africanus* and *Paranthropus robustus* (36 kg), *Paranthropus boisei* (44 kg), and *Homo ergaster* (58 kg) (Wood and Collard, 1999).

While there are inherent shortcomings of any referential model of hominin behavior (e.g., Tooby and DeVore, 1987; Moore, 1996; Aiello et al., 2000; Sayers and Lovejoy, 2008), cercopithecines have long been employed in scenarios of human evolution (e.g., Washburn and DeVore, 1961; DeVore and Washburn, 1963; Jolly, 1970, 2001; Elton, 2006; Macho, 2014).

Though there are some doubts about the accuracy of paleoecological reconstructions of hominoid fossil-bearing sites (Dominguez-Rodrigo and Musiba, 2010), hominins and many cercopithecines are thought to have evolved in the same types of highly complex and heterogeneous mosaic environments that characterized Africa between 4 and 1 Ma (e.g., Bobe and Behrensmeyer, 2003; Potts, 1998; Dunbar, 1983; Elton, 2006; DiMaggio et al., 2015). The frequent environmental fluctuations and general trend toward increasing aridity may have impacted hominins and cercopithecines in similar ways, forcing both to exploit new habitats and food resources (Elton, 2006; Fashing et al., 2014). Additionally, the current and historical geographic range of baboons, geladas, and their related fossil species overlap with those of hominins (e.g., Brain, 1981, 1993; Bobe and Behrensmeyer 2003; Codron et al., 2005; Copeland et al., 2011; Foley, 1993; Dunbar, 1983; Cerling et al., 2013). Hominins and fossil cercopithecines may have experienced the same ecological challenges under similar energetic constraints and the ways in which each group met these challenges can be understood through an examination of the extant species and their functional morphology.

A modern interpretation of Jolly's seed-eaters model allows us to again consider the evolutionary path of *Theropithecus gelada* when examining hominin evolution. The more we learn about chimpanzee tool cultures in conjunction with recent hominin hand discoveries, the clearer it seems that tool creation is less important for understanding hominin hand evolution and behavior than we have been led to believe. Comparisons of geladas and baboons have the potential to illuminate other important functional uses for hominin manual morphologies.

Gelada foraging ecology

Geladas have long been noted for their unique foraging and dietary strategy. Today, geladas are geographically restricted to the highland plateaus of Ethiopia (Dunbar, 1977). They are among the most terrestrial of the Old World monkeys (Krentz, 1993), perhaps due to the lack of trees in their montane habitat. While geladas do not frequently climb trees, they do climb the steep cliff faces where they retire to sleep each night (Dunbar, 1977; Krentz, 1993). Their habitat is largely devoid of fruit but abundant in grasses, which make up more than 90% the gelada diet across most habitats and seasons (Iwamoto, 1993).

This dietary specialization in geladas is evidenced in their dental and craniofacial morphology. Grasses are especially abrasive and can cause high tooth wear in geladas over their lifetime, reducing chewing efficiency with increased age (Venkataraman et al., 2014). Geladas have high-crowned, or hypsodont, molars. These enable geladas to shred blades of grass. Their teeth also have relatively thick enamel to resist the wear of silica phytoliths, which are especially prevalent in grasses (reviewed in Rabenold and Pearson, 2011; Dunbar and Bose, 1991). Geladas do not have the kind of specialized gut morphology that facilitates leaf eating in colobine monkeys. For this reason, dental architecture that facilitates high chewing efficiency is necessary to support a graminivorous diet in geladas. The adaptation to more powerful chewing is also manifested by large cross-sectional areas in the masseter muscles of geladas relative to baboons (Jablonski, 1993).

Geladas have very distinctive foraging behaviors associated with graminivory. While foraging, geladas sit upright plucking blades of grass and seeds between the thumb and second digit. They sit for extended periods of time and shuffle forward bipedally while maintaining a near-seated posture to allow for continuous feeding (Jolly, 1970; Wrangham, 1980). In this posture, both hands remain free from locomotor constraints. This is a contrast to the feeding posture typical of many baboons in which both one hand and both feet remain in contact with the ground, while the free hand is used for feeding. Notable changes in the femur of geladas to accommodate extended bouts of squatting and shuffling during feeding include laterally extended articular surfaces of the femoral head, laterally angled femoral shafts, and reduced heights on the greater trochanters (Krentz, 1988 cited in Krentz, 1993). Some soft tissue morphology helps to facilitate upright posture during feeding. Geladas possess fatty pads, or "accessory sitting pads", adjacent to their ischial callosities. Previous workers have considered that these fatty pads are a functional parallel to the fatty buttocks of humans (Jolly, 1970; Pocock, 1925).

The gelada hand also possesses distinctive morphology linked to their feeding ecology. Gelada hand morphology differs in important ways from that of other extant monkeys, particularly in the intrinsic hand proportions. One important measure of intrinsic hand proportions is the opposability index, a simple ratio of the length of the first ray (total length of metacarpal plus phalanges that comprise the thumb) to the length of the second ray (total length of metacarpal plus phalanges of the index finger) (Napier and Napier, 1967). Humans have a high opposability index, reflecting our long first ray, and specifically long thumb, compared to the length of the

second ray, including the index finger. Strong opposition of the thumb to the pads of the fingers facilitated by a high opposability index is considered an important prerequisite for some hominin behaviors including stone tool production and use (Toth and Schick, 1993; Rolian et al., 2011; Marzke, 1983; Marzke and Wullstein, 1996; Napier and Napier, 1967). While humans have a high opposability index, human hand proportions are less extreme than those of geladas. Geladas have the highest opposability index of any non-human primates, because they combine a relatively long first ray with a short second ray (Napier and Napier, 1967; Etter, 1973). The long first ray is largely due to elongation of the first metacarpal, whereas the reduction of ray 2 is due to abbreviation of the phalanges, especially the intermediate phalanx. Geladas represent the only other living primate with similar opposability index to humans and a thorough understanding of their manual regime may help us interpret the hominin fossil record. Their high opposability is often considered adaptive to their unique diet and feeding ecology, allowing geladas to efficiently pluck grasses and seeds between their thumb and second digit. Additionally, this kind of manual grazing might be facilitated by their strong thenar musculature, as outlined by Maier (1971; 1972; 1993).

The constraints of terrestrial locomotion on hand morphology

The opposability index illustrates only the most basic level of morphological uniqueness of the gelada hand morphology. Beyond the proportion of the first and second rays, few scientists have considered how other aspects of hand morphology may be involved in gelada foraging. Further, it is not clear how the overall gelada hand morphology may relate to tradeoffs between foraging and terrestrial locomotion. It is also not evident whether climbing on rocks, as geladas habitually do, may be different in some ways from arboreal climbing.

Much is known about the way that hominin hand morphology differs from that of the great apes. The opposing constraints of locomotion and manipulation have been important in the history of this subject. Living great apes and humans all use their hands for vertical climbing, though there might be a slight bias for hindlimb weight support (Hanna et al., 2017). Chimpanzees, gorillas, and bonobos also use their hands and wrists for knuckle-walking. This highly specialized form of quadrupedal terrestrial locomotion is characterized by distinct curvature patterns through the phalanges, ridging along the dorsal side of the metacarpal heads, and wrist stability in these primates (Orr, 2005; Tocheri et al., 2008; Matarazzo, 2008). Great apes and humans also all use their hands for manipulation. In humans and chimpanzees, and to some extent in orangutans, tool use is an important manipulatory activity. In gorillas as well as in other great apes, activities that involve manipulation include the extractive processing of foods with hidden or hard-to-access edible parts.

Cercopithecine hand morphology has also been examined relative to locomotion and manipulation. Etter (1973) found that cercopithecines, despite their great species diversity, all possess relatively similar hand morphology to other catarrhines, especially in their intrinsic hand proportions. Most of the differences in hand morphology that Etter observed within the cercopithecines were related to predator evasion (high speed terrestrial running) or food gathering. Human hands exhibit similar intrinsic proportions to those of many cercopithecines, suggesting that human hand proprtions are not particularly derived, but rather represent a more cercopithecine-like ancestral form. This ancestral form is also capable of precision

gripping and fine object manipulation as evidenced by extant taxa (reviewed in Fragaszy and Crast, 2016).

Metacarpal morphology can be informative for understanding the locomotor regimes of primates due to their exposure to compressive loads (Preuschoft, 1973; Siegel and Pernotto, 1975; Patel, 2010; Patel and Wunderlich, 2010; Tsegai et al., 2013). Preuschoft (1973) demonstrated that the metacarpals of knuckle-walking and brachiating primates are always under some degree of compressive force, regardless of locomotor regime, but the magnitude and distribution across the bone differs. Thus, specific morphology of the manual elements may be adaptive for resisting compressive forces associated with one type of locomotion. Siegel and Pernotto (1975) suggested that robusticity could be useful for determining modes of locomotion in primates associated with distinct patterns of compressive loading. Metacarpal head morphology, shaft cross-sectional morphology, and trabecular bone structure are also related to compressive joint reaction forces. These measures have been used to help distinguish palmigrady and digitigrady in cercopithecoid primates (Patel, 2010; Patel and Wunderlich, 2010) and knuckle-walking, suspensory, or manipulative hand postures in hominoids (Tsegai et al., 2013).

The morphology of the metacarpal base has been less thoroughly examined, but may be particularly informative regarding manipulation. Much of the previous work that discusses the metacarpal base morphology emphasizes the first metacarpal (Mc1) and trapezium (e.g., Rose, 1992, Tocheri et al., 2005). The second metacarpal (Mc2) has been largely ignored. It is an

essential element of the opposability index and may help facilitate independent movement of digit 2 (as in geladas during foraging behaviors, Jolly, 1970). Thus, the morphology of Mc2 should be considered in assessments of manipulative and locomotor functions of primates. Some studies have examined the carpals that form part of the second carpometacarpal joint (e.g., Tocheri et al., 2005). The trapezoid is one of the carpals that makes up the second carpometacarpal joint, and it has carried much weight in discussion of manipulation in fossil hominins. For example, the boot-shaped morphology of the trapezoid in *Homo* (as represented by *H. naledi*, Neanderthals, and *H. sapiens*) distinguishes from earlier hominins (Kivell, 2015). Examination of the trapezoid can be useful, but there are some incongruences between the articular surfaces of the carpals and metacarpals making it difficult to understand how the shape of the proximal end of the second metacarpal relates to overall joint function.

The activity at the carpometacarpal joints, specifically at Mc1 and Mc2 are essential for understanding the precision gripping capabilities of geladas. Metacarpal joint surface anatomy can indicate joint stability and range of motion at the carpometacarpal joints as well as habitual force patterns through the hands (Rose, 1992, Niewoehner, 2000; 2005, Marzke et al., 2010; Marchi et al., 2017). Comparing geladas and baboons in these features could reflect differences in behavior, especially related to opposition and forceful pad to pad precision gripping. A higher degree of flexibility and range of motion at these joints could suggest greater emphasis on manipulation relative to locomotion which would require greater passive stability.

Overall, geladas and baboons are both terrestrial quadrupeds. These two closely related primates do show some differences in locomotion during feeding, as discussed above, but they share most of their limb morphology and kinematics of terrestrial digitigrade locomotion characterized by extension at the carpometacarpal joints and contact with the substrate across the palmar surface of the fingers. As is typical of many primate and non-primate quadrupeds, geladas and baboons have roughly equal limb lengths (Krentz, 1993). Cercopithecine hands also have characteristic proportions that some researchers have connected to terrestrial quadrupedal locomotion. Etter (1973) noted that terrestrial cercopithecines have relatively long metacarpals 2 through 5 and short phalanges compared to highly arboreal monkeys. This is broadly true and is similarly expressed in geladas and baboons. Both geladas and baboons have similarly long metacarpals and short phalanges in rays 3 through 5. Habitually terrestrial digitigrade monkeys like geladas and baboons adopt hand positions that increase stride length and reduce strain at the distal joints during slow-speed walking (Patel, 2010; Patel and Wunderlich, 2010). Due to their similar locomotor regimes, the contact between the metacarpal head and the phalanges with the ground in digitigrade hand positions would likely place similar selective pressures on these aspects of hand morphology for geladas and baboons. Study of the differences between gelada and baboon manual skeletal morphology has been limited aside from the differences in intrinsic hand proportions noted above (Napier and Napier, 1967; Krentz, 1993; Etter, 1973).

Geladas do a considerable amount of rock climbing as they travel between their sleeping sites on the steep, rock faces and the grassy plateaus where they spend the day (Dunbar and

Dunbar, 1974; Ohsawa, 1979; Kawai and Iwamoto, 1979). Climbing rocks versus arboreal climbing is a relatively subtle locomotor difference. Rock climbing still engages all four limbs like tree climbing or terrestrial walking, but hand positions and force distribution across the manual elements differ in each of these modes of locomotion. While some populations of baboons in eastern and South Africa also traverse rocky substrates and climb rocks (e.g. Hamilton, 1982; Barrett et al., 2004), they do so at a lower frequency than gelada populations. These kinds of subtle differences in substrate use and manual behaviors could be difficult to discern through intrinsic hand proportions alone. Complex substrate use and high diversity between populations contribute to the need for other methods of examining manual morphology to understand unique gelada and baboon adaptations.

Ecology of fossil *Theropithecus* and implications for hand morphology

Interestingly, the intrinsic manual proportions of extant geladas are echoed in the fossil species *Theropithecus brumpti* (Guthrie, 2011) suggesting relatively long first rays and short second rays are ancestral for all *Theropithecus* taxa. Unfortunately, relevant manual elements are missing or incomplete for *Theropithecus oswaldi* which would further support the ancestral character of high opposability (Whitehead, 2018). The ancestral character of high opposability could indicate that manual grazing and a highly graminivorous diet characterizes the entire *Theropithecus* lineage. Stable isotope analyses of fossil *T. brumpti* and *Theropithecus oswaldi* teeth have offered some support for this assertion. These analyses have shown strong C_4 signals in the earliest *T. brumpti* specimens that increasing through more recent *T. oswaldi* specimens which show a diet almost entirely comprised of C_4-derived resources (Cerling et al., 2013). C_4 grasses may have comprised the bulk of fossil *Theropithecus* diets, though the proportion of other C_4-

derived resources like underground storage organs or leaves cannot be determined from stable isotopes alone. In contrast, extant geladas subsist almost exclusively on C_3 grasses which are abundant in the Ethiopian highlands (Dunbar and Bose, 1991).

Further complicating the functional interpretation of high opposability indices in fossil *Theropithecus,* dental microwear analyses indicate that *T. brumpti* consumed soft fruit in much higher proportions than modern geladas (Teaford, 1993). Likewise, *T. oswaldi* from Cueva Victoria in southeastern Spain exhibits a buccal microwear pattern of the molars and premolars that is likened to extant frugivorous mandrills (*Mandrillus sphinx)* and mangabeys (*Cercocebus* spp.) (Martínez et al., 2020). Mandrills and mangabeys consume abrasive diets including hard-shelled fruits and seeds that leave substantial striations on the buccal enamel. Martínez et al. (2020) suggest that the deep striations observed in *T. oswaldi* could be the result of extrinsic grit accumulated during terrestrial foraging of grasses and seeds, but it was not a grass specialist like extant geladas.

The presence of a high opposability index early in the *Theropithecus* lineage with the absence of a grass- and seed-dominant diet calls into question the traditional functional explanation for high opposability in extant geladas. While high opposability might still be explained by fine object manipulation throughout the *Theropithecus* lineage, the objects being manipulated might have been different from the food resources harvested by extant geladas. The simple explanation is that precision gripping capabilities used to harvest C_3 grasses by extant geladas were used to harvest C_4 grasses in fossil *Theropithecus* species. Alternatively, high opposability

that facilitates pad to pad precision gripping may not have been an adaptation to foraging behaviors at all, but was instead used during grooming through the *Theropithecus* lineage.

Grooming and hand morphology

One possible alternative use of pad to pad precision gripping between the first and second rays is during grooming behaviors. Given the hygienic and social importance of grooming to many primate groups, anatomical adaptations to efficient and effective grooming may be present in taxa that groom at especially high rates. Bishop (1962) suggested that opposition of the finger pads is essential for gripping fur which occurs during grooming activities. Furthermore, Bishop (1962) claimed that the hand positions used in grooming differ from those used in locomotion or food manipulation for prosimians, suggesting that fine motor control exhibited in ceboids and cercopithecoids may have evolved early in the primate lineage in large part due to grooming.

Primate allogrooming also has clear hygienic implications in addition to its social importance. Hutchins and Barash (1976) found that grooming performed by a partner was focused on areas of the body that were difficult for the grooming recipient to reach or that received minimum autogrooming. These authors suggested that there is a selective advantage for efficient ectoparasite removal through grooming, especially considering some ectoparasites that are found on primates negatively impact fitness (Lehmann, 1993). In a study of Japanese macaques (Tanaka and Takefushi, 1993), the items that were picked up during allogrooming by individuals in a free ranging group were catalogued. They found that macaques primarily picked up lice and the eggs of lice during grooming bouts. The macaques consumed all the lice and lice eggs they

picked up from grooming leading these researchers to additionally suggest that grooming could be related to nutritional needs.

Additional support for a potential link between grooming behaviors and manual morphology is found in some observational studies of Colobinae. Asian colobines tend to have lower levels of louse infestation than African colobines (Kuhn, 1968 as cited in Hutchins and Barash, 1976). This difference may be a consequence of a difference in hand proportions. African genera of colobines have a reduced thumb and less effective grooming postures than Asian colobines (Hutchins and Barash, 1976).

Pad to pad precision gripping postures were observed in a population of free ranging Japanese macaques (*Macaca fuscata*) during ectoparasite removal (Tanaka and Takefushi, 1993). Macaques gripped ectoparasites and hair between the thumb and index finger as they drew the hair through the closed pads of the digits. Similar pad to pad grip patterns were observed in semi-free ranging rhesus macaques (*Macaca mulatta*) (Macfarlane and Graziano, 2009). This precision grip occurred at a high frequency relative to all other manipulative postures, second only to pad to side grips, especially during grooming to pull fur aside and when holding pieces of grass or dirt.

Geladas devote a large percentage of their daily activity budget to grooming (Iwamoto and Dunbar, 1983). The species grooms for 17% of the day, on average. In one extreme case, 20% of the daily activity budget was devoted to grooming activities in a very large group (Dunbar,

2010). Baboons also groom at relatively high rates among primates, though the average across *Papio* is below that of geladas (Lehmann et al., 2007).

Geladas have a complex, multi-level social structure and form large herds. Gelada exhibit some of the largest group sizes among natural populations of primates, regularly numbering in the hundreds (reviewed in Dunbar, 1988; 1993). In the open grassland plateaus of Ethiopia, there are few natural refuges from predators and large group sizes help to reduce predation risk.

This high density of individuals can increase stress within large groups and grooming is one way to reduce stress and strengthen social cohesion (reviewed in Lehmann et al., 2007; Dunbar, 2018). Dunbar (1991) found that the frequency of social grooming was strongly positively correlated with group size, but not with body size, in catarrhine primates concluding that there is a significant social function of grooming rather than a strictly hygienic function. Also, grooming-based alliances between female geladas may help buffer them against the negative fitness consequences of stressful altercations. Reproductive endocrinology of primates is very sensitive to stress and geladas seem to be able to mitigate declines in fertility associated with the stress of large groups through these strong grooming-based alliances (Dunbar, 2018).

Another indicator of the importance of grooming behaviors in geladas is the relationship between foraging, resting, and grooming within the activity budget. Within seasonal and altitudinal changes, foraging time fluctuates to meet energetic demands at the expense of

resting time (Iwamoto and Dunbar, 1983). Grooming time does not change in response to increased foraging time but instead remains constant within a given group.

However, it is important to note that some baboons also live in relatively large groups and likely experience high levels of stress associated with social interactions (Lehmann et al., 2007). Proportionally high grooming rates in baboons could also be important for social cohesion in these species. An important difference between most gelada and baboon groups is their habitat which could have important implications for their grooming behaviors. Geladas live exclusively in the northern highlands of Ethiopia (Dunbar, 1977). There is some overlap with *Papio anubis* in the Ethiopian valley, but geladas consistently live at higher and therefore colder altitudes (Dunbar and Dunbar, 1974).

There are also thermoregulatory benefits of grooming. Grooming not only removes debris and ectoparasites that would keep fur matted, but it also detangles fur and thereby enhances pelt loft. McFarland et al. (2016) found that backcombed *Chlorocebus pygerthrus* pelts had significantly better thermal performance than flattened pelts in wind-tunnel experiments, reducing the amount of radiant heat absorbed by the skin. This concept can be applied to cold temperatures as well. Grooming increases pelt depth and increases total insulation. For geladas living in cold temperatures, grooming and the maintenance of pelt loft could be an essential thermoregulatory behavior.

The stresses associated with thermoregulation are important to fitness in wild geladas. Reduced birth rates and increased death rates associated with increases in altitude are the likely the result of cold stress (Ohsawa and Dunbar, 1984 as cited in Dunbar, 1988, Beehner and McCann, 2008). Despite greater availability of food resources at higher altitudes, group sizes decreased and more daily activity budget is devoted to feeding to account for the increased energetic demands of thermoregulation at cold temperatures (Iwamoto and Dunbar, 1983). Ho (2009) examined grooming frequency relative to ambient temperature in a population of captive geladas at the Bronx Zoo. This work demonstrated that grooming frequency increased as temperature decreased. It is possible that the high rates of grooming in geladas is linked to thermoregulatory benefits of increased pelt loft. Because grooming includes simple brushing and combing of fur in addition to pad to pad precision grips, the relationship between grooming and manual morphology is likely complex and deserves additional attention.

Conclusions

A detailed examination of the hand morphology of baboons and geladas has potential to further our understanding of primate hand evolution and, more specifically, the hominin evolutionary path. The grooming behaviors and foraging ecology of geladas are specialized among the cercopithecines and are intimately tied to hand function. Geladas also form the foundation of the seed-eaters inferential model of hominin evolution, offering a different perspective from the chimpanzee-human comparison so frequently used to examine hominin hand adaptation.

Looking forward to the analytical chapters, I aim to provide a detailed description of the manual skeletal morphology of extant geladas and provide insight into additional morphological differences between gelada and baboon hands. Special attention is paid to the carpometacarpal joints of rays one and two and potential relationships between opposability and grooming.

Works Cited

Aiello, L.C., Collard, M., Thackeray, J.F., & Wood, B.A. (2000). Assessing exact randomization-based methods for determining the taxonomic significance of variability in the human fossil record. *South African Journal of Science*, *96*(4), 179-183.

Almécija, S., Smaers, J.B., & Jungers, W.L. (2015). The evolution of human and ape hand proportions. *Nature communications*, *6*(1), 1-11.

Barrett, L., Gaynor, D., Rendall, D., Mitchell, D., & Henzi, S.P. (2004). Habitual cave use and thermoregulation in chacma baboons (*Papio hamadryas ursinus*). *Journal of Human Evolution*, *46*(2), 215-222.

Beehner, J.C., & McCann, C. (2008). Seasonal and altitudinal effects on glucocorticoid metabolites in a wild primate (Theropithecus gelada). *Physiology & behavior*, *95*(3), 508-514.

Bishop, A. (1962). Control of the hand in lower primates. *Annals of the New York Academy of Sciences*.

Bobe, R., & Behrensmeyer, A.K. (2004). The expansion of grassland ecosystems in Africa in relation to mammalian evolution and the origin of the genus Homo. *Palaeogeography, Palaeoclimatology, Palaeoecology*, *207*(3), 399-420.

Bobe, R., & Behrensmeyer, A.K. (2004). The expansion of grassland ecosystems in Africa in relation to mammalian evolution and the origin of the genus Homo. *Palaeogeography, Palaeoclimatology, Palaeoecology*, *207*(3), 399-420.

Brain, C.K. (1981). *The hunters or the hunted?*. University of Chicago Press.

Brain, C.K. (1993). A taphonomic overview of the Swartkrans fossil assemblages. *Swartkrans: A Cave's Chronicle of Early Man. Transvaal Museum, Pretoria*, 257-264.

Cerling, T.E., Chritz, K.L., Jablonski, N.G., Leakey, M.G., & Manthi, F.K. (2013). Diet of *Theropithecus* from 4 to 1 Ma in Kenya. *Proceedings of the National Academy of Sciences*, *110*(26), 10507-10512.

Codron, D., Luyt, J., Lee-Thorp, J.A., Sponheimer, M., De Ruiter, D., & Codron, J. (2005). Utilization of savanna-based resources by Plio-Pleistocene baboons: research letter. *South African Journal of Science*, *101*(5-6), 245-248.

Copeland, S.R., Sponheimer, M., de Ruiter, D.J., Lee-Thorp, J.A., Codron, D., le Roux, P.J., ... & Richards, M.P. (2011). Strontium isotope evidence for landscape use by early hominins. *Nature*, *474*(7349), 76-78.

Darwin, C. (1871). The descent of man, and selection in relation to sex. *Princeton: Princeton UP*.

Delson, E., Terranova, C.J., Jungers, W.L., Sargis, E.J., Jablonski, N.G., & Dechow, P.C. (2000). Body mass in Cercopithecidae (Primates, Mammalia): estimation and scaling in extinct and extant taxa. *Anthropological Papers of the American Museum of Natural History*, (83), 1-159.

DeVore, I., & Washburn, S.L. (1963). Baboon ecology and human evolution. *African Ecology and Human Evolution*, 335-367.

DiMaggio, E.N., Campisano, C.J., Rowan, J., Dupont-Nivet, G., Deino, A.L., Bibi, F., ... & Reed, K.E. (2015). Late Pliocene fossiliferous sedimentary record and the environmental context of early *Homo* from Afar, Ethiopia. *Science*, *347*(6228), 1355-1359.

Domínguez-Rodrigo, M., & Musiba, C.M. (2010). How accurate are paleoecological reconstructions of early paleontological and archaeological sites?. *Evolutionary Biology*, *37*(2-3), 128-140.

Dunbar, R.I.M. (1977). Feeding ecology of gelada baboons: a preliminary report. In *Primate ecology: Studies of feeding and ranging behaviour in lemurs, monkeys and apes.* Clutton-Brock, T. H. (ed.).London: Academic Press.

Dunbar, R.I.M. (1983). Theropithecines and hominids: contrasting solutions to the same ecological problem. *Journal of Human Evolution*, *12*(7), 647-658.

Dunbar, R.I.M. (1988). *Primate social systems.* Ithaca, New York. Cornell University Press.

Dunbar, R.I.M. (1991). Functional significance of social grooming in primates. *Folia primatologica*, *57*(3), 121-131.

Dunbar, R.I.M. (1993). Conservation Status of the Gelada, in: Jablonksi, N.G. (Ed.), *Theropithecus*: The Rise and Fall of a Primate Genus. Cambridge University Press,

Cambridge, pp. 527-531.

Dunbar, R.I.M. (2018). Social structure as a strategy to mitigate the costs of group living: a comparison of gelada and guereza monkeys. *Animal behaviour*, *136*, 53-64.

Dunbar, R.I.M., & Bose, U. (1991). Adaptation to grass-eating in gelada baboons. *Primates*, *32*(1), 1-7.

Dunbar, R.I.M., & Dunbar, E.P. (1974). Ecological relations and niche separation between sympatric terrestrial primates in Ethiopia. *Folia Primatologica*, *21*(1), 36-60.

Elton, S. (2006). Forty years on and still going strong: the use of hominin-cercopithecid comparisons in palaeoanthropology. *Journal of the Royal Anthropological Institute*, *12*(1), 19-38.

Etter, H.F. (1973). Terrestrial adaptations in the hands of Cercopithecinae. *Folia Primatologica*, *20*(5-6), 331-350.

Fashing, P.J., Nguyen, N., Venkataraman, V.V., & Kerby, J.T. (2014). Gelada feeding ecology in an intact ecosystem at Guassa, Ethiopia: variability over time and implications for theropith and hominin dietary evolution. *American Journal of Physical Anthropology*, *155*(1), 1-16.

Fleagle, J.G. (1999). Primate adaptation and evolution, Academic Press. *New York*.

Foley, R.A. (1993). The influence of seasonality on hominid evolution. *Seasonality and Human Ecology*, 17-37.

Fragaszy, D.M., & Crast, J. (2016). Functions of the hand in primates. In *The evolution of the primate hand* (pp. 313-344). Springer, New York, NY.

Grabowski, M., Hatala, K.G., Jungers, W.L., & Richmond, B.G. (2015). Body mass estimates of hominin fossils and the evolution of human body size. *Journal of Human Evolution*, *85*, 75-93.

Guthrie, E.H. (2011). *Functional morphology of the postcranium of Theropithecus brumpti (Primates: Cercopithecidae)* (Doctoral dissertation, University of Oregon).

Hamilton, W.J. (1982). Baboon sleeping site preferences and relationships to primate grouping patterns. *American Journal of Primatology*, *3*(1-4), 41-53.

Ho, R.C.L. (2009). A Cross-Species Comparative Study: Grooming Patterns in Captive Populations of Hamadryas Baboons and Geladas. *Queens College senior honors thesis*.

Hutchins, M., & Barash, D.P. (1976). Grooming in primates: implications for its utilitarian function. *Primates*, *17*(2), 145-150.

Iwamoto, T. (1993). The ecology of Theropithecus gelada. *Theropithecus: The rise and fall of a primate genus*, 441-452.

Iwamoto, T., & Dunbar, R.I.M. (1983). Thermoregulation, habitat quality and the behavioural ecology of gelada baboons. *The Journal of animal ecology*, 357-366.

Jablonski, N.G. (1993). Evolution of the masticatory apparatus in Theropithecus. *Theropithecus: The rise and fall of a primate genus*, 299-329.

Jolly, C.J. (1970). The seed-eaters: a new model of hominid differentiation based on a baboon analogy. In *Primate Evolution and Human Origins* (pp. 323-332). Routledge.

Jolly, C.J. (2001). A proper study for mankind: analogies from the papionin monkeys and their implications for human evolution. *American Journal of Physical Anthropology: The Official Publication of the American Association of Physical Anthropologists*, *116*(S33), 177-204.

Kawai, M. & Iwamoto, T. (1979). Nomadism and activities. In M. Kawai (Ed.) *Ecological and Sociological Students of Gelada Baboons* (3-45). Tokyo: Kodansha.

Kivell, T.L., Deane, A.S., Tocheri, M.W., Orr, C.M., Schmid, P., Hawks, J., ... & Churchill, S.E. (2015). The hand of Homo naledi. *Nature communications*, *6*(1), 1-9.

Krentz, H. (1988). The femur of *Theropithecus* – evidence for the appearance of shuffling behavior. In *American Journal of Physical Anthropology* (Vol. 75, No. 2, pp. 234-234). Div John Wiley & Sons Inc 605 Third Ave, New York, NY 10158-0012: Wiley-Liss.

Krentz, H.B. (1993). Postcranial anatomy of extant and extinct species of Theropithecus. In *Theropithecus: the rise and fall of a primate genus* (pp. 383-422). Cambridge University Press Cambridge.

Kuhn, H.J. (1968). Parasites and the phylogeny of the catarrhine primates. *Taxonomy and phylogeny of Old World Primates with references to the origin of Man*, 187-195.

Leakey, L.S., Tobias, P.V., & Napier, J.R. (1964). A new species of the genus Homo from Olduvai Gorge. *Nature*, *202*(4927), 7-9.

Lee-Thorp, J.A., Sponheimer, M., & van der Merwe, N.J. (2003). What do stable isotopes tell us about hominid dietary and ecological niches in the Pliocene?. *International Journal of Osteoarchaeology*, *13*(1-2), 104-113.

Lehmann, J., Korstjens, A.H., & Dunbar, R.I.M. (2007). Group size, grooming and social cohesion in primates. *Animal Behaviour*, *74*(6), 1617-1629.

Lehmann, T. (1993). Ectoparasites: direct impact on host fitness. *Parasitology today*, *9*(1), 8-13.

Lovejoy, C.O., Simpson, S.W., White, T.D., Asfaw, B., & Suwa, G. (2009). Careful climbing in the Miocene: the forelimbs of Ardipithecus ramidus and humans are primitive. *Science*, *326*(5949), 70-70e8.

Macfarlane, N.B., & Graziano, M.S. (2009). Diversity of grip in *Macaca mulatta*. *Experimental brain research*, *197*(3), 255-268.

Macho, G.A. (2014). Baboon feeding ecology informs the dietary niche of Paranthropus boisei. *PLoS One*, *9*(1).

Maier, W. (1971): Vergleichend- und funktionell-anatomische Untersuchungen an der Vorderextremität von *Theropithecus gelada* (Ruppell 1835). Abhdl. Senckenb. Naturf. Ges., No. 527, 1-284, Frankfurt a. M.

Maier, W. (1972). Anpassungstyp und systematische Stellung von Theropithecus gelada Rüppell, 1835. *Zeitschrift für Morphologie und Anthropologie*, (H. 3), 370-384.

Maier, W. (1993). Adaptations in the hands of cercopithecoids and callitrichids. In: Preuschoft H., Chivers, D.J. (eds) *Hands of primates*. Springer-Verlag, Vienna, pp 191–198.

Marchi, D. (2005). The cross-sectional geometry of the hand and foot bones of the Hominoidea and its relationship to locomotor behavior. *Journal of Human Evolution*, *49*(6), 743-761.

Marchi, D., Proctor, D.J., Huston, E., Nicholas, C.L., & Fischer, F. (2017). Morphological correlates of the first metacarpal proximal articular surface with manipulative capabilities in apes, humans and South African early hominins. *Comptes Rendus Palevol*, *16*(5-6), 645-654.

Marzke, M.W. (1983). Joint functions and grips of the Australopithecus afarensis hand, with special reference to the region of the capitate. *Journal of Human Evolution*, *12*(2), 197-211.

Marzke, M.W., & Wullstein, K.L. (1996). Chimpanzee and human grips: a new classification with a focus on evolutionary morphology. *International Journal of Primatology*, *17*(1), 117-139.

Marzke, M.W., Tocheri, M.W., Steinberg, B., Femiani, J.D., Reece, S.P., Linscheid, R.L., ... & Marzke, R.F. (2010). Comparative 3D quantitative analyses of trapeziometacarpal joint surface curvatures among living catarrhines and fossil hominins. *American Journal of*

Physical Anthropology: The Official Publication of the American Association of Physical Anthropologists, *141*(1), 38-51.

McFarland, R., Henzi, S.P., Barrett, L., Wanigaratne, A., Coetzee, E., Fuller, A., Hetem, R.S., Mitchell, D. & Maloney, S.K. (2016). Thermal consequences of increased pelt loft infer an additional utilitarian function for grooming. *American Journal of Primatology*, *78*(4), 456-461.

Moore, J. (1996). Savanna chimpanzees, referential models and the last common ancestor. In W. C. McGrew, L. F. Marchant, & T. Nishida (Eds.) *Great Ape Societies* (275). Cambridge University Press.

Napier, J.R. & Napier, P.H. (1967): A handbook of living Primates. Academic Press, London.

Niewoehner, W.A. (2000). *The functional anatomy of Late Pleistocene and recent human carpometacarpal and metacarpophalangeal articulations*. (Doctoral dissertation) University of New Mexico, New Mexico.

Niewoehner, W.A. (2005). A geometric morphometric analysis of Late Pleistocene human metacarpal 1 base shape. In *Modern morphometrics in physical anthropology* (pp. 285-298). Springer, Boston, MA.

Ohsawa, H. (1979). The local gelada population and environment of the Gich area. In M. Kawai (Ed.) *Ecological and Sociological Students of Gelada Baboons* (3-45). Tokyo: Kodansha.

Ohsawa, H., & Dunbar, R.I.M. (1984). Variations in the demographic structure and dynamics of gelada baboon populations. *Behavioral Ecology and Sociobiology*, *15*(3), 231-240.

Orr, C.M. (2005). Knuckle-walking anteater: A convergence test of adaptation for purported knuckle-walking features of African Hominidae. *American Journal of Physical Anthropology*, *128*(3), 639-658.

Patel, B.A. (2010). Functional morphology of cercopithecoid primate metacarpals. *Journal of human evolution*, *58*(4), 320-337.

Patel, B.A., & Wunderlich, R.E. (2010). Dynamic pressure patterns in the hands of olive baboons (*Papio anubis*) during terrestrial locomotion: implications for cercopithecoid primate hand morphology. *The Anatomical Record: Advances in Integrative Anatomy and Evolutionary Biology*, *293*(4), 710-718.

Pocock, R.I. (1925). 57. The External Characters of the Catarrhine Monkeys and Apes. In *Proceedings of the Zoological Society of London* (Vol. 95, No. 4, pp. 1479-1579). Oxford, UK: Blackwell Publishing Ltd.

Potts, R. (1998). Environmental hypotheses of hominin evolution. *American Journal of Physical Anthropology*, *107*(S27), 93-136.

Preuschoft, H. (1973). Functional anatomy of the upper extremity. *The chimpanzee*, *6*, 34-120.

Rabenold, D., & Pearson, O.M. (2011). Abrasive, silica phytoliths and the evolution of thick molar enamel in primates, with implications for the diet of Paranthropus boisei. *PLoS One*, *6*(12).

Rein, T.R. (2019). A geometric morphometric examination of hominoid third metacarpal shape and its implications for inferring the precursor to terrestrial bipedalism. *The Anatomical Record*, *302*(6), 983-998.

Richmond, B.G., Begun, D.R., & Strait, D.S. (2001). Origin of human bipedalism: the knuckle-walking hypothesis revisited. *American Journal of Physical Anthropology: The Official Publication of the American Association of Physical Anthropologists*, *116*(S33), 70-105.

Rolian, C., Lieberman, D.E., & Zermeno, J.P. (2011). Hand biomechanics during simulated stone tool use. *Journal of Human Evolution*, *61*(1), 26-41.

Rose, M.D. (1992). Kinematics of the trapezium-1st metacarpal joint in extant anthropoids and Miocene hominoids. *Journal of Human Evolution*, *22*(4-5), 255-266.

Sayers, K., & Lovejoy, C.O. (2008). The Chimpanzee Has No Clothes: A Critical Examination of Pan troglodytes in Models of Human Evolution. *Current Anthropology*, *49*(1), 87.

Siegel, M.I., & Pernotto, B. (1975). Hand use and metacarpal robusticity in Catarrhini. *Primates*, *16*(4), 371-377.

Strasser, E., & Delson, E. (1987). Cladistic analysis of cercopithecid relationships. *Journal of Human Evolution*, *16*(1), 81-99.

Susman, R.L. (1979). Comparative and functional morphology of hominoid fingers. *American Journal of Physical Anthropology*, *50*(2), 215-236.

Tanaka, I., & Takefushi, H. (1993). Elimination of external parasites (lice) is the primary function of grooming in free-ranging Japanese macaques. *Anthropological Science*, *101*(2), 187-193.

Teaford, M.F. (1993). Dental microwear and diet in extant and extinct *Theropithecus*: preliminary analysis, in: Jablonksi, N.G. (Ed.), *Theropithecus*: Rise and Fall of a Primate Genus. Cambridge University Press, Cambridge, pp. 331-349.

Tocheri, M.W., Orr, C.M., Jacofsky, M.C., & Marzke, M.W. (2008). The evolutionary history of the hominin hand since the last common ancestor of *Pan* and *Homo*. *Journal of Anatomy*, *212*(4), 544-562.

Tocheri, M.W., Razdan, A., Williams, R.C., & Marzke, M.W. (2005). A 3D quantitative comparison of trapezium and trapezoid relative articular and nonarticular surface areas in modern humans and great apes. *Journal of Human Evolution*, *49*(5), 570-586.

Tooby, J. & DeVore, I. (1987). The reconstruction of hominid behavioral evolution through strategic modeling. In W. Kinzey (Ed.) *The evolution of human behavior: Primate models* (183-237). Albany: State University of New York Press.

Toth, N., & Schick, K. (1993). Early stone industries and inferences regarding language and cognition. In K. R. Gibson & T. Ingold (Eds.) *Tools, language and cognition in human evolution* (346-362). Cambridge: Cambridge University Press.

Tsegai, Z.J., Kivell, T.L., Gross, T., Nguyen, N.H., Pahr, D.H., Smaers, J.B., & Skinner, M.M. (2013). Trabecular bone structure correlates with hand posture and use in hominoids. *PLoS One*, *8*(11).

Venkataraman, V.V., Glowacka, H., Fritz, J., Clauss, M., Seyoum, C., Nguyen, N., & Fashing, P.J. (2014). Effects of dietary fracture toughness and dental wear on chewing efficiency in geladas (T heropithecus gelada). *American Journal of Physical Anthropology*, *155*(1), 17-32.

Washburn, S.L., & DeVore, I. (1961). Social behavior of baboons and early man. *Yearbook of Physical Anthropology* 9, 91-105.

White, T.D., Lovejoy, C.O., Asfaw, B., Carlson, J.P., & Suwa, G. (2015). Neither chimpanzee nor human, *Ardipithecus* reveals the surprising ancestry of both. *Proceedings of the National Academy of Sciences*, *112*(16), 4877-4884.

Whitehead, P.F. (2018). *Functional Anatomy of the Forelimb in Terrestrial and Arboreal African Cercopithecoids* (Doctoral dissertation, Yale University).

Wood, B., & Collard, M. (1999). The human genus. *Science*, *284*(5411), 65-71.

Wrangham, R.W. (1980). Bipedal locomotion as a feeding adaptation in gelada baboons, and its implications for hominid evolution. *Journal of Human Evolution*, *9*(4), 329-331.

Young, R.W. (2003). Evolution of the human hand: the role of throwing and clubbing. *Journal of Anatomy*, *202*(1), 165-174.

Chapter 3
Manual skeletal morphology of *Theropithecus gelada*

Introduction

Multiple descriptions of the manual elements of fossil *Theropithecus* species exist (Jablonski et al., 2002; Guthrie, 2011), though a comprehensive description of extant *Theropithecus gelada* manual elements in missing from the available literature. Available descriptions are limited to the manual proportions of the musculature of geladas (Maier, 1971), lacking detailed accounts of the skeletal elements. The following description is derived from specimen M-200108, a young adult male from a wild population in Ethiopia currently curated at the American Museum of Natural History (AMNH) in New York, NY. All skeletal elements of the left hand were available and identifiable for this individual, not including sesamoids. Given the limited number of disarticulated gelada specimens available, many comparisons were made with articulated or partially articulated adult specimens also curated at the AMNH including M-238034 (unknown sex, unknown provenience), M-200763 (male, Ethiopia), and M-19006 (male, zoo) when possible. Individual variation exists between specimens and the descriptions provided here are as characteristic of the species as possible given the limited sample. Skeletal elements of the gelada hand described in this study from specimen M-200108 at the AMNH are depicted in Figure 3.1 in articulation. Figure 3.1 was hand-drawn by the author using photo references included in this chapter. As a comparative reference, the manual skeletal elements of one *Papio cynocephalus* individual are shown in articulation in Figure 3.2. Figure 3.2 was hand-drawn by the author using images from Swindler and Wood (1973).

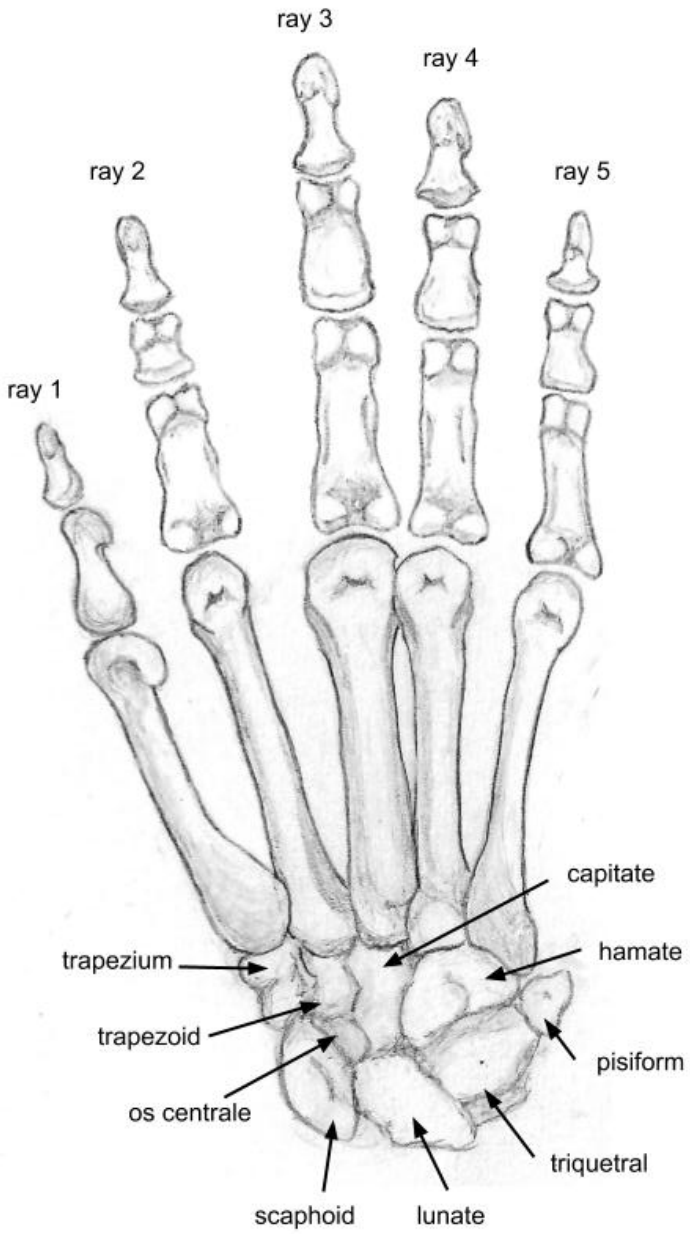

Figure 3.1
Palmar view of *Theropithecus gelada* left hand with labelled rays and carpals.

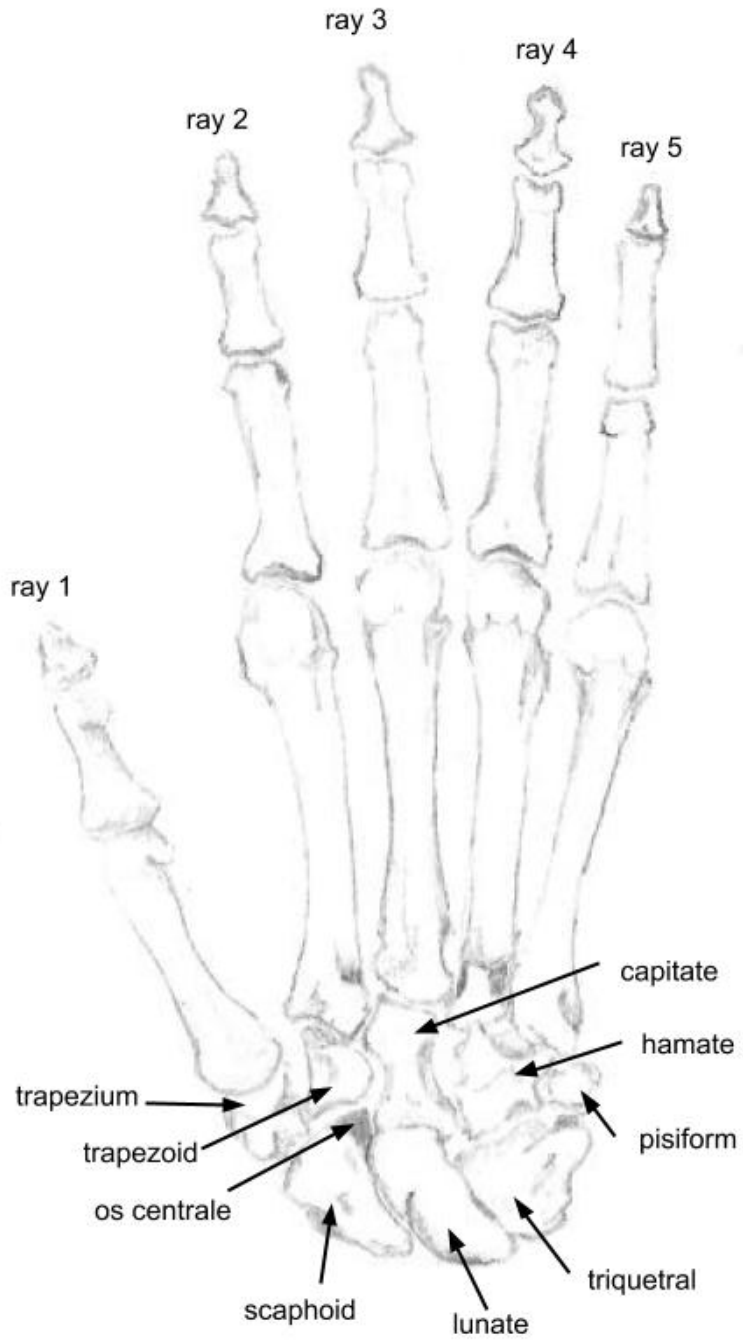

Figure 3.2
Palmar view of *Papio cynocephalus* left hand, drawn from Swindler and Wood (1973), with labelled rays and carpals.

Though the general cercopithecine pattern of manual morphology may be expected for *Theropithecus gelada*, relatively long thumbs and short second digits are frequently cited as unique traits that set geladas apart from other African monkeys (e.g, Jolly, 1970; Etter, 1973; Dunbar, 1983; Elton, 2006; Patel and Maiolino, 2016). In the following detailed examination of gelada manual skeletal morphology, this pattern of intrinsic hand proportions is expected. Any additional departures from the general cercopithecine pattern are expected in the first and second rays and may be related to precision manipulative activities. Broad similarities between geladas and baboons (*Papio* spp.) are expected across the carpals and metacarpals.

Carpals

Geladas have nine carpals: the os centrale, scaphoid, lunate, triquetral, and pisiform in the proximal row and the trapezium, trapezoid, capitate, and hamate in the distal row. In some other primate species (like many hominoids), the os centrale is fused with the scaphoid and there are only eight carpals.

Os centrale

The os centrale is a small carpal that nests largely within the distal surface curve of the scaphoid. It is sharply concave on the distal surface with a clear crescent shape. The distal surface is an articular facet for the capitate head and angles proximally on the ulnar side and tips in the palmar-ulnar direction. The proximal side is mainly an articular facet with the scaphoid, rounding convexly. The radial-most edge contains a small area that is not part of the articular facet. The radial side has a triangular articular facet on the palmar half which articulates with the trapezoid and part of the trapezium. The dorsal half is also roughly

triangular but does not contain any articular facets. Both dorsal and palmar aspects are triangles of non-articular bone. The dorsal face triangle is flat on the proximal edge with the most distal point on the ulnar side. The palmar face triangle is a rough tendon attachment site for the joint between the scaphoid and os centrale. The ulnar side is yet another small triangle and an articular surface for the lunate (Figure 3.3).

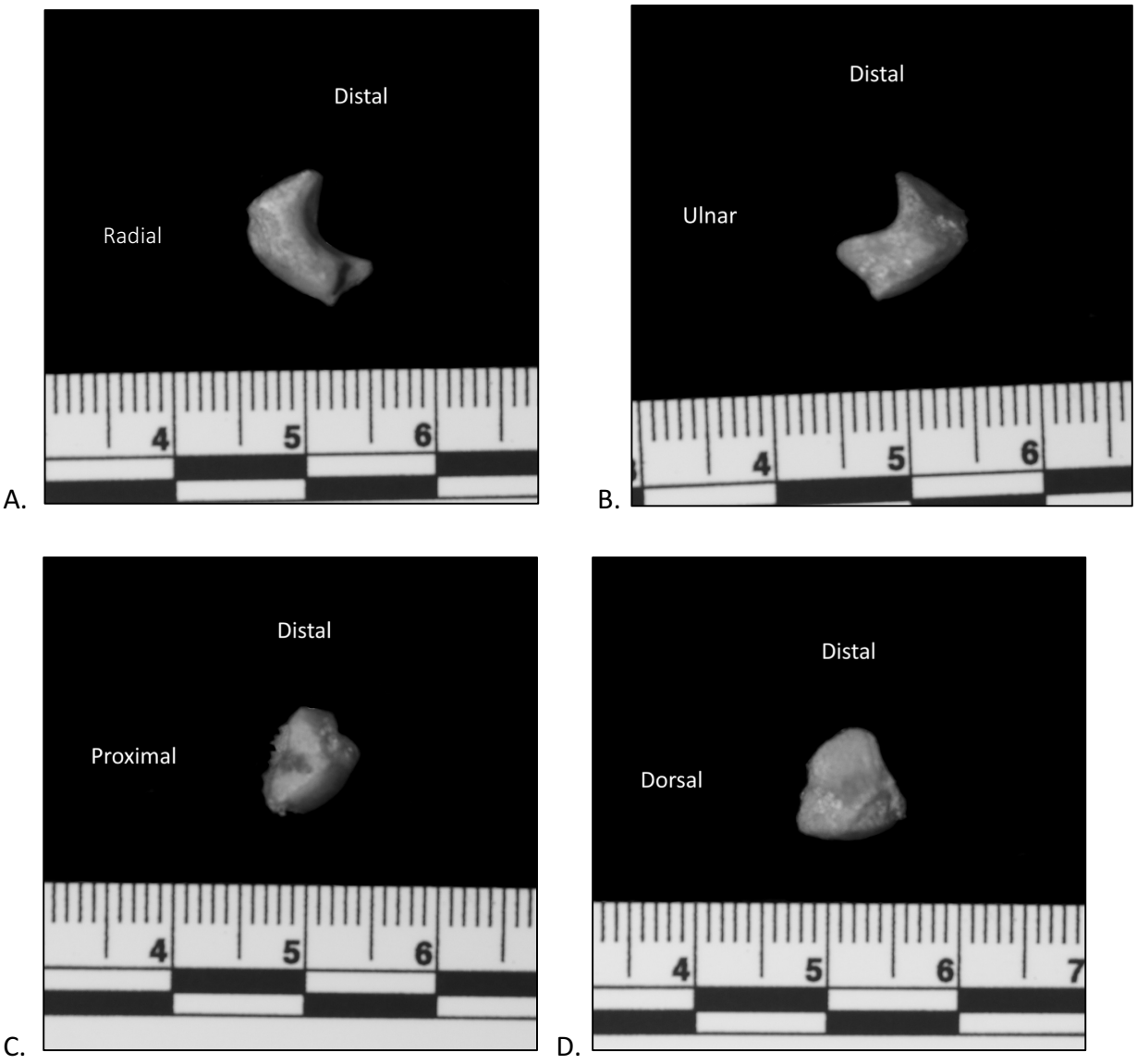

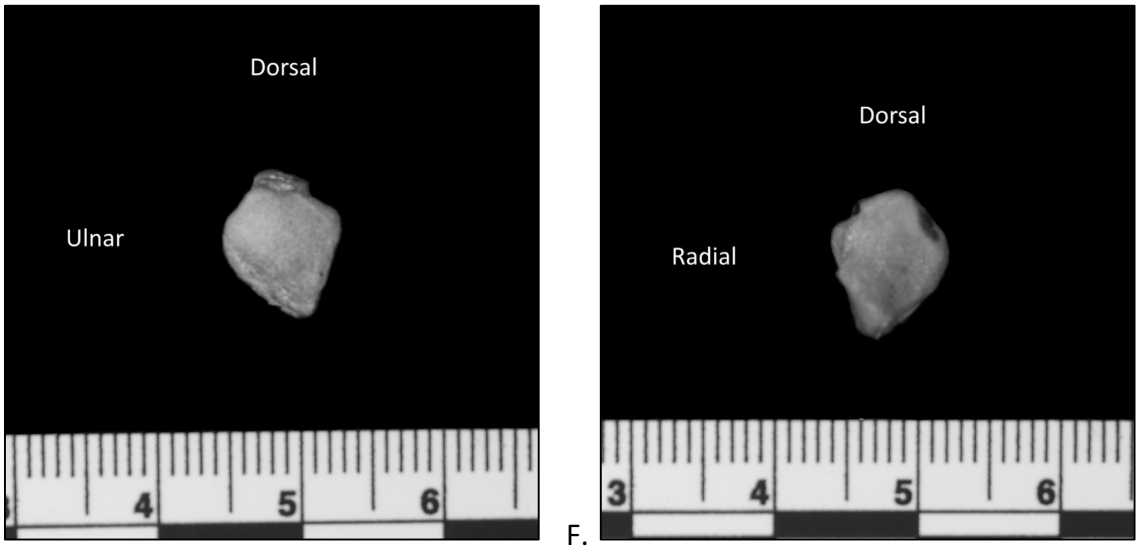

Figure 3.3
Left os centrale viewed from the standard anatomical aspects: palmar (A), dorsal (B), radial (C), ulnar (D), proximal (E), and distal (F). Scale is in centimeters (cm).

Scaphoid

The scaphoid is a distinct sickle-shaped carpal bone. It is radioulnarly broad in the dorsal direction and narrows palmarly. The dorsal portion is flattened proximodistally whereas the palmar side is tall. The proximal side contains a large articular facet for the distal radius. The radial side of the facet is slightly concave for the articulation with the styloid process of the radius. The ulnar-palmar surface of the facet is broad and convex. There is no ridge or groove distinguishing these two parts of the radial articular surface. The palmar-most portion of the distal side is non-articular and forms a small square, separated from the articular facets by a shallow groove through which the palmar radiocarpal ligament passes. Projecting from the radial side of the radial articular surface and perpendicular to the body of the scaphoid is a large tubercle. On the distal side is a large concave articular surface for the os centrale. It is large and circular on the dorsal portion and narrows as it continues palmarly toward the beak.

The tip of the beak projects distally with a small rectangular facet angled radially and proximally for the articulation with the trapezoid. The palmar surface of the beak is non-articular with a clear ridge running proximodistally (slightly diagonally) down the middle. On the ulnar aspect, there is a large triangular fossa connecting to the groove on the proximal surface. Running the length of the bone dorsopalmarly, there is a smooth articular facet. The dorsal and middle portion articulates with the lunate and the palmar section, curving distally, articulates with the head of the capitate. The lunate facet is a long, shallow S curve convex on the dorsal portion and concave at the middle (palmar extent of the lunate articulation). The dorsal aspect of the scaphoid body is thin and non-articular (Figure 3.4).

A. 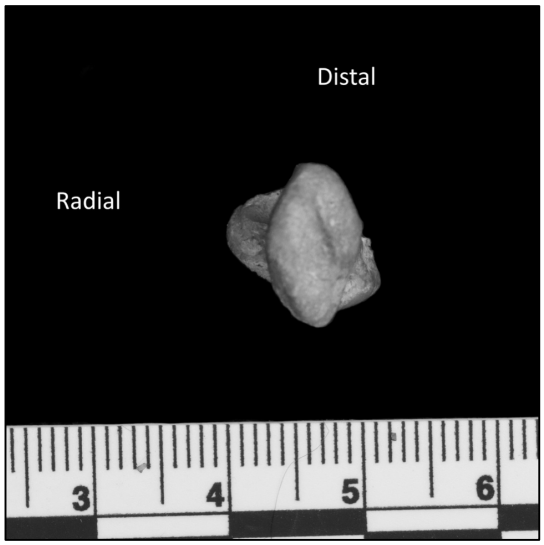

B. 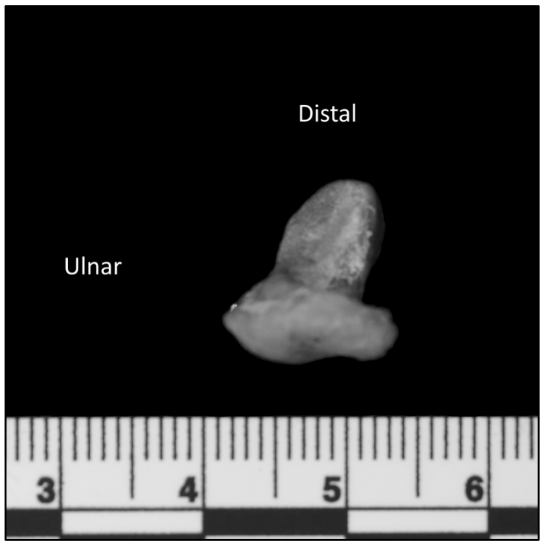

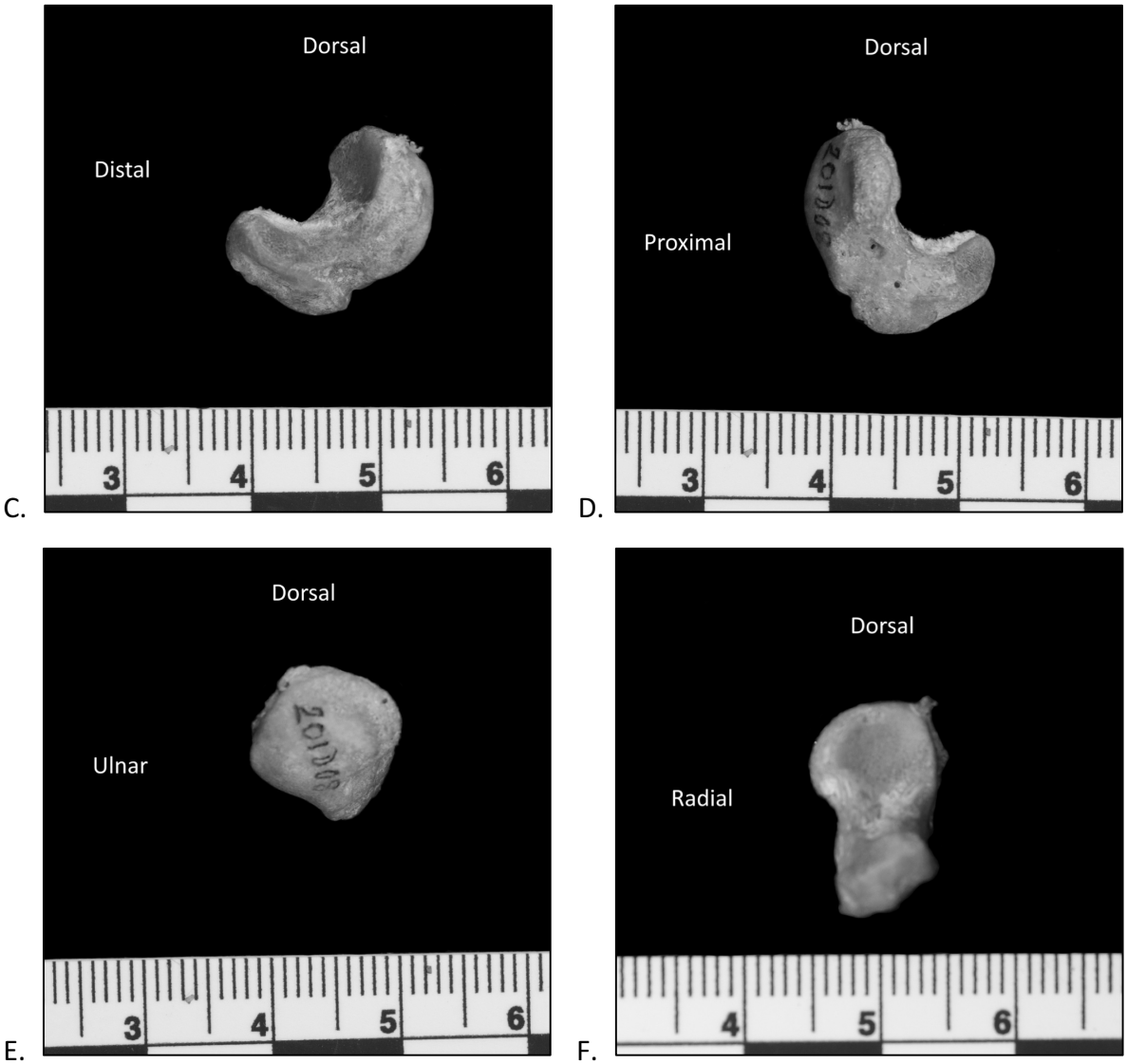

Figure 3.4
Left scaphoid viewed from the standard anatomical aspects: palmar (A), dorsal (B), radial (C), ulnar (D), proximal (E), and distal (F). Scale is in centimeters (cm).

Lunate

The lunate is mid-sized carpal with a cube-like shape with a clear crescent-shaped articular facet on the distal side. This distal articulation is with the capitate head and is concave dorsally and narrow in the radioulnar dimension. On the radial side, the palmar edge of this facet extends further radially than the dorsal edge. At the dorsal point, there is a point of non-

articular bone. The palmar side is a rectangular non-articular surface with few defining characteristics. It is tall proximodistally and narrow radioulnarly. Likewise, the dorsal aspect is non-articular but much narrower proximodistally and more triangular. The proximal face is smooth and rounded, forming the radial articulation. It is convex and proximodistally long, narrow radioulnarly on the palmar side and broadening in the radioulnar direction as it runs to the dorsal edge. This broader dorsal edge also bends distally along the radial edge. On the radial face of the lunate is a long smooth articular surface running the entire dorsopalmar length containing facets for the os centrale and the scaphoid. The palmar portion of the facet is convex while the dorsal portion is flatter on the proximal half with a small, oblong depression on the distal half. The small concavity is the facet for the os centrale and the remaining articular surface is for the scaphoid-lunate connection. The proximal surface curves distally to meet the scaphoid facet on the dorsal part of the radial side. The proximal half of the palmar side of the radial face is non-articular. The ulnar aspect features a rectangular articular facet for the triquetral running proximodistally down the dorsopalmar middle. This facet is smooth, flat, and narrow dorsopalmarly. Proximal to the facet is a thin strip of non-articular bone with a rounded point proximally where it meets the proximal-radial extreme of the proximal face. Dorsal to the facet is a strip of non-articular bone. Palmar to the facet is non-articular bone and a small fossa at the proximal extreme (Figure 3.5).

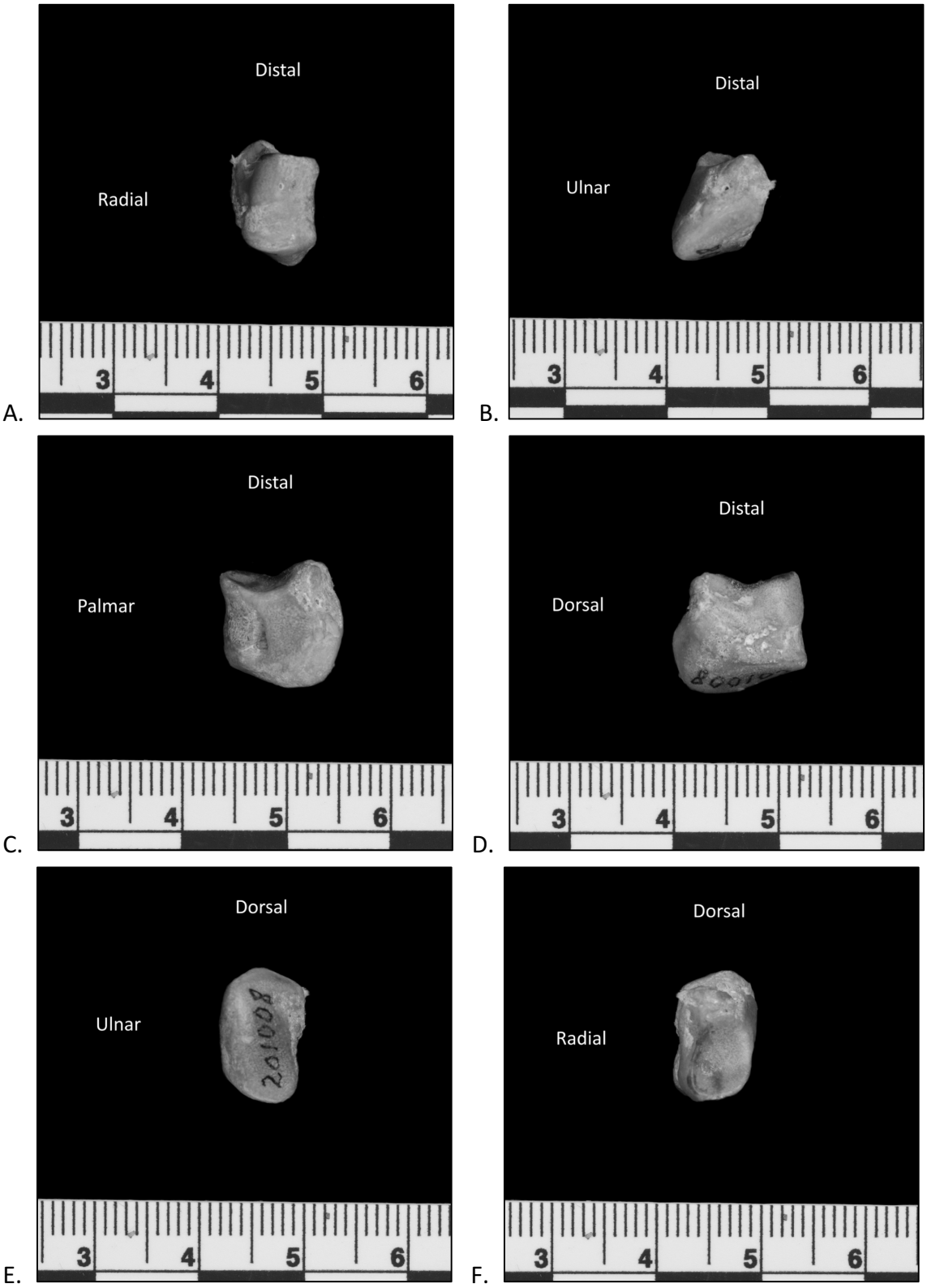

Figure 3.5
Left lunate viewed from the standard anatomical aspects: palmar (A), dorsal (B), radial (C), ulnar (D), proximal (E), and distal (F). Scale is in centimeters (cm).

Triquetral

The triquetral is a relatively large ovoid carpal. The distal surface has a large rectangular facet for the hamate. It is long in the dorsopalmar direction and narrow in the radioulnar dimension. The facet has a twist - the palmar-radial corner is pushed distally and the palmar-ulnar corner is pushed proximally whereas the dorsal-radial corner quite flat and the dorsal-ulnar corner is pushed distally. The surrounding bone on the distal surface is non-articular, bordering the facet along the palmar side. Proximal and radial to the hamate facet is the smaller, flat facet for the lunate. Proximal to the lunate facet and running the length of the radial side is a rounded ridge of non-articular bone. This ridge extends to the palmar side and creates a softly curved tip to the egg-shaped triquetral. On the proximal surface, there is a rectangular, slightly concave facet for the pisiform. It runs most of the dorsopalmar length of the proximal surface with a curved portion of non-articular bone at the palmar end. The pisiform articulation is defined on the ulnar side by a clear ridge. The dorsal end of this ridge comes to a small point. Ulnar to this ridge is the large, concave facet for the styloid process of the ulna. At the ulnar-dorsal extreme of this facet is a rounded point projecting slightly in the proximal direction. The ulnar face of the triquetral is non-articular bone that is compressed proximodistally on the palmar side and tall proximodistally on the dorsal side (Figure 3.6).

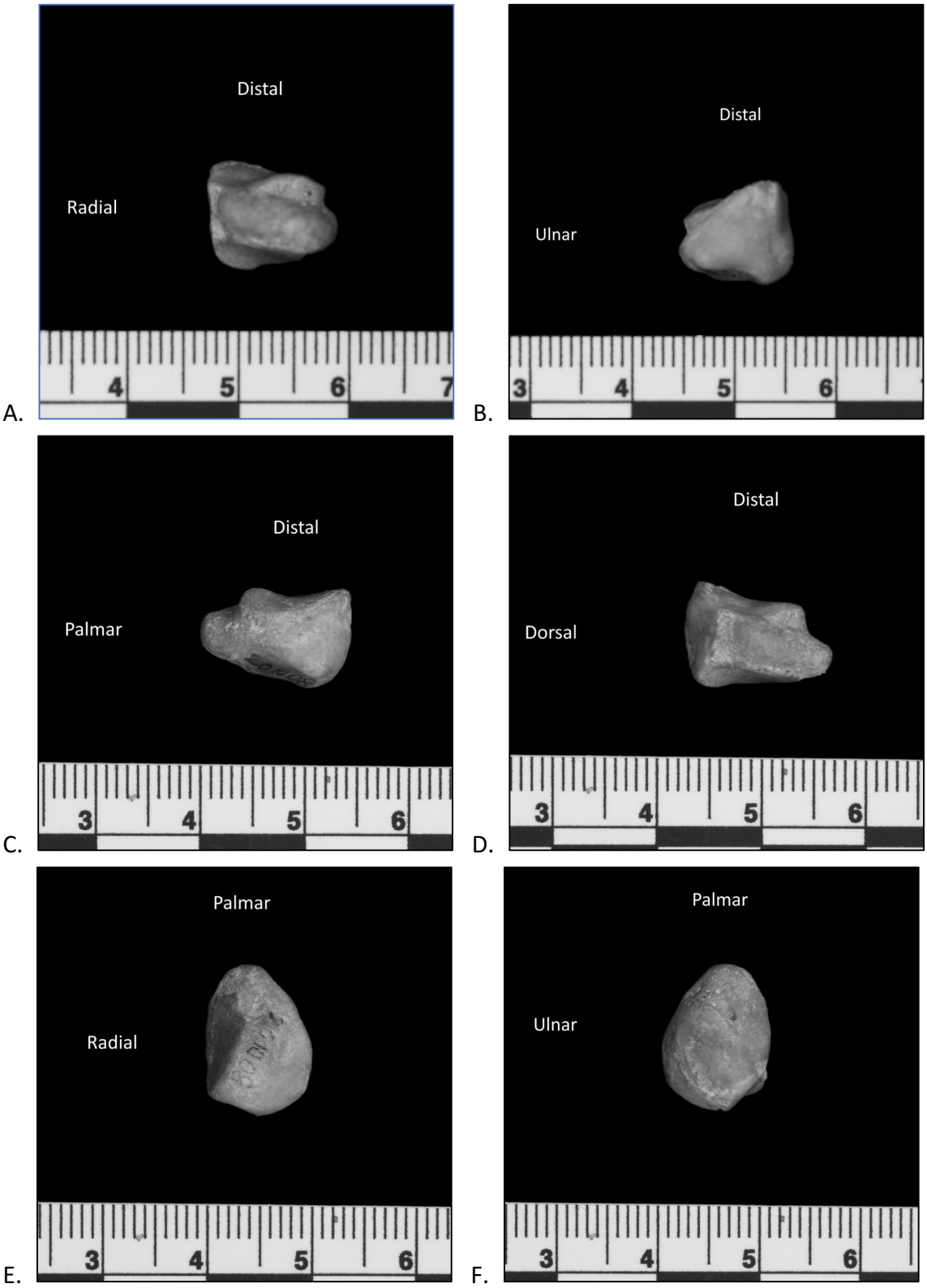

Figure 3.6
Left triquetral viewed from the standard anatomical aspects: palmar (A), dorsal (B), radial (C), ulnar (D), proximal (E), and distal (F). Scale is in centimeters (cm).

Pisiform

The pisiform is a relatively cylindrical carpal with flattened dorsal end. The shaft of the pisiform is narrow compared to the palmar and dorsal ends. On the proximal portion at the dorsal end is the articulation with the triquetral and styloid process of the ulna. This is a slightly convex rectangular facet that is longer radioulnarly than dorsopalmarly. There is no clear distinction on the facet for the articulation with these two bones like a ridge or depression. The dorsal end of the bone is flattened to nearly straight line running radioulnarly. When viewed from the proximal or distal aspect, if flares ulnarly and radially from the shaft. The palmar end of the bone is egg-shaped with the smaller point positioned distally. There is a small sulcus running radioulnarly across the palmar surface of the ovoid portion that approximately bisects the surface. From the ulnar or radial view, the bone is shallowly concave from the distal end (the dorsal and palmar extremes extend further distally than the midpoint of the shaft) (Figure 3.7).

A. 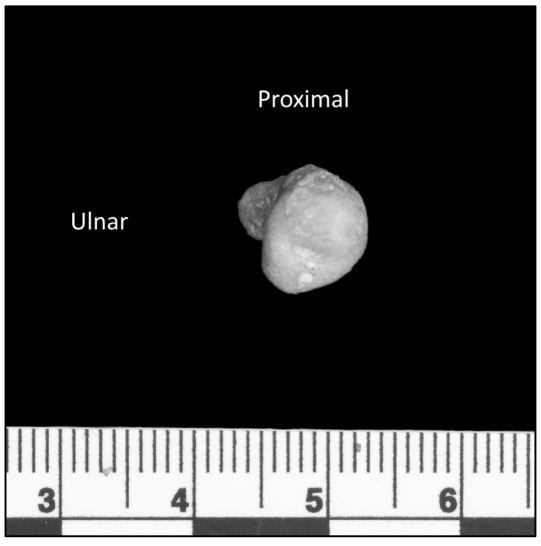

B. 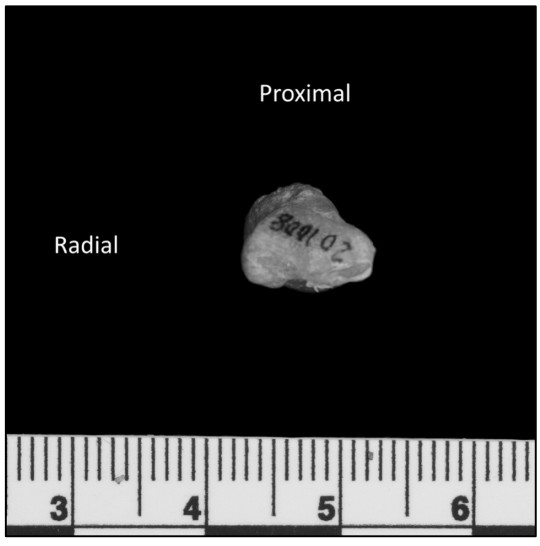

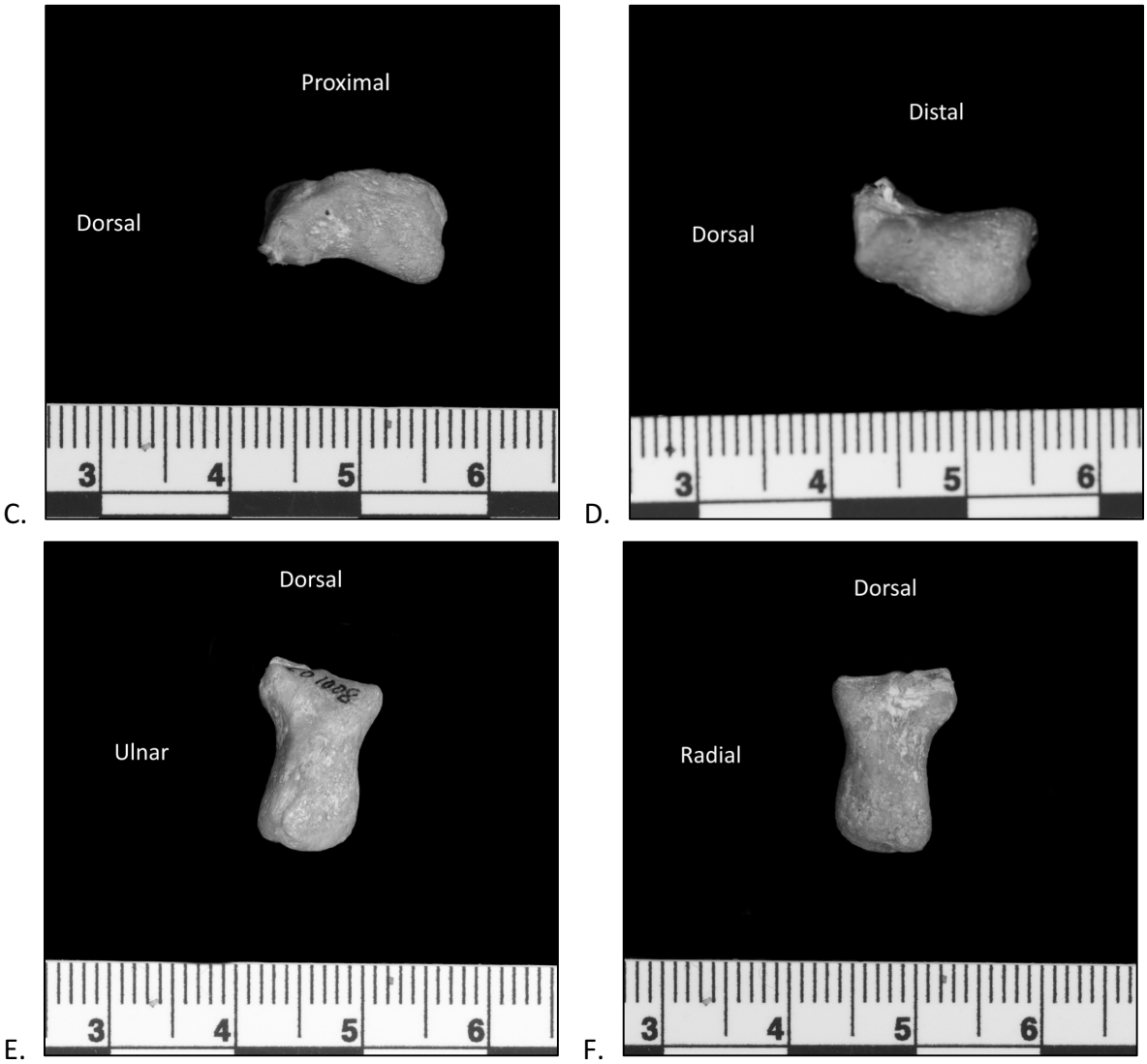

Figure 3.7
Left pisiform viewed from the standard anatomical aspects: palmar (A), dorsal (B), radial (C), ulnar (D), proximal (E), and distal (F). Scale is in centimeters (cm).

Trapezium

The trapezium is located on the radial and distal sides of the wrist, proximal to the Mc1. It is a relatively small bone in the carpal complex. There is a sellar articular surface for the Mc1 joint on the distal surface. It is convex radioulnarly and concave dorsopalmarly (though this line is angled from the ulnar toward the dorsal side to radial on the palmar side) on the distal face.

The palmar aspect of the trapezium has a small rounded tubercle that extends toward the ulnar and palmar directions. On the ulnar side, there are two articular facets. The palmar one is larger and roughly square, articulating with the trapezoid. The smaller, oblong facet is on the dorsal half of the ulnar aspect and articulates with both the trapezoid and the Mc2. There is a very small ridge that approximately bisects the smaller facet with the Mc2 articulation on the distal side and the trapezoid articulation on the proximal side. There is a groove distal to the Mc2 facet that runs from the dorsal edge of the ulnar surface palmarly to the edge of the Mc2 facet at its palmar extreme. The proximal surface is almost entirely a roughly triangular articular facet for the scaphoid and os centrale. The scaphoid tubercle articulates radially and the os centrale articulates degree ulnarly. There is no clear distinction between these two facets on the proximal surface of the trapezium in geladas. Contrary to some fossil specimens (see Guthrie, 2011) half or less of this surface articulates with the os centrale. The dorsal surface contains no articulations and is rough. This specimen lacks the pronounced tubercle on the dorsal surface that characterizes *Theropithecus brumpti* and some *Papio* individuals (Guthrie, 2011). The dorsal surface does have two rounded tubercles on the distal half, one radial and one ulnar. There is also a low ridge running along the proximal edge of the dorsal surface (Figure 3.8).

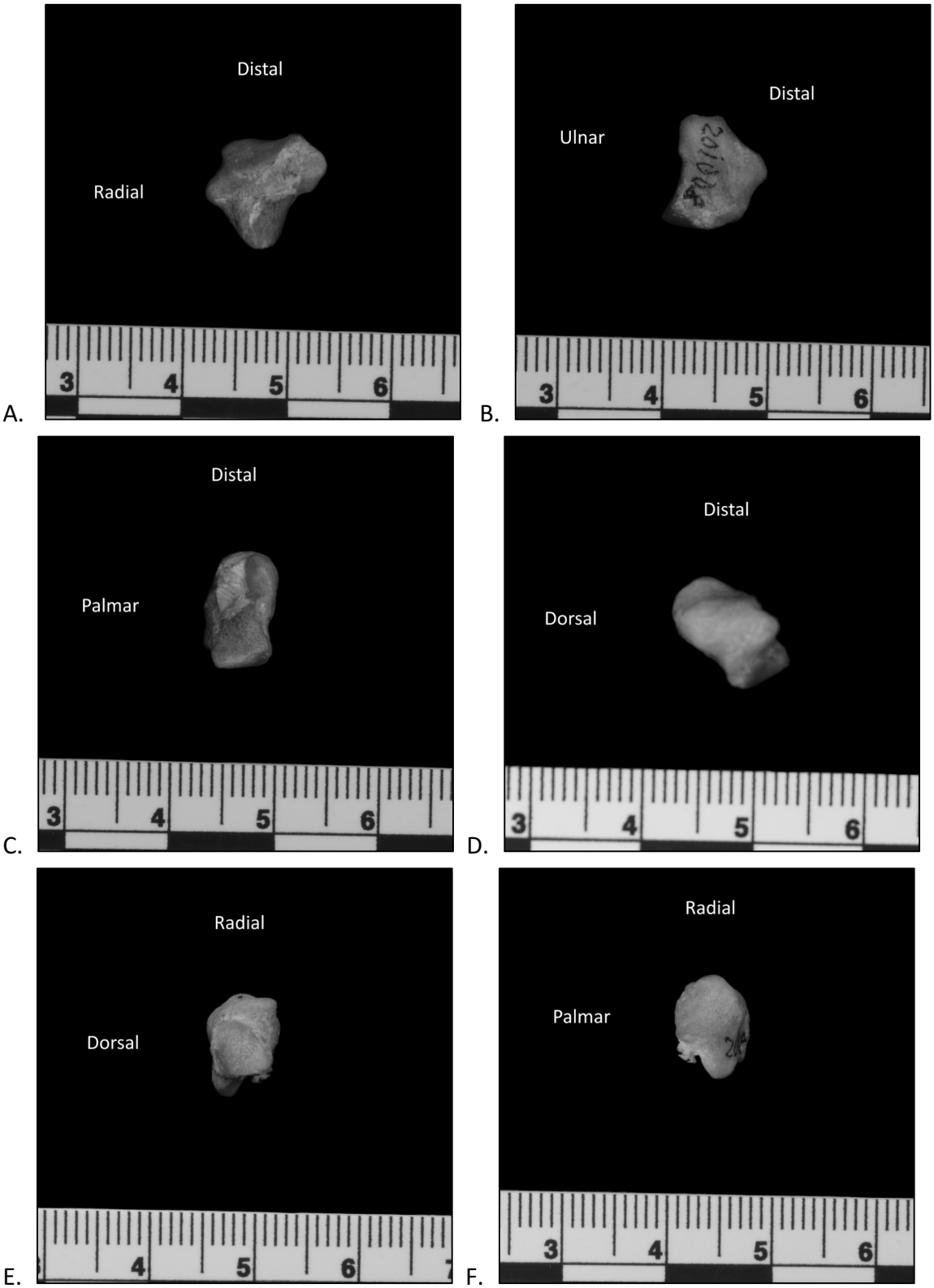

Figure 3.8
Left trapezium viewed from the standard anatomical aspects: palmar (A), dorsal (B), radial (C), ulnar (D), proximal (E), and distal (F). Scale is in centimeters (cm).

Trapezoid

The trapezoid is another small carpal bone located ulnar to the trapezium. Viewed from the dorsal aspect, the shape is pentagonal with the distal edges making up three sides of approximately equal length. The ulnar and radial edges are approximately equal and double the length of the other three sides. The ulnar and radial edges come together and form a point at the proximal extreme of the dorsal surface. This extended pentagonal surface looks much like a cartoon gem. The dorsal surface curves toward the palmar side proximally (the proximal point is more palmar than the distal point). The palmar edge is formed by the union of articular facets on the proximal and radial surfaces and a non-articular surface on the ulnar side. On the radial side, the trapezium articulates via a rhomboidal facet placed palmarly with a thin strip along the distal edge that extends to the dorsal edge. The radial side angles ulnarly from the distal to proximal sides (the distal edge is more radial than the proximal edge). The small remaining portion of the radial side is non-articular. The ulnar side is approximately triangular and provides the articular facet for the capitate. There is a small strip on the distal edge running from the palmar side to just beyond the midpoint dorsopalmarly that is non-articular. The ulnar face angles radially from distal to proximal (the opposite of the radial side). The proximal edge is a point rather than a face. The distal face is the articular surface for the Mc2-trapezoid joint. It is approximately triangular with the triangle base along the dorsal edge. There is a ridge that runs down the middle from dorsal to palmar bisecting the facet. The radial half slopes proximally as it extends to the radial extreme. Likewise, the ulnar half slopes proximally as it extends to the ulnar extreme. The face is also curved in the dorsopalmar dimension, with the dorsal edge and palmar point lying further distal than the midpoint of the face (Figure 3.9).

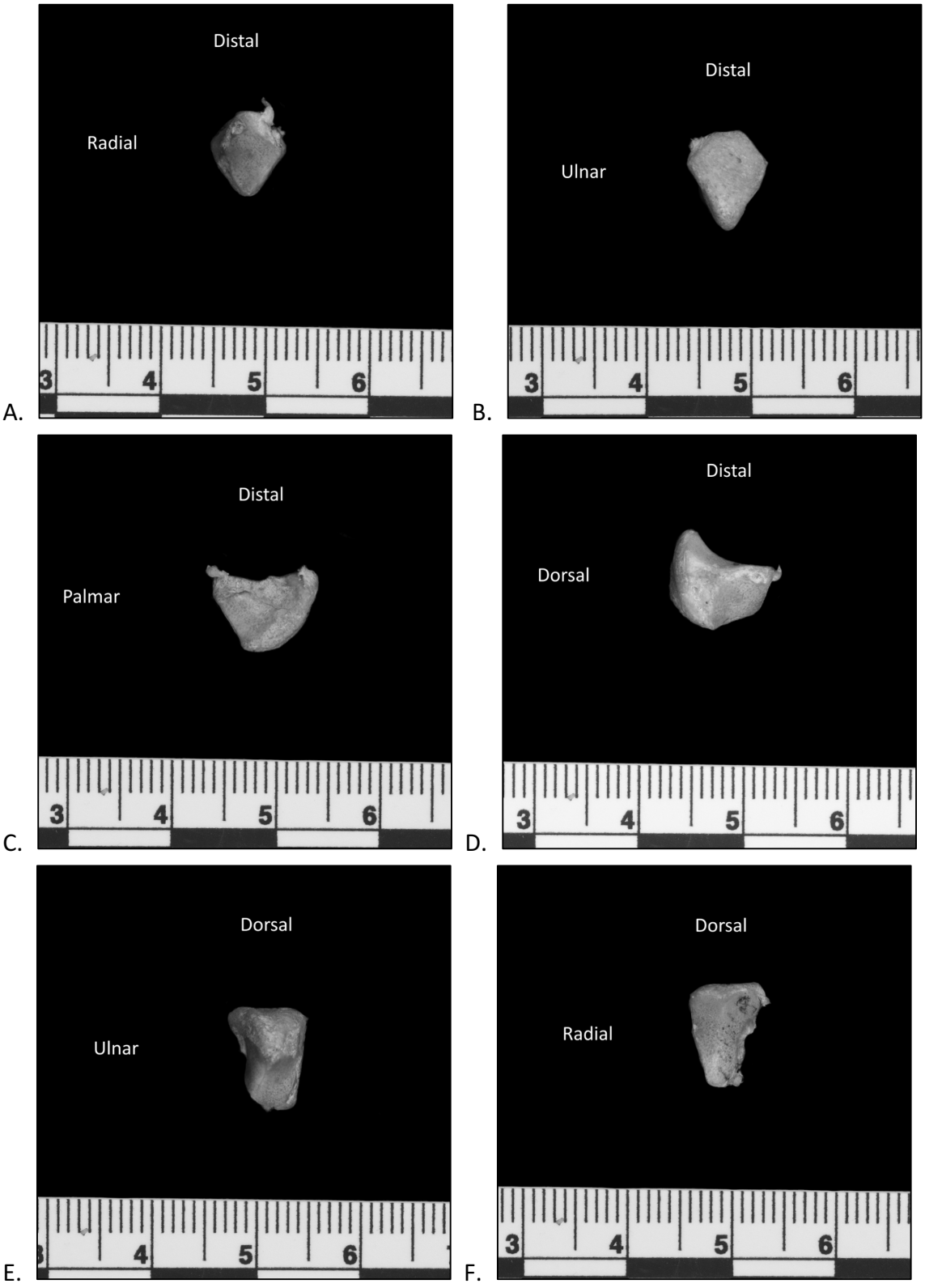

Figure 3.9
Left trapeziod viewed from the standard anatomical aspects: palmar (A), dorsal (B), radial (C), ulnar (D), proximal (E), and distal (F). Scale is in centimeters (cm).

Capitate

The capitate is one of the larger bones in the wrist with a distinctive, proximally projecting head. On the palmar surface, there is a non-articular surface that projects palmarly below which is a groove defining the head of the capitate proximally. The head articulates with the os centrale, scaphoid, lunate, and hamate. The large distal surface is deeply concave with sharp distally projecting dorsal and palmar edges. The surface serves primarily as the articulation for the base of Mc3. A small portion of the radial-most edge of the base of Mc4 articulates with the ulnar edge of the distal face of the capitate. There is a small semicircular notch at the approximate midpoint of the ulnar edge of the distal face. On the ulnar face, two articular facets are present. The very small oval facet at the distal-palmar corner of the ulnar face articulates with the Mc4. The long articular facet running the length of the face from proximal to distal provides the articular surface for the hamate and is positioned with one edge at the dorsal extreme and the palmar edge at the approximate middle dorsopalmarly. This facet is rounded at the proximal extension and has uneven edges running the remaining length. The hamate articular facet is concave with the proximal and distal edges projecting more ulnarly than the midpoint. Additionally, there is a deep groove separating the two facets and making up the rest of the face. The proximal side of the capitate head is the articulation with the lunate. The capitate head is rounded with a slight elongation on the radial-palmar and ulnar-dorsal diagonal. On the radial side, four bones articulate with the capitate. There are two facets (one on the palmar half, one on the dorsal half) for the Mc2 articulation. The palmar facet is round and the dorsal is crescent-shaped, concave on the distal edge. Immediately proximal to the dorsal Mc2 facet is a small triangular facet for the trapezoid. A subtle ridge separates these

two facets. The bulk of the capitate head on the radial side articulates with the os centrale. This facet wraps around to the dorsal side of the capitate as well, allowing the os centrale to cup the distal portion of the capitate head. The proximal and palmar edge of the capitate head on the radial aspect articulates with the scaphoid, though the distinction between the os central and scaphoid facets is not well-defined. There is a deep groove and large depression proximal to the Mc2 facets and separating the capitate head from the rest of the bone in a line running from the midpoint dorsopalmarly to the palmar edge. On the dorsal aspect, the capitate head slopes in the palmar direction. The head articulates with the lunate proximally and os centrale distally on the dorsal face. Distally, there is an irregular rectangle of non-articular, rough bone (Figure 3.10).

A. 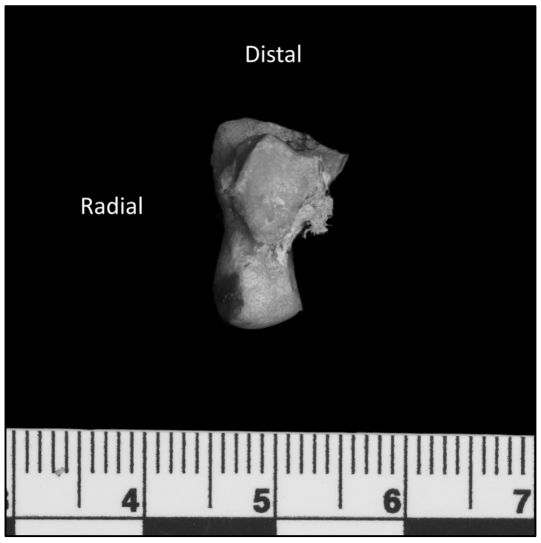

B. 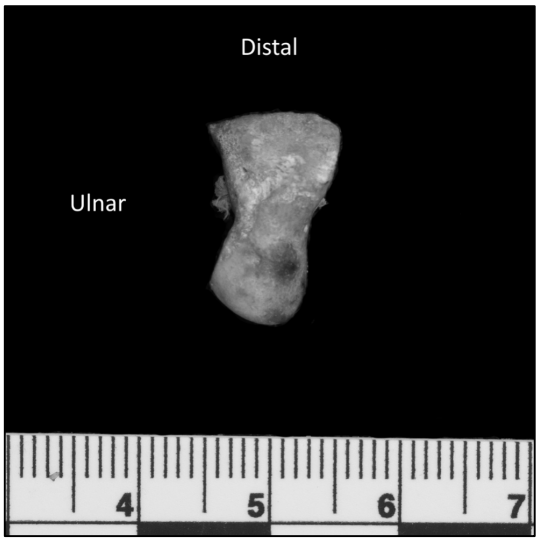

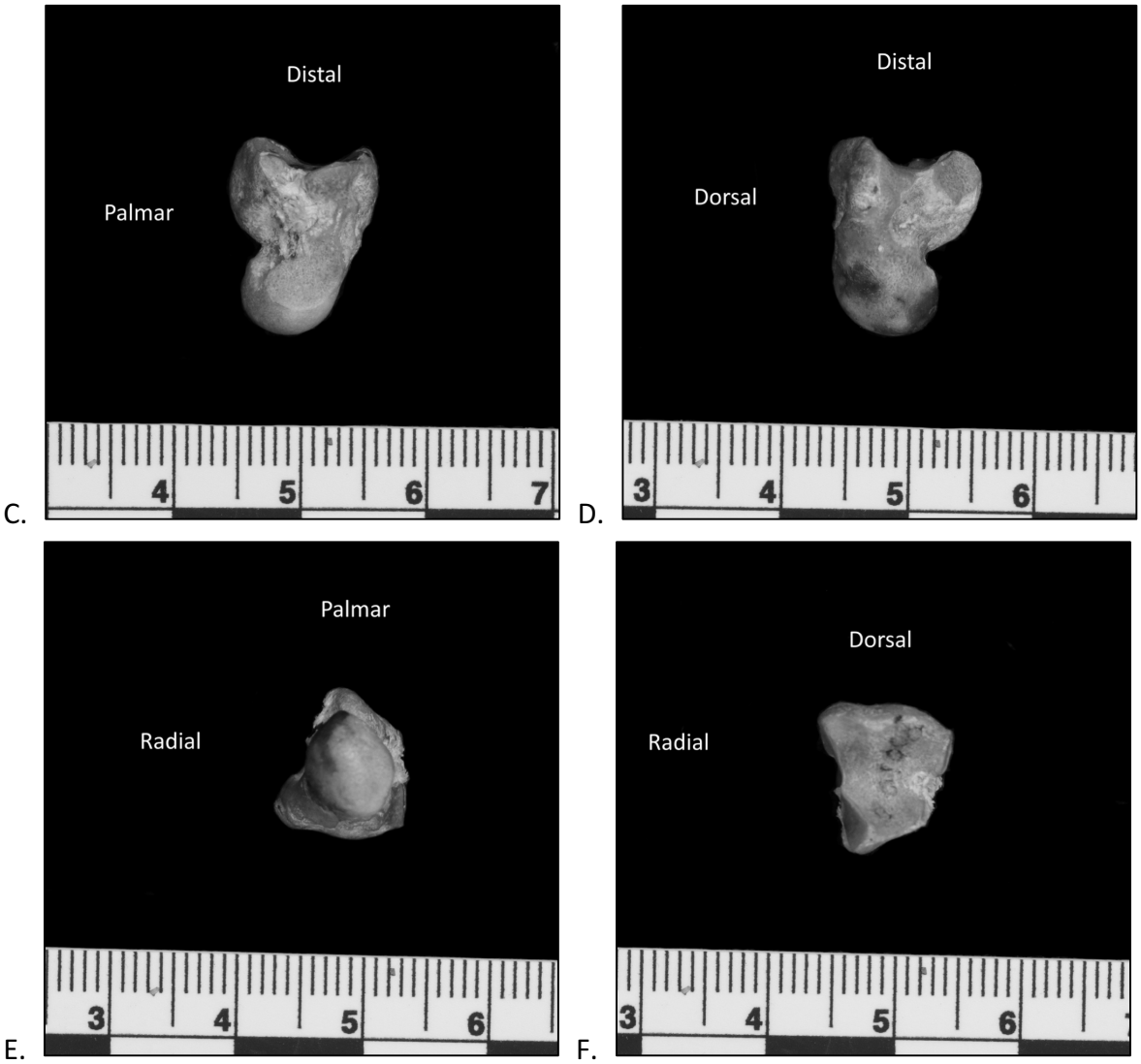

Figure 3.10
Left capitate viewed from the standard anatomical aspects: palmar (A), dorsal (B), radial (C), ulnar (D), proximal (E), and distal (F). Scale is in centimeters (cm).

Hamate

The hamate is a large carpal bone with a distinct hamulus projecting palmarly from the ulnar side of the palmar face. The dorsal side is non-articular and irregular in shape. The radial side forms a “J” when viewed from the dorsal aspect. The distal edge is gently concave with the radial and ulnar corners projecting further distally than the midpoint. The proximal edge is

longest and runs diagonally from the ulnar edge of the “J”” to the ulnar extreme of the face. From this ulnar extreme, the ulnar edge is rounded and connects the proximal and distal edges. The palmar face is also irregular and non-articular, however there are some soft tissue articulations visible. Notably, the hamulus is on the proximal-ulnar portion of the palmar face, hooking radially. On the ulnar face, there is a long, rectangular articular facet for the triquetral. This facet slopes from the distal edge of the ulnar face to the proximal extreme. It is also twisted with the proximal-palmar corner pushing ulnarly and the proximal-dorsal corner pushing radially. This pattern is also seen on the distal half of this facet (distal-palmar corner pushing radially and the distal-dorsal corner pushing ulnarly). The remaining portion of the ulnar face contains a large, deep fossa just palmar to the distal end of the articular facet. The radial side contains the articular facet for the capitate, running proximodistally along the dorsal edge and expanding at the proximal and distal edges in the palmar direction. The middle portion, proximodistally, of the radial face contains a deep fossa for soft tissue attachment. On the proximal surface, there is a small ridge of non-articular bone that runs between the proximal edges of the articular facets for the triquetral on the ulnar side and the lunate on the radial side. The distal face is divided into two articular facets in addition to some non-articular surface, including the hamulus. The radial half of the distal face has the articular facet for the Mc4 and a thin strip of non-articular bone on the dorsal edge. Separated by a small ridge from the Mc4 articular facet is the small, rectangular Mc5 articular facet on the ulnar side. This facet is bordered on the palmar aspect by the hamulus and by a small triangle of non-articular surface on the dorsal edge. Both facets are concave with the furthest distal extreme at the

dorsal edge where both facets meet and the hamulus on the palmar side – both are equally distal (Figure 3.11).

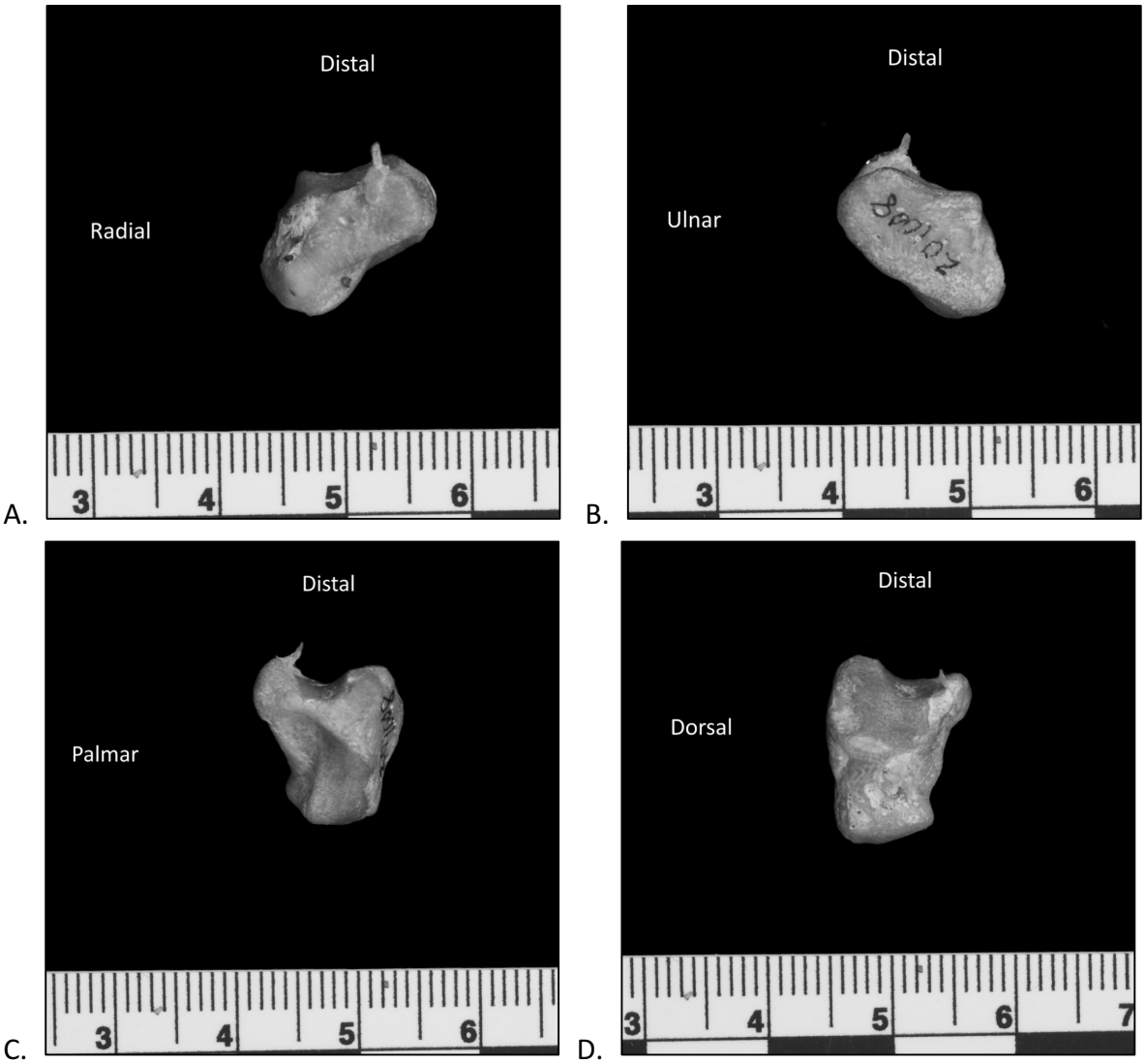

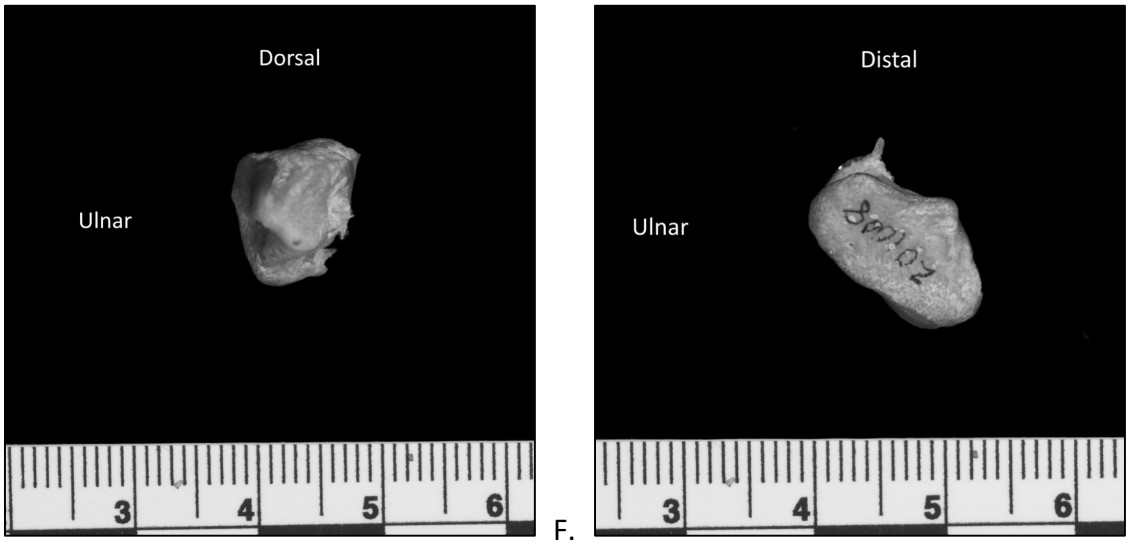

Figure 3.11
Left hamate viewed from the standard anatomical aspects: palmar (A), dorsal (B), radial (C), ulnar (D), proximal (E), and distal (F). Scale is in centimeters (cm).

Metacarpals

All the metacarpals are relatively straight in the dorsal-palmar direction, showing no clear curvature along the dorsal surface. Mc1 is relatively long in *Theropithecus* compared to other cercopithecoids. This is often linked to their unique feeding ecology in which they manipulate small grasses and seeds between their thumb and forefinger (manual grazing) (Dunbar, 1983). Interestingly, Mc2 does not show any associated modifications in length. Among other primates, *Theropithecus gelada* has relatively short and narrow metacarpals. This trait might be linked to digitigrade hand posture during terrestrial quadrupedal locomotion (Patel, 2010) as it is also present in *Papio* and *Mandrillus*.

Metacarpal 1

The metacarpal of ray 1 is very straight and thin with a largely cylindrical diaphysis. The metacarpal base flares radioulnarly to a greater degree than the head. Furthermore, the base

flares more on the radial side and extends further proximally than on the ulnar side. The ulnar side exhibits a tiny, shallow, convex facet for the articulation with the trapezium. Viewed in the radioulnar aspect, the dorsal surface is very straight with only the slightest expansion dorsally at the metacarpal head. The palmar surface exhibits minimal concave curvature. The curve is smooth from just proximal to the metacarpal head and extending to the proximal end, but the metacarpal head sharply projects in the palmar direction. The metacarpal head is rounded and slightly compressed radioulnarly. On the metacarpal of ray 1, the head narrows dorsally and the maximum radioulnar breadth on the dorsal aspect of the metacarpal head is less than half of the radioulnar breadth on the palmar aspect. There are two very shallow sesamoid gutters splitting the palmar edge into three blunt points. Viewed from the distal end, this gives the typical metacarpal head appearance of a tulip with three petals, possessing a rounded and tapered dorsal side and a wider and squarer palmar side. The Additionally, the palmar portion of head is offset radially from the shaft. Just proximal to the head, there is a small epicondyle on the ulnar and radial sides for the attachment of the collateral ligament of the metacarpophalangeal joint. The base is saddle-shaped where it articulates with the trapezium, though shallow. It is rounded on the palmar and radial side and flattened on the dorsal side (Figure 3.12).

A.


Radial
Proximal
2
3
4
5
6
7

B.


Radial
Proximal
2
3
4
5
6
7

C.


Palmar
Proximal
2
3
4
5
6
7

D.

E.

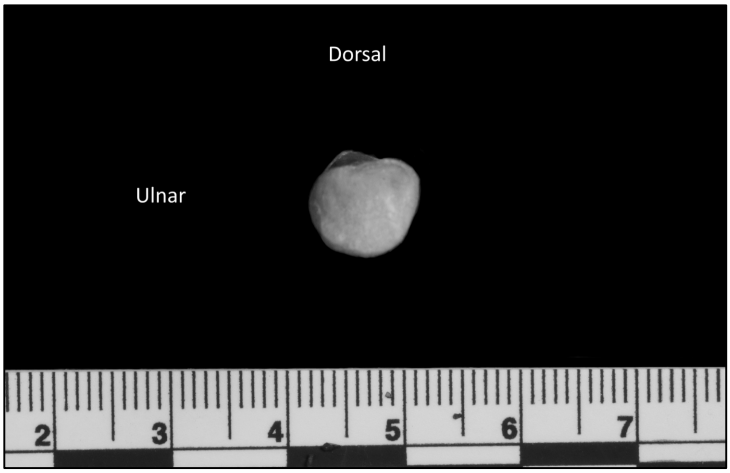

F.

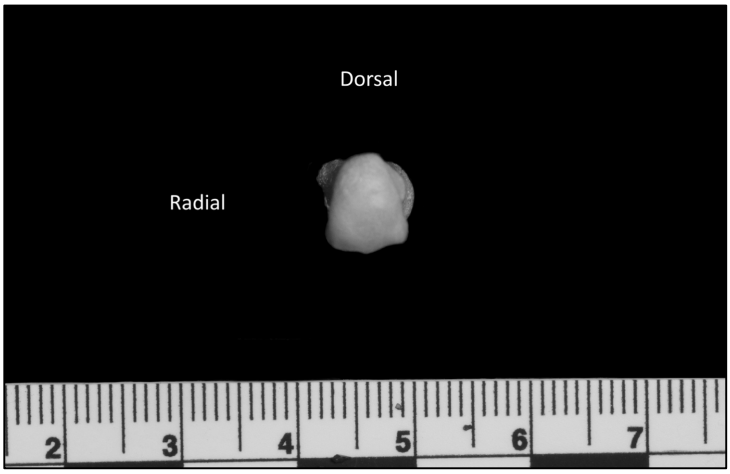

Figure 3.12

Left metacarpal 1 viewed from the standard anatomical aspects: palmar (A), dorsal (B), radial (C), ulnar (D), proximal (E), and distal (F). Scale is in centimeters (cm).

Metacarpal 2

The metacarpal of the second ray is also quite thin and straight in the dorsopalmar direction. The diaphysis is relatively cylindrical with some flattening on the dorsal side and very slight ridging down the middle of the diaphysis creating an almost triangular shape in cross-section. This ridging is more pronounced toward the proximal end of the shaft and is an attachment site for the interosseous muscles. There is a subtle curvature in the radioulnar direction that is concave from the radial side (head and base are more radial than the midshaft). There are small epicondyles just below the metacarpal head, one on the radial side and one on the ulnar side for the attachment of the collateral ligaments of the metacarpophalangeal joint. The metacarpal head is rounded and slightly compressed radioulnarly. The head narrows dorsally as in Mc1. The angles at which the radial and ulnar sides narrow are uneven. The radial side narrows more drastically, creating a more acute angle than on the ulnar side. The gutters in which the sesamoids sit are deeper than in Mc1. The base of Mc2 exhibits perhaps the most complex morphology of all the metacarpal bases. The Mc2 articulates with the trapezium at a small oblong facet on the dorsal portion of the radial side of the base of the bone. The large triangular facet on the proximal surface articulates with the trapezoid. The facet is much like an isosceles triangle with small semicircular notches at the midpoint of each side of the triangle. One of the two longer sides of the triangle extends dorsopalmarly with the dorsal end in line with the midpoint of the diaphysis and the palmar end angled ulnarly. There is an indent that approximately bisects the facet, extending from the middle of the dorsal edge to just palmar to the midpoint of the radial edge. This creates a blade-like projection extending proximally, the extreme of which is the ulnar edge of the trapezoid articulation triangle. The ulnar side of this

blade-like projection is two separate facets. On the palmar half of the ulnar aspect, there is a flat, round facet for the articulation with the capitate. There is a second articular facet for the capitate on the dorsal half of the ulnar aspect. This is a larger facet that contains a very small and subtle ridge differentiating the articulation with the capitate proximally and the Mc3 distally. There is a fossa on the dorsal side of the base, just above the semicircular notch that is in the center of the dorsal edge of the triangle that forms the proximal face (Figure 3.13).

A.

B.

C.


Palmar
Proximal
TRIC 1
2
3
4
5
6
7

D.


Dorsal
Proximal
IC 1
2
3
4
5
6
7

E.

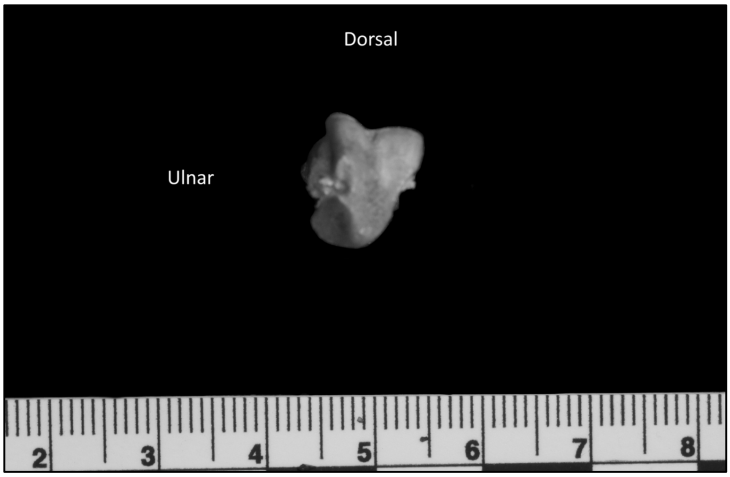
Dorsal
Ulnar
2
3
4
5
6
7
8

F. 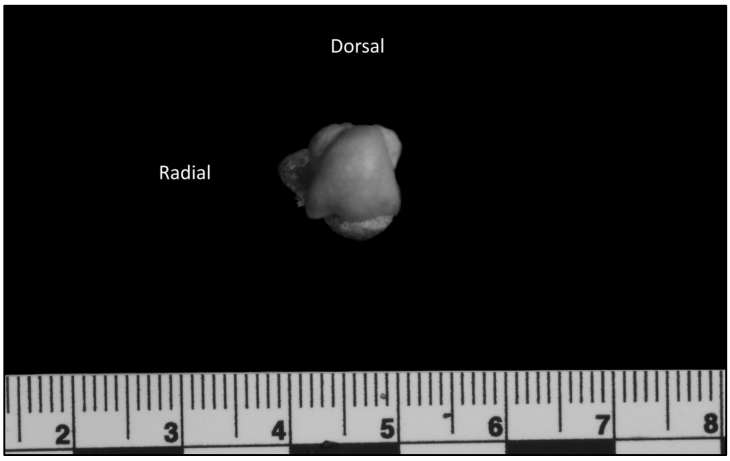

Figure 3.13
Left metacarpal 2 viewed from the standard anatomical aspects: palmar (A), dorsal (B), radial (C), ulnar (D), proximal (E), and distal (F). Scale is in centimeters (cm).

Metacarpal 3

The third metacarpal is only very slightly shorter than the Mc2. It is also broader than all the other metacarpals in the radioulnar direction, showing the greatest robusticity. The shaft is very flat on the dorsal side with slight curvature on the palmar side (similar in degree to that of Mc1 without the sharp distinction between shaft and metacarpal head). The diaphysis is flattened dorsopalmarly and is less cylindrical than Mc1, Mc2, and Mc4. There is very minimal flaring in the radioulnar direction at the base. Two epicondyles (one on the radial and one on the ulnar side) serve as attachments for the collateral ligaments of the metacarpophalangeal joint just proximal to the metacarpal head. The metacarpal head is rounded and only slightly narrowed. Unlike in Mc1, Mc2, and Mc5, the head of Mc3 has parallel ulnar and radial sides. The palmar edge exhibits two rounded gutters in which the sesamoids lie. The metacarpal head is flatter than the Mc1, Mc2, and Mc5 though still rounded. The radial side of the metacarpal articular surface with the proximal phalanx flattens slightly as it approaches the radial edge. This is most

apparent when viewed from the dorsal or palmar aspect. The base of Mc3 contains articular surfaces for the Mc2, Mc4, and capitate. The Mc2 articulates with the Mc3 at the small, oblong facet on the radial side of the Mc3 base. This facet is on the dorsal half of the radial side, running roughly perpendicular to the dorsal edge. The entirety of the proximal face is an articular facet with the capitate. It is approximately triangular, nearly equilateral in shape. The face is convex to the proximal direction, extending proximal to the greatest extent on the ulnar side. The palmar tip of the triangular facet curves toward the palmar surface and toward the ulnar side. The ulnar and dorsal edges of the triangle are approximately bisected by semicircular notches. On the dorsal side of the bone, there is a small circular fossa just above the semicircular notch bisecting the dorsal edge of the proximal articular facet. The dorsal edge of the triangle also extends distally to a similar degree that the palmar tip extends toward the palmar surface. At the most proximal end of the ulnar side, there are two facets for the articulation with the Mc4. The palmar facet is very small and triangular. The dorsal facet is much larger and nearly diamond-shaped. The dorsal facet is angled radially, causing the facet to face both the palmar and, to a greater extent, the ulnar aspects (Figure 3.14).

A.

B.


Ulnar
Proximal
20/008
RIC 1
2
3
4
5
6
7

C.


Palmar
Proximal
C 1
2
3
4
5
6
7

D.


Dorsal
Proximal
1
2
3
4
5
6
7

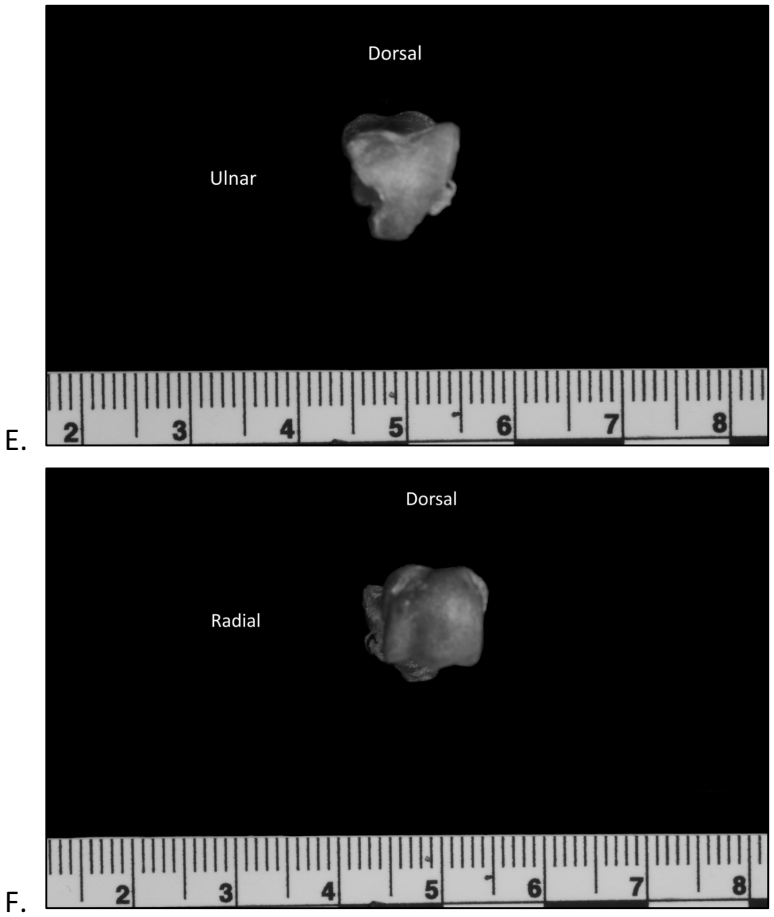

Figure 3.14
Left metacarpal 3 viewed from the standard anatomical aspects: palmar (A), dorsal (B), radial (C), ulnar (D), proximal (E), and distal (F). Scale is in centimeters (cm).

Metacarpal 4

The fourth metacarpal is also thin and very straight on the dorsal aspect. There is some very slight curvature concave on the ulnar aspect (head and base are a small distance further to the ulnar direction than the shaft), similar in degree to what we see in Mc2. There is also a small hump on the distal end of the shaft on the palmar aspect. The two small epicondyles on the ulnar and radial sides are present again just proximal to the metacarpal head for the attachment of the collateral ligaments of the metacarpophalangeal joint. The shaft is slightly

flattened on the dorsal aspect and pinched through the palmar surface of the radial aspect, creating a sharper edge to the radial side of the shaft than the ulnar side. The metacarpal head is rounded evenly in both the radioulnar and dorsopalmar directions. The ulnar and radial edges of the metacarpal head are close to parallel, giving the head an outline that is squarer in dimension with a subtle rounding of the dorsal edge, when viewed from the distal surface. There are two gutters on the palmar edge of the head in which the sesamoids lie. The base of the Mc4 articulates with the Mc3, Mc5, capitate, and hamate. On the radial side, there are two articular facets. The palmar facet is smaller and round compared to the larger oval articular facet on the dorsal half of the radial side of the base. The palmar facet articulates with the Mc3 and with the capitate. The dorsal facet only articulates with the Mc3. On the palmar point of the base, there is a small smooth facet that articulates with the hamulus of the hamate. The proximal surface of the Mc4 base is angled down from the dorsal side to the palmar side (the dorsal edge is more distal and the palmar edge is more proximal). The facet articulates with the capitate on the radial side along a very thin rectangular strip. There is almost no differentiation between the capitate and hamate articular facet on the proximal face. The radial side of the proximal facet is almost perpendicular to the dorsal side forming an angle at the dorsal-radial connection that is just greater than 90 degrees. The ulnar edge is angled more sharply, creating closer to a 60 degree angle at the junction of the dorsal and ulnar edges. The palmar edge of the proximal face is rounded (Figure 3.15).

A.


Radial
Proximal
2
3
4
5
6
7
8

B.


Ulnar
Proximal
TRIC 1
2
3
4
5
6
7

C.


Palmar
Proximal
C 1
2
3
4
5
6
7

D.

E.

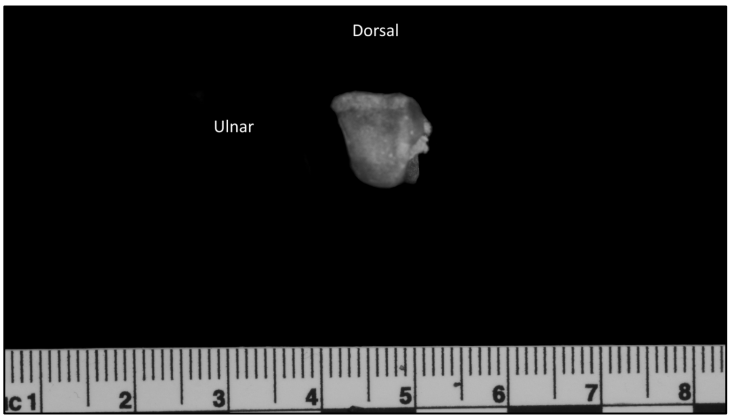

F.

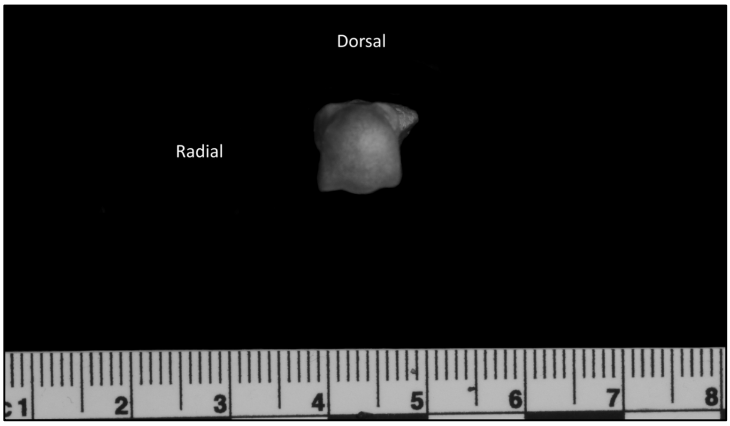

Figure 3.15

Left metacarpal 4 viewed from the standard anatomical aspects: palmar (A), dorsal (B), radial (C), ulnar (D), proximal (E), and distal (F). Scale is in centimeters (cm).

Metacarpal 5

The Mc5 is the thinnest of the metacarpals in the radioulnar direction. It is similar in proximodistal length to Mc2 – Mc5. It also has the greatest degree of dorsopalmar curvature of all the metacarpals, though it is still slight (concave on the palmar surface). There is also obvious curvature in the radioulnar direction (concave in on the ulnar surface with the head and base extending further ulnar than the midshaft). The diaphysis is flattened in the radioulnar direction and relatively thick in the dorsopalmar direction, a feature unlike any of the other metacarpals. Additionally, the shaft is tilted with the dorsal side being further in the radial direction and the palmar edge being further in the ulnar direction, starting at midshaft and extending through the proximal end. The two small epicondyles on the ulnar and radial sides are also present in Mc5 just proximal to the metacarpal head for the attachment of the collateral ligaments of the metacarpophalangeal joint. The metacarpal head is very similar in shape to the head of Mc2, though it is slightly smaller. It is rounded and slightly compressed on the dorsal side, forming a symmetrical triangle with a base on the palmar edge. On the palmar edge there are two evenly spaced gutters in which the sesamoids lie on the palmar aspect. The base of the Mc5 articulates with the Mc4 and the hamate. The palmar surface of the base is raised and rough, extending toward the proximal and ulnar sides and coming to a rounded point. The radial side does not extend as far in the proximal direction, creating an angled palmar edge of the proximal surface. The ulnarly projecting point of the base also contains a shallow but broad fossa on the ulnar side. On the radial side, there is an articular facet for the Mc4-Mc5 connection. This is a long curved facet with a subtle crescent shape positioned on the dorsal and proximal edges of the radial side. The furthest extension of the facet in the palmar

direction projects slightly radially whereas the side furthest dorsal bends slightly toward the dorsal aspect of the bone. The bulk of the proximal surface is an articular facet for the hamate. The large facet is boot-shaped with the sole of the boot forming the edge along the radial side between the facets for the Mc4 and the hamate. This edge angles from the radioulnar midpoint of the dorsal side of the proximal face to the radial side. The “toe” of the boot points toward the dorsal and slightly ulnar sides. The leg of the boot extends proximally on the reverse of the long point extending proximally and ulnarly. On the ulnar aspect, there is a small, shallow, triangular fossa that sits between the “toe” and “leg” of the boot (Figure 3.16).

A.

B.

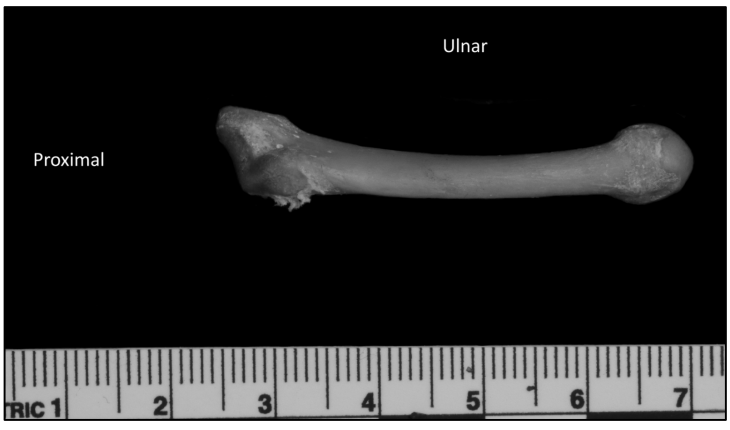

C.


Palmar
Proximal
1
2
3
4
5
6
7

D.


Dorsal
Proximal
201008
1
2
3
4
5
6
7

E.

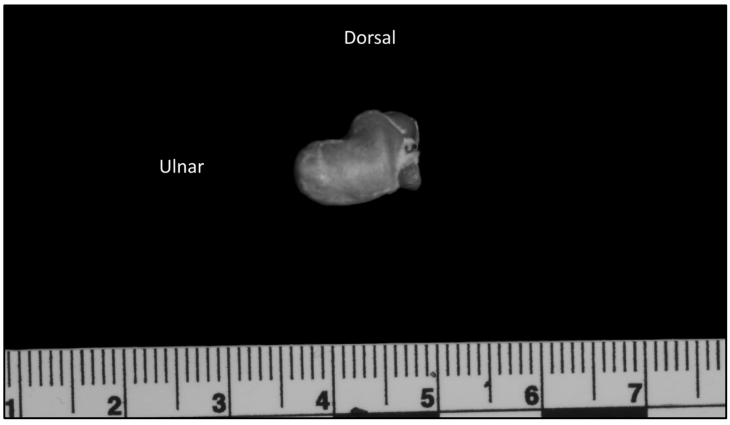
Dorsal
Ulnar
1
2
3
4
5
6
7

F. 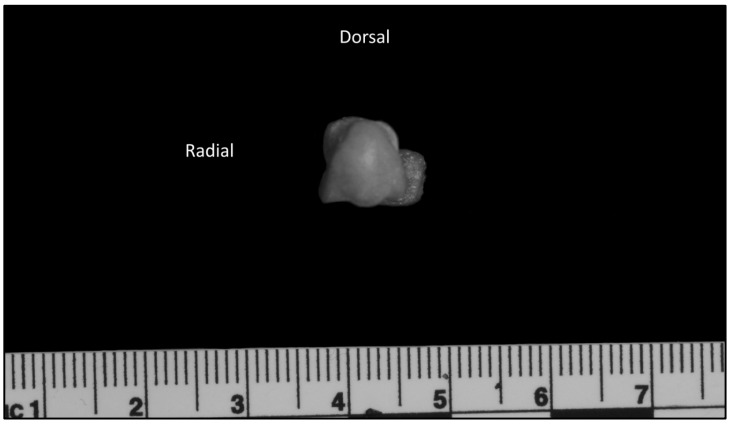

Figure 3.16
Left metacarpal 5 viewed from the standard anatomical aspects: palmar (A), dorsal (B), radial (C), ulnar (D), proximal (E), and distal (F). Scale is in centimeters (cm).

Proximal phalanges

Proximal phalanx 1

The palmar aspect of the proximal phalanx of the first ray shows a clear distinction between the head, shaft, and base. The shaft is narrow proximal to the head and broadens radioulnarly from the midshaft to the base. The ulnar and radial edges of the palmar and dorsal faces are concave toward the midline with the radial curve being deeper than the ulnar curve. The radial extension of the base at the proximal end of the shaft is greater than the ulnar extension contributing to the differences in curvature on each side. The proximal edge of the dorsal and palmar faces is rounded and concave with the ulnar and radial edges extending further proximally than the midpoint. The head is also uneven in the radioulnar dimensions. The radial condyle is larger than the ulnar and a smooth intercondylar groove separates the two condyles. This groove is also visible by the small dip on distal edge of the head positioned to the ulnar side of the midline. The breadth of the proximal shaft is greater than the articular surface of the base due to a ridge of roughened bone that runs along the proximal edge of the shaft on the

dorsal, palmar, ulnar, and distal faces. This ridge of bone is least pronounced on the palmar and dorsal faces though there are still rough areas for the insertion of the flexor pollicis brevis (radial) and adductor pollicis (ulnar) on the palmar side and the extensor pollicis brevis on the dorsal side. There are no distinct palmar tubercles as seen in the other proximal phalanges. The shaft narrows just proximal to the head in the dorsopalmar direction as well. It also broadens from approximately the midpoint of the shaft to the proximal end. Viewed from the ulnar and radial aspects, the dorsal edge is straight and the palmar edge shows concave curvature. The dorsopalmar height is greater at the proximal end of the shaft than at the condyles of the head. On the radial side of the base there is a small tubercle for the insertion of the abductor pollicis brevis. The base is rounded and convex from the ulnar and radial aspects. The head is also rounded and convex, though it is smaller than the base and slightly flattened on the palmar edge. This creates a small point where the head meets the shaft on the palmar edge when viewed from the ulnar and radial aspects. The head articulates with the proximal end of the first distal phalanx. From the distal view, the size imbalance between the two condyles is easy to identify. The radial condyle is larger, extending further from the midpoint that the ulnar condyle. It is rounded along the dorsal and radial sides, coming to a rounded point where the radial and palmer edges meet. The ulnar condyle is flattened on the dorsal edge and to a lesser extent on the ulnar edge. The palmar edge of the head is sharply angled with two flat edges (on running from the dorsal-radial extreme and another from the dorsal-ulnar extreme) meeting at the intercondylar groove. The articular facet on the base is smooth and concave with round edges along the dorsal, ulnar, and radial sides. The palmar edge is flattened with a very subtle

palmar channel. From the proximal aspect, the ridge of roughened bone distal to the base is visible projecting beyond the articular facet ulnarly and radially (Figure 3.17).

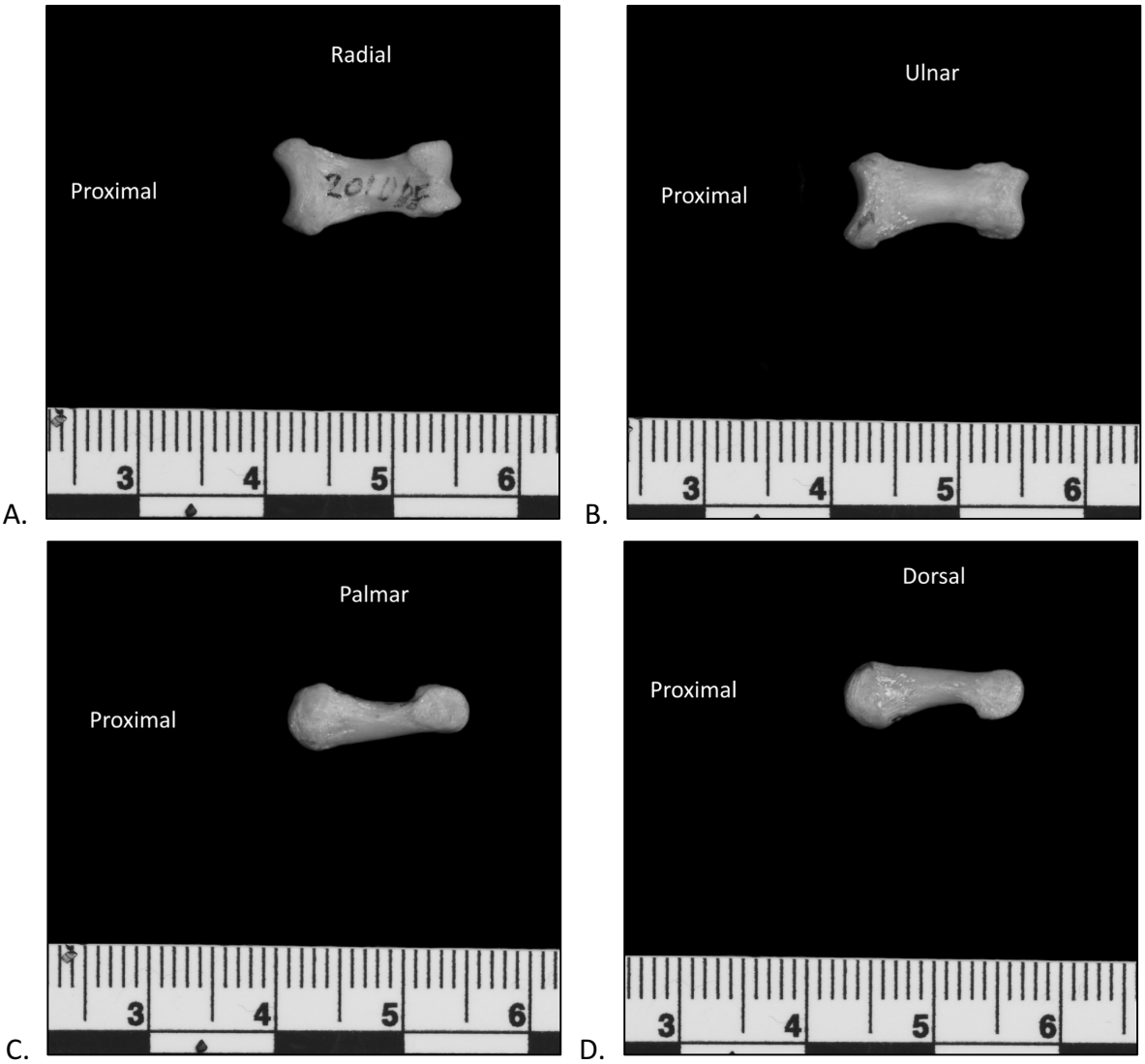

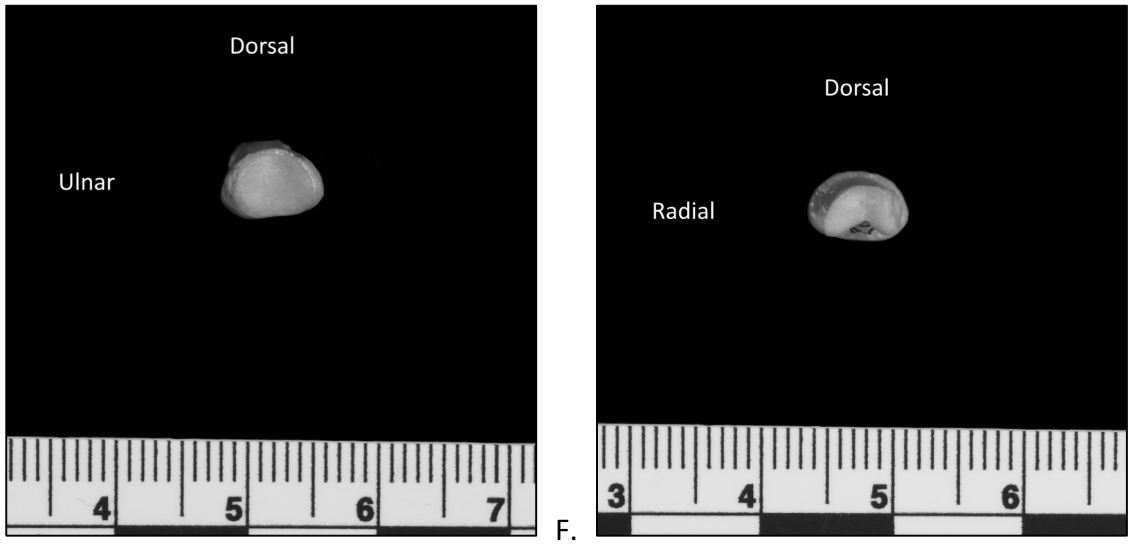

Figure 3.17
Left proximal phalanx 1 viewed from the standard anatomical aspects: palmar (A), dorsal (B), radial (C), ulnar (D), proximal (E), and distal (F). Scale is in centimeters (cm).

Proximal phalanges 2-5

The proximal phalanges of rays 2 through 5 have similar relative lengths to those of other papionins. On each proximal phalanx for rays 2 through 5, the dorsal surface of the shaft is smooth and convex radioulnarly. The palmar surface of the shaft is flat with slightly raised ulnar and radial edges, giving the surface a small degree of concavity. Near the midpoint of the shaft on the palmar surface there are two flexor sheath ridges, one on the ulnar edge and one on the radial. The development of these ridges varies between rays. The flexor sheath ridges are most well developed on PP2 and PP3 and very minimal on PP4 and PP5 in this individual. In many other primate species, the flexor sheath ridges are most well developed in PP3 and PP4 (Patel and Maiolino, 2016) and at least one other gelada specimen showed a similar pattern. Proximal to the head, the shaft narrows minimally and expands at the midpoint where the flexor sheath ridges project slightly to the ulnar and radial sides. The shaft narrows proximal to the flexor

sheath ridges and broadens radioulnarly at the base. There are two distinct palmar tubercles at the proximal end of the shaft on the palmar face with a well-defined palmar channel separating the ulnar and radial tubercles at which tendons of the metacarpophalangeal joint capsule attach. On the radial and ulnar sides, the collateral fossae sit in the center of the circular profile of the condyles, serving as an attachment site for the collateral ligaments of the proximal interphalangeal joint (PIP). The proximal articular surface is concave and oblong. It is broad radioulnarly and short dorsopalmarly. Within this general pattern, there are some unique aspects of the proximal phalanges for rays 2 through 5 in *Theropithecus gelada*. The proximal phalangeal length pattern for geladas is 3>4>5>2>1 whereas African apes, hylobatids, humans, and most orangutans show a 3>4>2>5>1 length pattern for the proximal phalanges (Susman, 1979).

Proximal phalanx 2

This bone differs from the general pattern of proximal phalanges in the following ways. The radioulnar expansion at the base is greater on the radial side than on the ulnar side. From the dorsal view, it is easy to identify that the radial side of the base extends proximally more than the ulnar side as well. The proximal edge of the base on the ulnar side is rounded. The radial side is much flatter on the dorsal side of the proximal edge with rounding along the palmar-proximal edge. Additionally, the flexor sheath ridge on the ulnar side is more pronounced than that of the radial side. The breadth of the condyles on the head is even for the proximal phalanx of ray 2 but the ulnar condyle extends in the distal direction a very small amount more than the radial condyle (Figure 3.18).

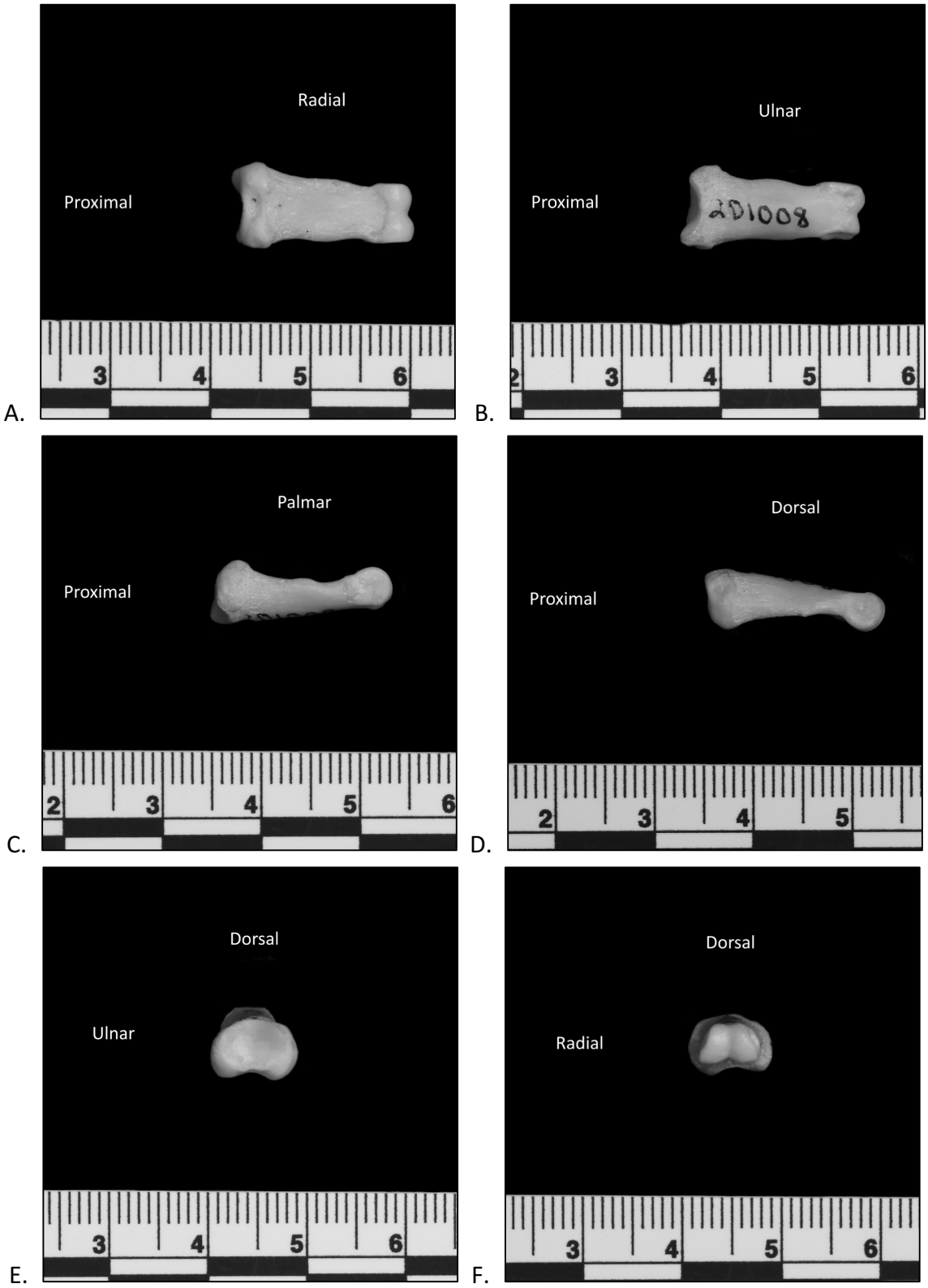

Figure 3.18

Left proximal phalanx 2 viewed from the standard anatomical aspects: palmar (A), dorsal (B), radial (C), ulnar (D), proximal (E), and distal (F). Scale is in centimeters (cm).

Proximal phalanx 3

This bone differs from the general pattern of proximal phalanges in the following ways. The radioulnar expansion at the base is greater on the ulnar side than on the radial side. Additionally, the ulnar condyle at the distal end is broader than the radial condyle in PP3. The flexor sheath ridge is more well developed on the radial side than the ulnar side (Figure 3.19).

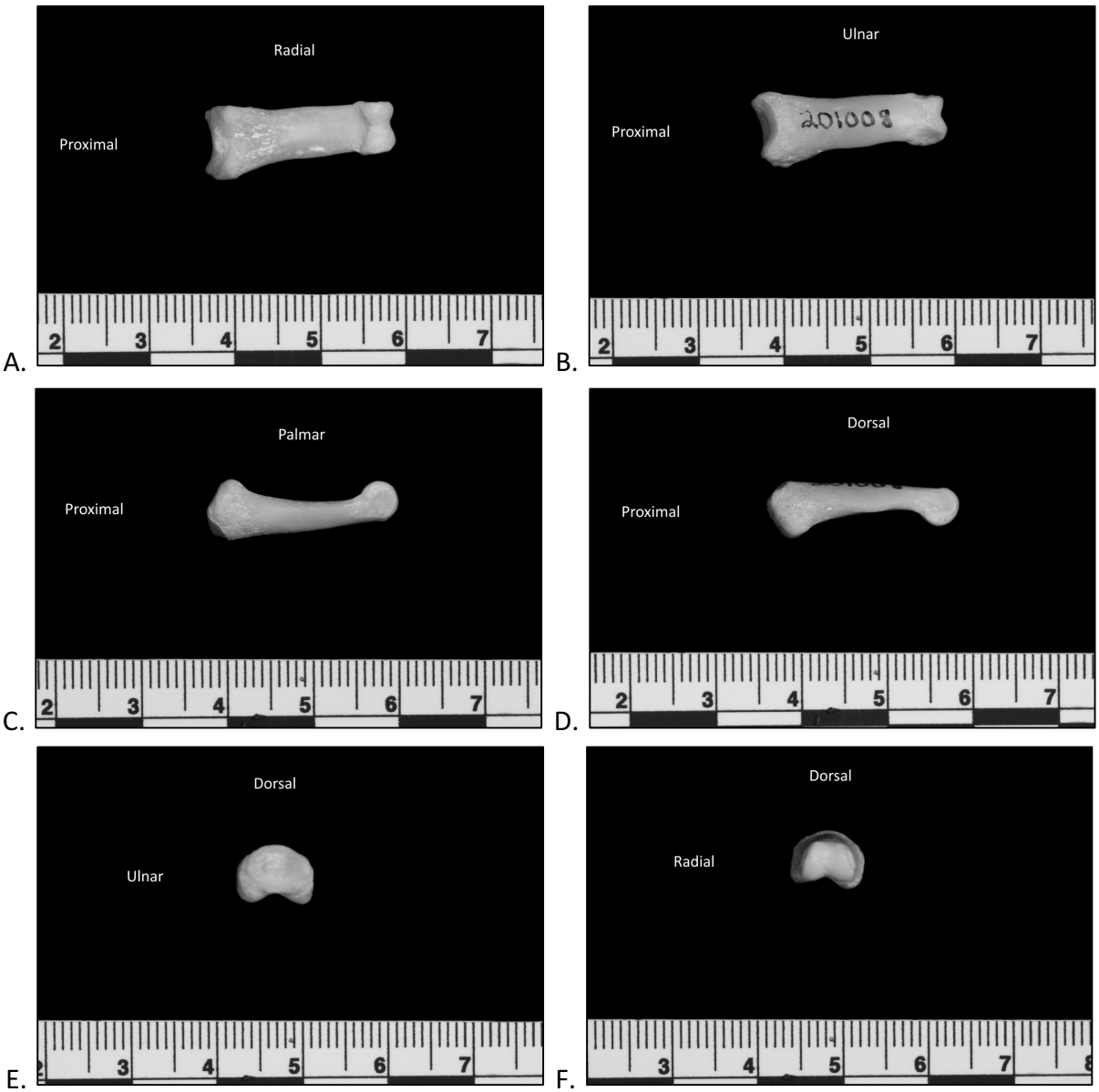

Figure 3.19
Left proximal phalanx 3 viewed from the standard anatomical aspects: palmar (A), dorsal (B), radial (C), ulnar (D), proximal (E), and distal (F). Scale is in centimeters (cm).

Proximal phalanx 4

This bone differs from the general pattern of proximal phalanges in the following ways. The ulnar condyle at the distal end is broader than the radial condyle. The flexor sheath ridges are minimal and almost not apparent, especially when viewed from the ulnar and radial aspects (Figure 3.20).

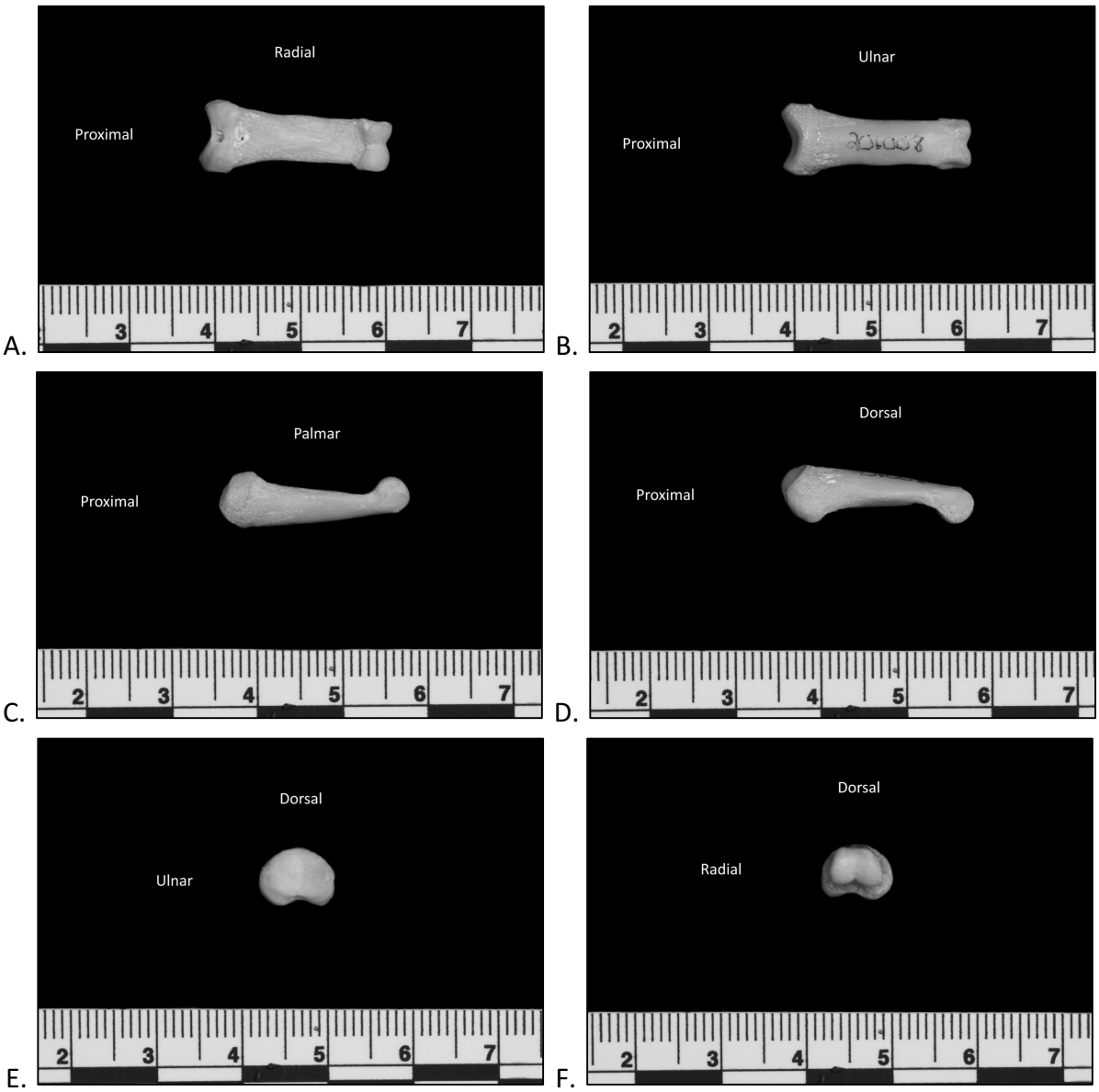

Figure 3.20
Left proximal phalanx 4 viewed from the standard anatomical aspects: palmar (A), dorsal (B), radial (C), ulnar (D), proximal (E), and distal (F). Scale is in centimeters (cm).

Proximal phalanx 5

This bone differs from the general pattern of proximal phalanges in the following ways. The radioulnar expansion at the base is greater on the ulnar side than on the radial side. Additionally, the ulnar condyle is broader than the radial condyle in PP5. The flexor sheath ridges are minimal and almost not apparent, though there is a very small palmar expansion of the ridge on the radial edge that is not shown on the ulnar side (Figure 3.21).

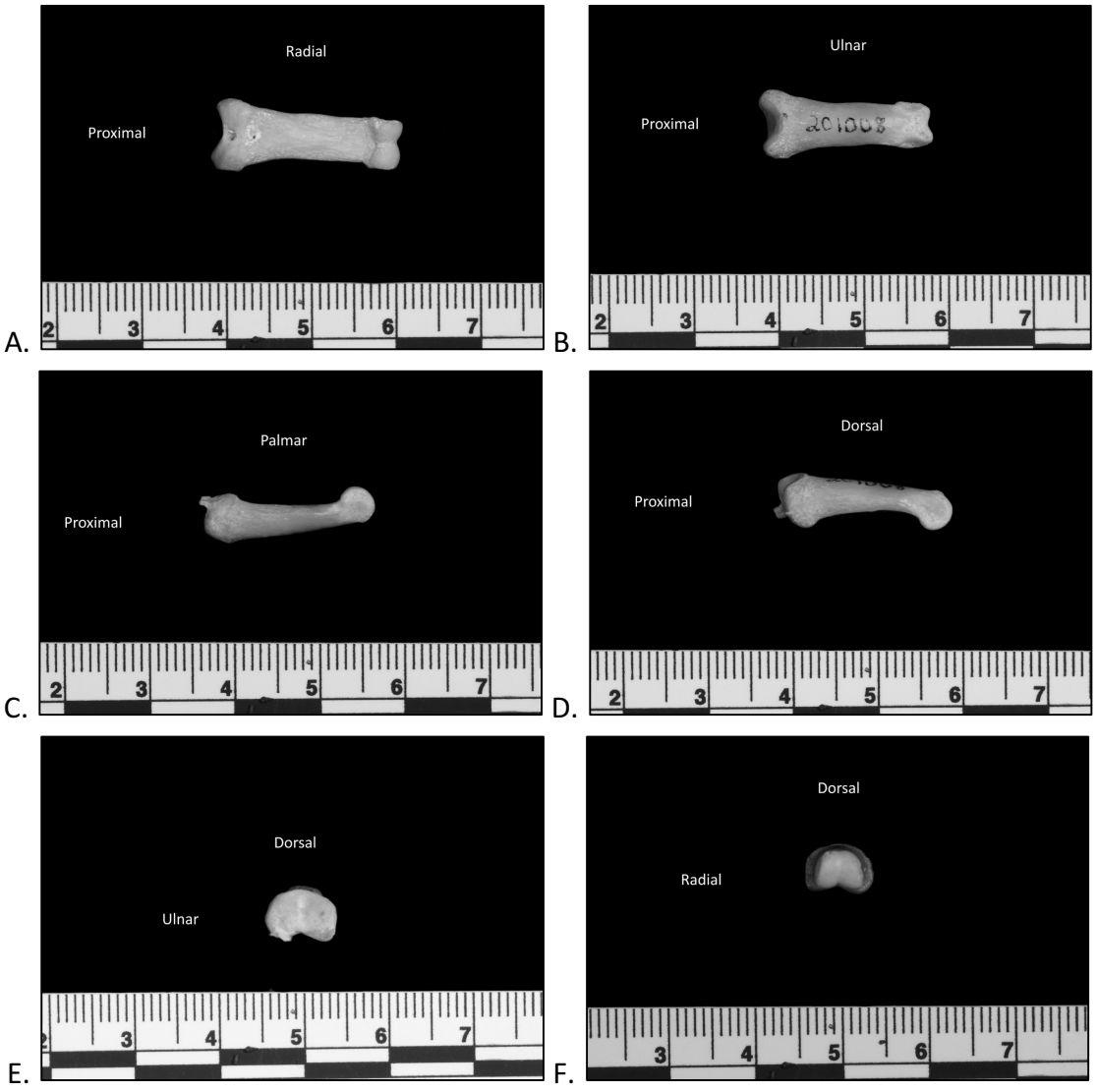

Figure 3.21
Left proximal phalanx 5 viewed from the standard anatomical aspects: palmar (A), dorsal (B), radial (C), ulnar (D), proximal (E), and distal (F). Scale is in centimeters (cm).

Intermediate phalanges

Intermediate phalanx 2

Of all the manual elements, the relative size of the intermediate phalanx of ray 2 distinguishes geladas from baboons most clearly. This is a very short phalanx relative to the other rays and, in conjunction with a relative increase in the length of ray 1, is often considered an adaptation to manual grazing. The palmar face is largely square, showing only a slight reduction in radioulnar breadth across the middle of the shaft with subtle radioulnar expansion at the distal and proximal ends. There is a ridge that distinguishes the shaft from the head on both the palmar and dorsal aspects. At the base, there is a small, rough ridge that runs along the edge of the proximal end where the shaft meets the proximal articular surface. The proximal edge is rounded on the palmar side with a very small beak at the radioulnar midpoint whereas the proximal edge displays a distinct beak at the radioulnar midpoint on the dorsal aspect, corresponding to the intercondylar groove of proximal phalanx 2 with which it articulates. On this specimen, the radial edge is longer than the ulnar edge as viewed from the palmar and dorsal aspects though that pattern might not hold for all individuals. Additionally, the ulnar edge is more concave than the radial edge from these views. The distal articular facet projects distally more on the radial half than the ulnar half with a smooth intercondylar groove running the dorsopalmar length of the distal facet at the radioulnar midline. There are two proximal articular facets of approximately equal size for the articulation with the condyles of the distal end of proximal phalanx 2, split down the radioulnar midline by the interarticular keel. The distal end is smooth and convex, articulating with the proximal end of distal phalanx 2. The intercondylar groove approximately bisects the head radioulnarly. The ulnar condyle is slightly

larger than the radial condyle. The palmar edge of the head is concave with the ulnar and radial edges extending further toward the palmar aspect than the midpoint. The dorsal edge of the head is straight and perpendicular to the ulnar and radial aspects. Additionally, the palmar extreme of the radial condyle flares radially and the palmar extreme of the ulnar articular condyle flares ulnarly. The ulnar and radial views are very similar, both showing the proximal and palmar projection of the palmar side of the proximal edge and straight dorsal edge. Comparing the radial and ulnar aspects, the radial edge is slightly longer and completely obscures morphology of the articular facets on the proximal and distal edges, whereas small portions of both the radial condyle and radial proximal articular facet can be seen from the ulnar aspect (Figure 3.22).

A. 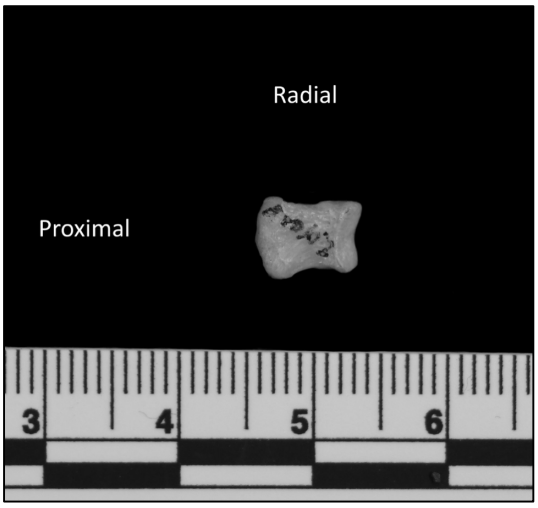

B. 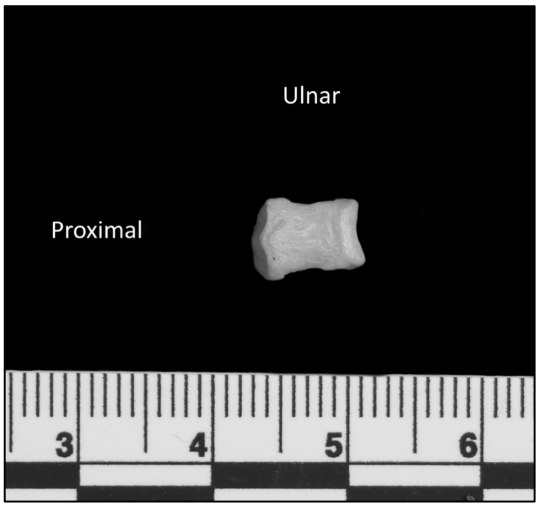

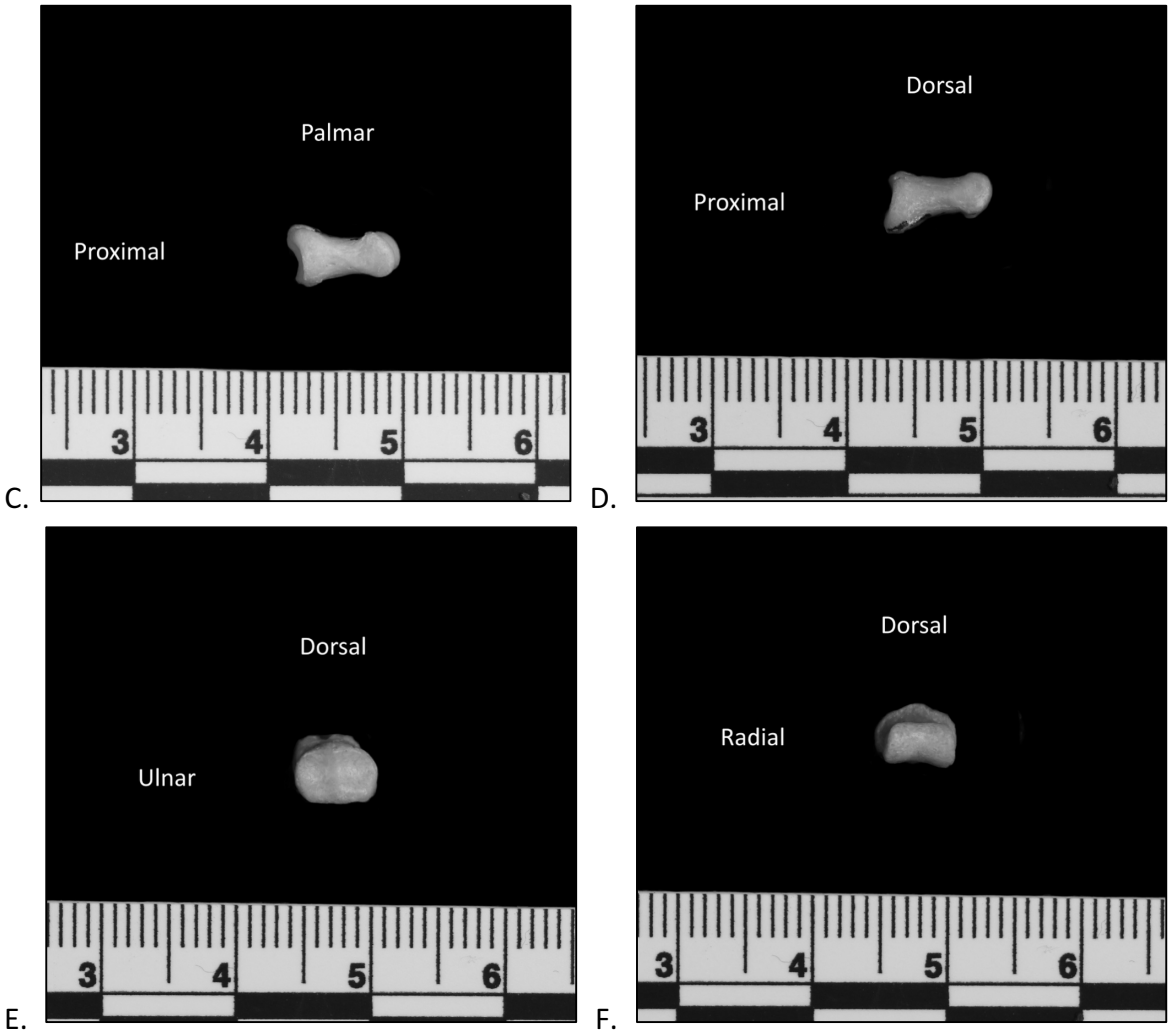

Figure 3.22
Left intermediate phalanx 2 viewed from the standard anatomical aspects: palmar (A), dorsal (B), radial (C), ulnar (D), proximal (E), and distal (F). Scale is in centimeters (cm).

Intermediate phalanges 3 – 5

In general, these phalanges are more symmetrical radioulnarly than IP2. They are also longer than IP2 and of a similar relative size length as in other papionins. Just proximal to the head of IP3, the shaft narrows radioulnarly only to expand radioulnarly at the proximal 1/3 of the shaft, matching the breadth of the base on the proximal end. The small beak is visible on the palmar edge of the base, corresponding to the intercondylar groove of the head of the proximal

phalanges with which they articulate. This beak is sharper and more clearly defined on the dorsal aspect of the intermediate phalanges than on the palmar aspect. On the proximal half of the palmar surface along the ulnar and radial edges, there are rough areas of bone for the insertion of the flexor digitorum superficialis tendons. These are more pronounced on IP3 and IP4 than the other intermediate phalanges. The shaft is narrow dorsopalmarly immediately proximal to the head and expands dorsopalmarly beginning at midshaft and extending proximally. The base is dorsopalmarly tall (as compared to head and shaft) and has concave curvature from the radial and ulnar aspects. The head is convex distally and round from the ulnar and radial views. The distal face has two condyles, one ulnar and one distal, that are separated at the medioradial midpoint by a smooth intercondylar groove. The dorsal edge of the distal articular surface is straight (parallel to the dorsal face) whereas the palmar edge is concave with the ulnar and radial edges extending further in the palmar direction than the midpoint. The base has two similar sized concave articular facets, one on the ulnar half and one on the radial half, that articulate with the condyles of the head of the corresponding proximal phalanges. These facets are separated by an interarticular keel at the midline of the proximal face. The dorsal edge of the base is rounded with a smooth curve continuing down the ulnar and radial edges until the straight palmar edge which is parallel to the palmar aspect. Intermediate phalanges 3 and 4 are extremely similar in all aspects. The intermediate phalanx of ray 5 is shorter than those of rays 3 and 4 and the medioradial expansion of the shaft at the proximal end is less pronounced in IP5 (Figures 3.23-3.25).

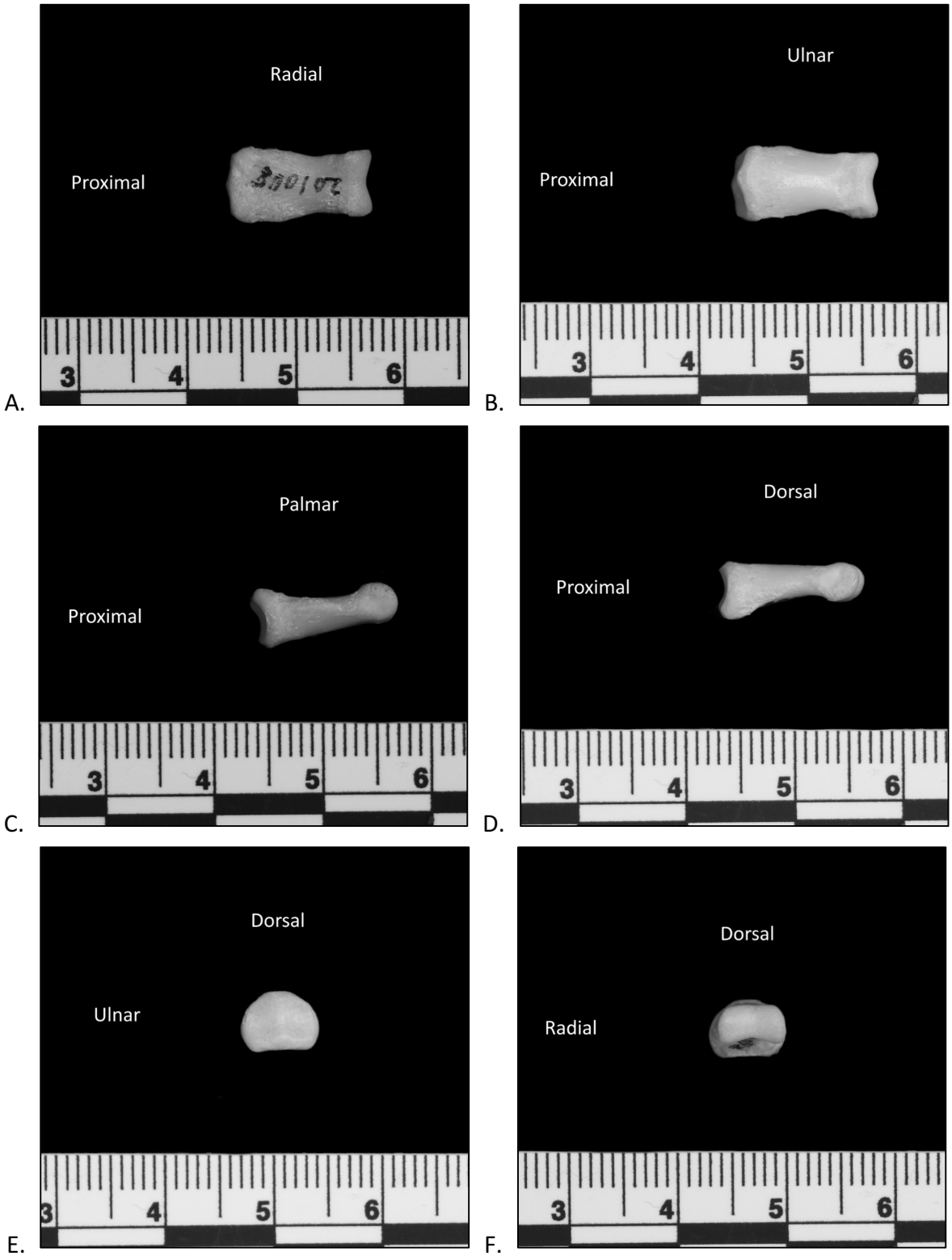

Figure 3.23

Left intermediate phalanx 3 viewed from the standard anatomical aspects: palmar (A), dorsal (B), radial (C), ulnar (D), proximal (E), and distal (F). Scale is in centimeters (cm).

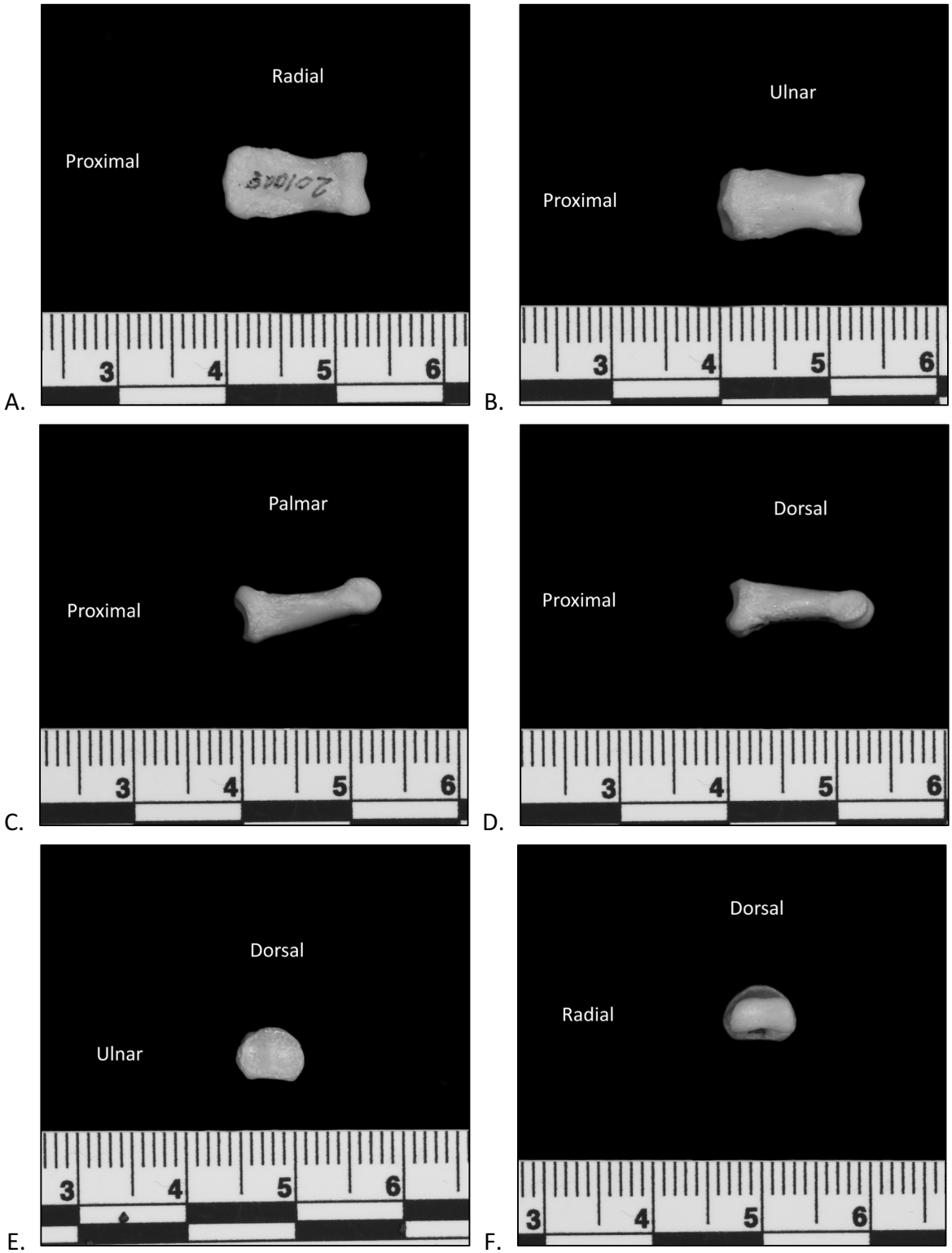

Figure 3.24

Left intermediate phalanx 4 viewed from the standard anatomical aspects: palmar (A), dorsal (B), radial (C), ulnar (D), proximal (E), and distal (F). Scale is in centimeters (cm).

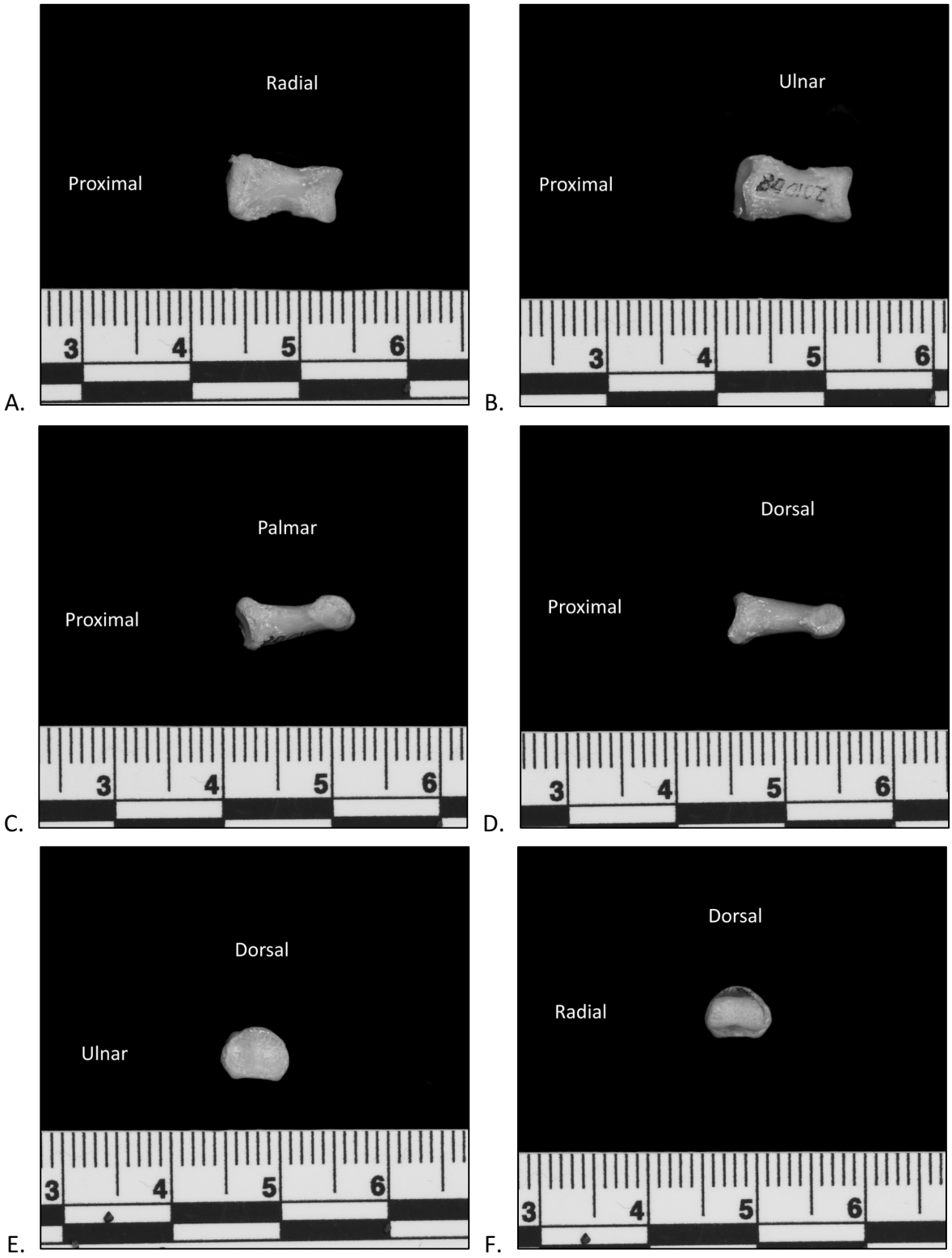

Figure 3.25

Left intermediate phalanx 5 viewed from the standard anatomical aspects: palmar (A), dorsal (B), radial (C), ulnar (D), proximal (E), and distal (F). Scale is in centimeters (cm).

Distal phalanges

Distal phalanx 1

This is a very small bone with medioradial expansion at the apical tuft and base. This expansion is greater at the base than at the tuft. The articular surface of the base forms a rough oval when viewed from the proximal aspect, with the intercondylar crest projecting proximally at the radioulnar midpoint. The intercondylar crest is more pronounced on the palmar side of the articular surface than on the dorsal side. On the ulnar and radial halves of the base there are rounded depressions for the articulation of the proximal articular base with the distal condyles of the first proximal phalanx. Additionally, at the radioulnar midline of the palmar surface at the proximal edge, there is a concavity, giving the base of distal phalanx 1 a thick crescent or kidney shape. The apical tuft on the distal end is softly rounded and flattened dorsopalmarly. On the ulnar and radial sides, the apical tuft is cut off sharply on its proximal extreme. In this specimen, the ulnar side is more sharply pointed whereas the “corner” of this edge is rounded on the radial side. Distal phalanx 1 does show greater apical tuft expansion in the radioulnar direction than the other distal phalanges which is also typical in baboons and great apes. On the palmar surface, the insertion of the flexor tendon is obvious from a ridge running radioulnarly distal to the base. Between the ridge and the proximal edge of the base on the proximal surface, the proximal volar fossa is visible by a shallow depression (Figure 3.26).

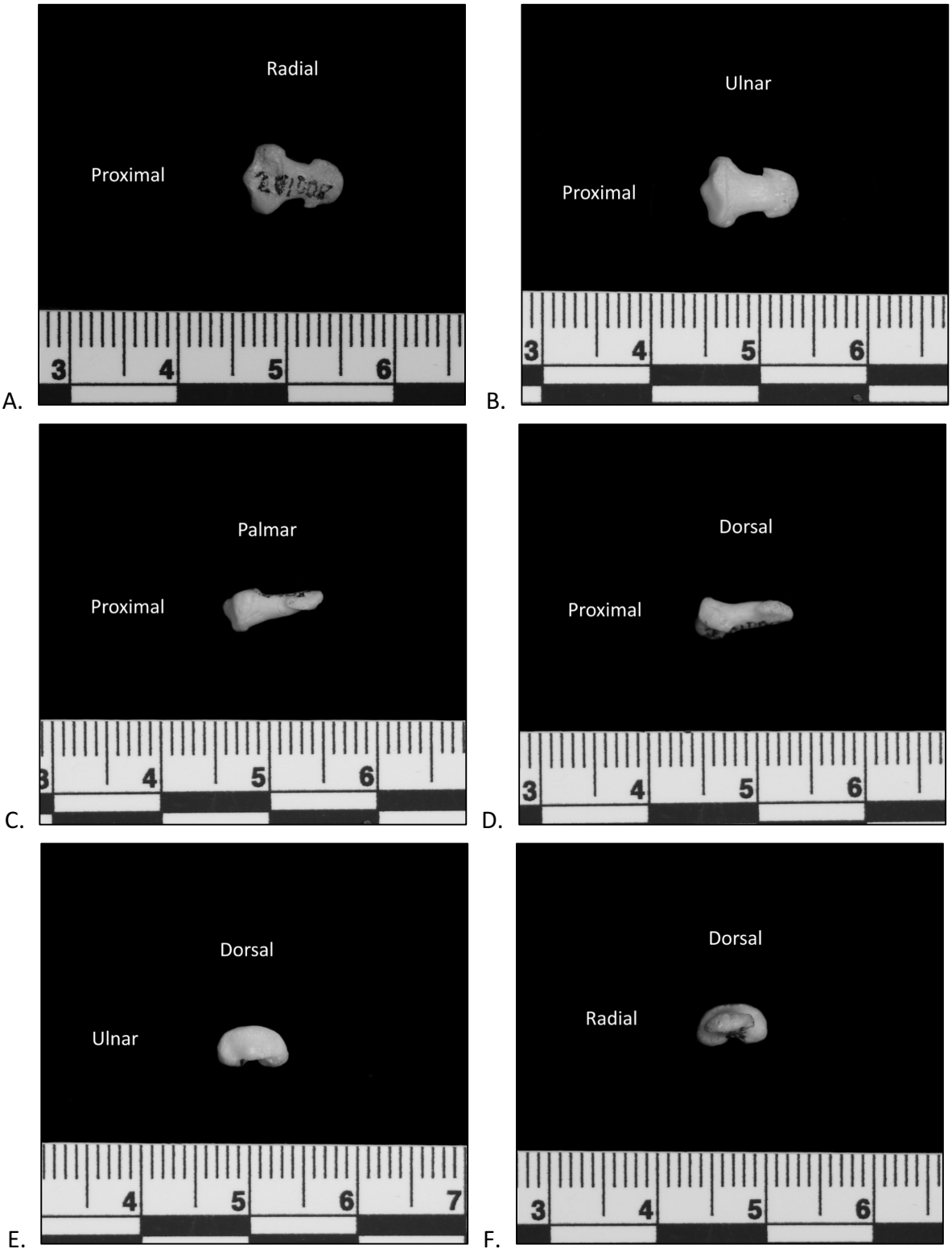

Figure 3.26

Left distal phalanx 1 viewed from the standard anatomical aspects: palmar (A), dorsal (B), radial (C), ulnar (D), proximal (E), and distal (F). Scale is in centimeters (cm).

Distal phalanges 2- 5

The distal manual phalanges are small and narrow. The apical tuft has very slight expansion in the radioulnar direction where it meets the shaft. This expansion is absent on the fifth distal phalanx. The distal tip of the apical tuft is pointed, unlike that of the first distal phalanx which is much rounder. The distal phalanx of the fourth digit is rounded more than that of the second, third, or fifth digit though less than the first distal phalanx. On the second distal phalanx, there is a depression where the apical tuft meets the shaft on the radial side. This is unique to the M-201008 individual and not characteristic of the species. The proximal ends of the distal phalanges 2-5 are radioulnarly wide, matching the width of the distal articular surface of the intermediate phalanges with which they articulate. The proximal end articulates with the distal end of the intermediate phalanges for rays 2-5. The intercondylar crest approximately bisects the articular surface separating the ulnar and radial halves. The articular surface is oblong in shape, lacking the crescent or kidney shape of the surface of DP1. On the distal phalanges of rays 2-5, Tendon insertion sites for flexors and extensors are not well-defined. The manual distal phalanges for rays 2-5 are very similar in morphology to the pedal distal phalanges for the corresponding pedal rays. In isolation, it would be almost impossible to distinguish between a manual or pedal distal phalanx from rays 2 through 5. Additionally, assigning an isolated manual phalanx from digits 2-5 to a specific ray would be difficult because of the many morphological similarities (Figures 3.27-3.30).

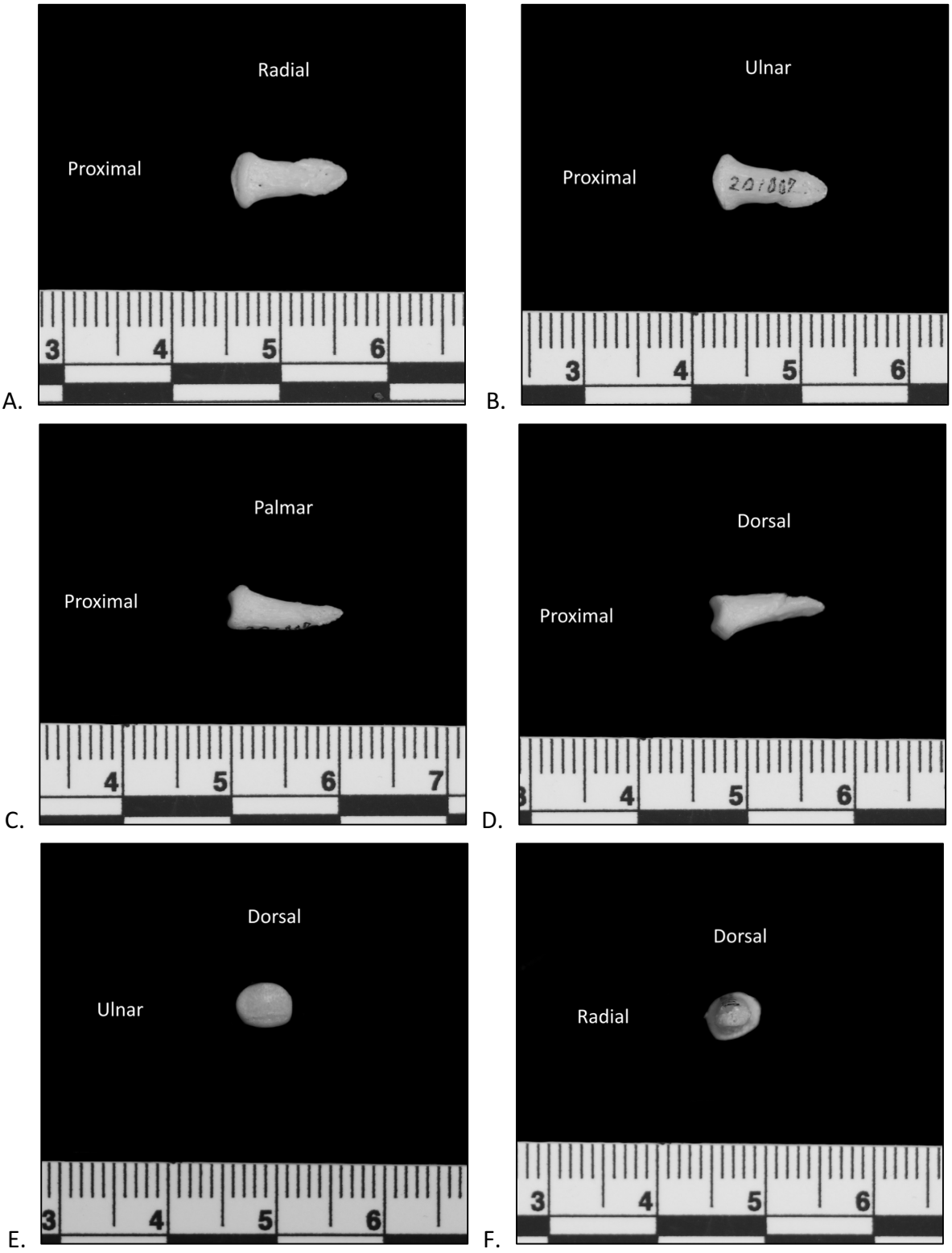

Figure 3.27

Left distal phalanx 2 viewed from the standard anatomical aspects: palmar (A), dorsal (B), radial (C), ulnar (D), proximal (E), and distal (F). Scale is in centimeters (cm).

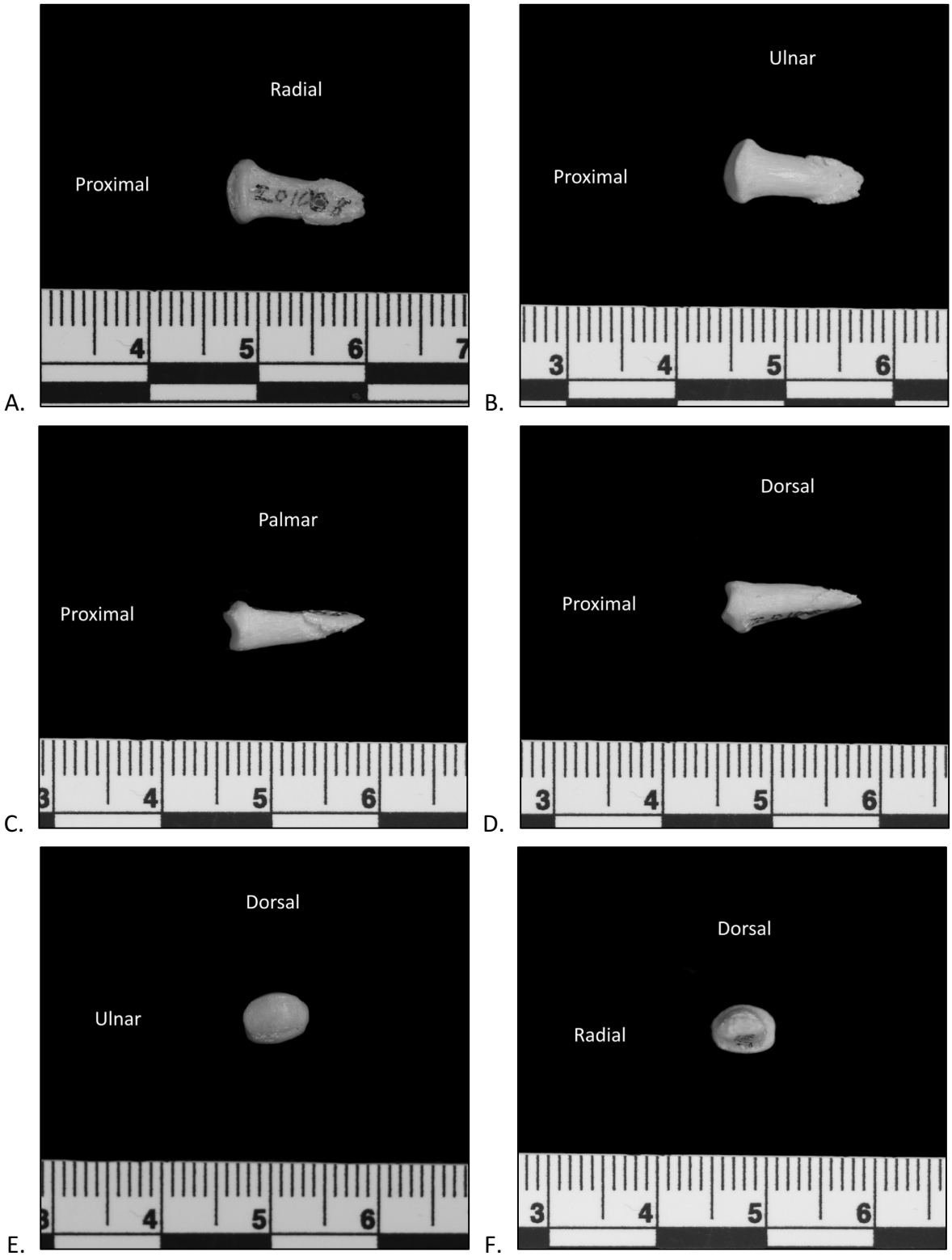

Figure 3.28

Left distal phalanx 3 viewed from the standard anatomical aspects: palmar (A), dorsal (B), radial (C), ulnar (D), proximal (E), and distal (F). Scale is in centimeters (cm).

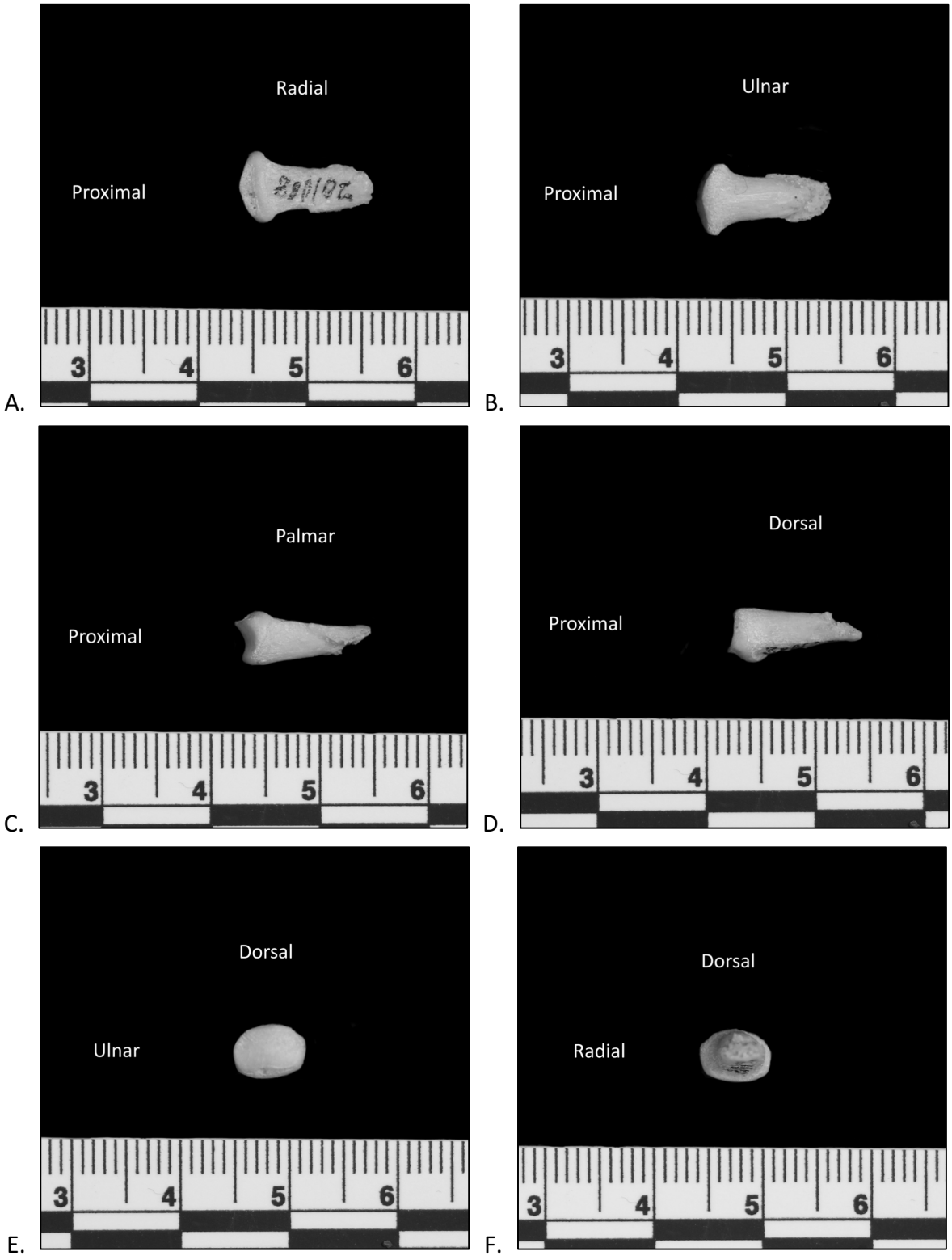

Figure 3.29

Left distal phalanx 4 viewed from the standard anatomical aspects: palmar (A), dorsal (B), radial (C), ulnar (D), proximal (E), and distal (F). Scale is in centimeters (cm).

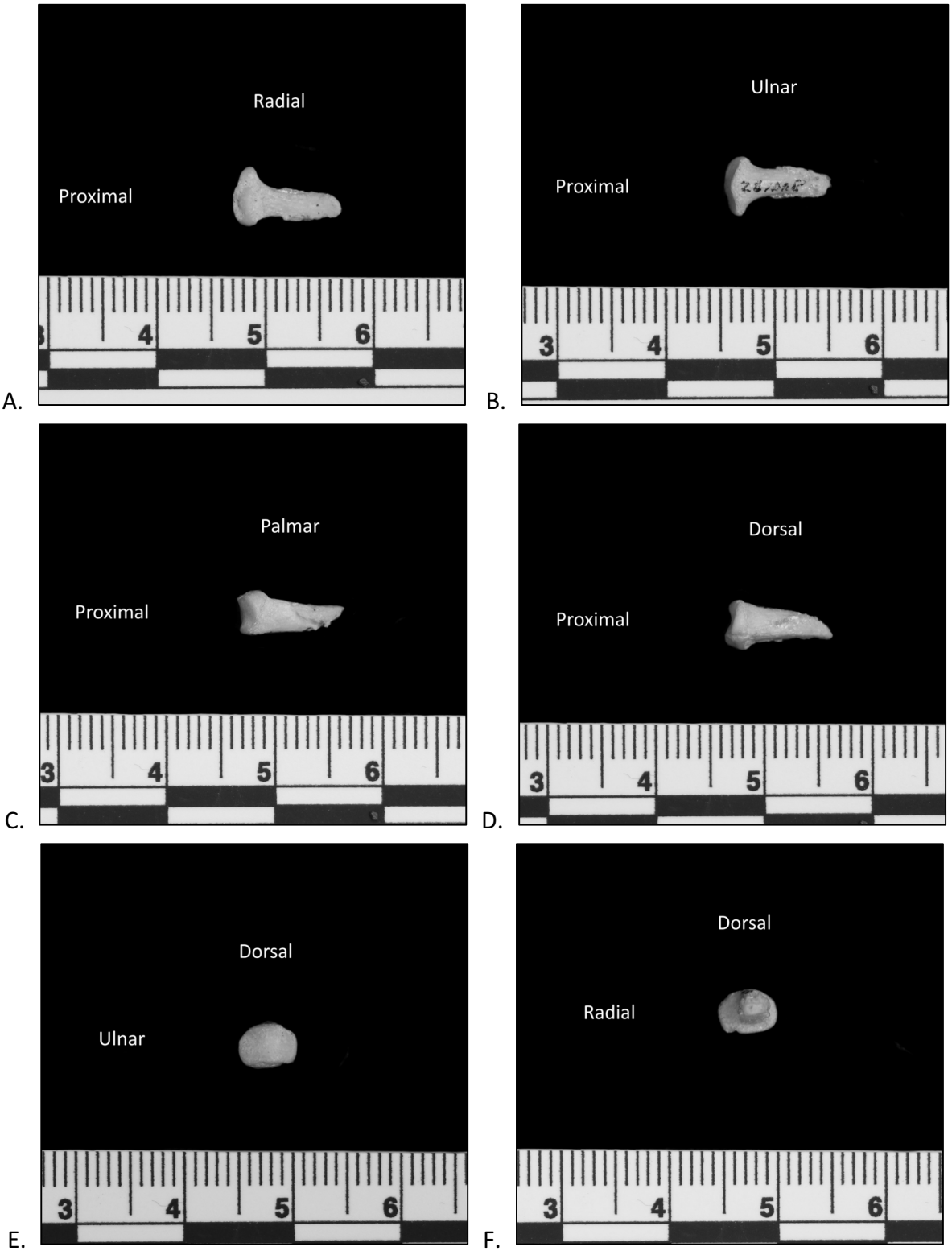

Figure 3.30

Left distal phalanx 5 viewed from the standard anatomical aspects: palmar (A), dorsal (B), radial (C), ulnar (D), proximal (E), and distal (F). Scale is in centimeters (cm).

Sesamiods

Geladas have one carpal sesamoid, known as the prepollex, located proximal to the Mc1. The sesamoids on the palmar side of the metacarpal heads are asymmetrical. They lie in the sesamoid gutters of each metacarpal. On ray 1, the sesamoids are usually very similar in size though the ulnar sesamoid is slightly larger in some individuals. This contrasts with the pattern of the sesamoids of the other rays. The radial sesamoids are larger (longer in the proximodistal direction) than the ulnar sesamoids for rays 2-5. The sesamoids were not present on this individual and were therefore unavailable for photography.

Conclusions

Though broadly following the general cercopithecine pattern of manual morphology, some important details unique to the geladas examined in this study are present. The relatively long first ray compared to second ray of geladas is evidenced by the elongation of the Mc1 and shortening of the intermediate phalanx of ray 2, supporting previous assessments of their specific intrinsic hand proportions (e.g, Jolly, 1970; Etter, 1973; Dunbar, 1983; Elton, 2006; Patel and Maiolino, 2016). Additionally, some aspects of metacarpals 2 through 5 differed from the expected general morphology of terrestrial African monkeys. Namely, the relatively great radioulnar breadth of Mc3 compared to the other metacarpals and the pronounced radioulnar curvature of Mc5 and extension of the base in the ulnar direction are subtle departures from the morphology seen in baboons. These differences in metacarpal morphology could be linked to distinct locomotor behaviors. For example, geladas traverse steep, rocky cliffs daily as they move from their sleeping sites to the plateaus where they spend the bulk of the day (Dunbar

and Dunbar, 1974; Ohsawa, 1979; Kawai and Iwamoto, 1979). Though some populations of baboons also use rocky substrates (e.g., Hamilton, 1982; Barret et al., 2004), most do so at frequencies lower than geladas which could explain these differences in metacarpal morphology.

This detailed description of the manual skeletal morphology of *Theropithecus gelada* offers comparative data for further analyses of manipulative and locomotor behaviors related to the hands of these primates. Some aspects of their hand morphology are well-known (i.e., opposability index, Napier and Napier, 1967). Much of their hand anatomy has not been discussed at length, though it may be linked to unique facets of gelada behavior. While geladas broadly exhibit hand morphology expected of the cercopithecines as a whole (Etter, 1973), subtle distinctions in posture during terrestrial locomotion or fine object manipulation could be reflected in their unique manual morphology. These descriptions form the foundation of further detailed analyses of throughout this dissertation.

Works Cited

Barrett, L., Gaynor, D., Rendall, D., Mitchell, D., & Henzi, S.P. (2004). Habitual cave use and thermoregulation in chacma baboons (*Papio hamadryas ursinus*). *Journal of Human Evolution*, *46*(2), 215-222.

Dunbar, R.I.M. (1983). Theropithecines and hominids: Contrasting solutions to the same ecological problem. *Journal of Human Evolution*, *12*(7), 647-658.

Dunbar, R.I.M., & Dunbar, E.P. (1974). Ecological relations and niche separation between sympatric terrestrial primates in Ethiopia. *Folia Primatologica*, *21*(1), 36-60.

Elton, S. (2006). Forty years on and still going strong: the use of hominin-cercopithecid comparisons in palaeoanthropology. *Journal of the Royal Anthropological Institute*, *12*(1), 19-38.

Etter, H.F. (1973). Terrestrial adaptations in the hands of Cercopithecinae. *Folia Primatologica*, *20*(5-6), 331-350.

Guthrie, E.H. (2011). *Functional morphology of the postcranium of Theropithecus brumpti (Primates: Cercopithecidae)* (Doctoral dissertation, University of Oregon).

Hamilton, W.J. (1982). Baboon sleeping site preferences and relationships to primate grouping patterns. *American Journal of Primatology*, *3*(1-4), 41-53.

Jablonski, N.G., Leakey, M.G., Kiarie, C., & Antón, M. (2002). A new skeleton of Theropithecus brumpti (Primates: cercopithecidae) from Lomekwi, west turkana, Kenya. *Journal of Human Evolution*, *43*(6), 887-923.

Jolly, C.J. (1970). The seed-eaters: a new model of hominid differentiation based on a baboon analogy. In *Primate Evolution and Human Origins* (pp. 323-332). Routledge.

Kawai, M. & Iwamoto, T. (1979). Nomadism and activities. In M. Kawai (Ed.) *Ecological and Sociological Students of Gelada Baboons* (3-45). Tokyo: Kodansha

Maier, W. (1971): Vergleichend- und funktionell-anatomische Untersuchungen an der Vorderextremität von *Theropithecus gelada* (Ruppell 1835). Abhdl. Senckenb. Naturf. Ges., No. 527, 1-284, Frankfurt a. M.

Napier, J.R. & Napier, P.H. (1967): A handbook of living Primates. Academic Press, London.

Ohsawa, H. (1979). The local gelada population and environment of the Gich area. In M. Kawai (Ed.) *Ecological and Sociological Students of Gelada Baboons* (3-45). Tokyo: Kodansha.

Patel, B.A., & Maiolino, S.A. (2016). Morphological diversity in the digital rays of primate hands. In *The evolution of the primate hand* (pp. 55-100). Springer, New York, NY.

Susman, R.L. (1979). Comparative and functional morphology of hominoid fingers. *American Journal of Physical Anthropology*, *50*(2), 215-236.

Swindler, D.R., & Wood, C.D. (1973). Part 1 Osteology. In *An atlas of primate gross anatomy: Baboon, chimpanzee, and man* (pp. 36-38). Seattle, WA: University of Washington Press.

Chapter 4
Proximal articular surface morphology of metacarpals 1 and 2 in geladas and baboons

Abstract

This study uses 3D geometric morphometrics to examine the morphology of the carpometacarpal joint surfaces of first and second metacarpals in two groups of highly terrestrial African primates – geladas (*Theropithecus gelada)* and baboons (*Papio* spp.). The proximal joint surface of the first metacarpal is significant for understanding manipulative capabilities in primates, especially related to forceful opposition and pad to pad precision gripping. The morphology of the second metacarpal has been largely ignored in previous work. Assessing functional differences of the first and second rays in geladas and baboons is important due to the behavioral differences observed for these taxa. 3D geometric morphometric analyses and principal components analyses (PCA) were used to compare the proximal articular surfaces of the first and second metacarpals of geladas and baboons. The results highlight many broad similarities between these two groups as well as significant differences in morphology primarily related to joint stability. Geladas exhibit morphology reflective of greater stability at the first metacarpal-trapezium joint for resisting axial loads compared to baboons. At the second metacarpal-trapezoid joint, geladas exhibit less passive stability and greater flexion-extension range relative to baboons. These subtle differences are likely indicative of differences in manipulative and locomotor patterns between these two taxa.

Introduction

Geladas (*Theropithecus gelada*) and baboons (*Papio* spp.) are closely related, terrestrial large-bodied monkeys. The two groups share many behavioral characteristics but differ in several

important ways. Many of their behavioral differences are rooted in their different feeding ecologies. Geladas are known as manual grazers, picking grasses and rhizomes from the ground by pinching them between their first and second digits. Some aspects of the manual adaptations that make this unique behavior possible have are well-known. Geladas possess a very high opposability index resulting primarily from the shortening of the intermediate phalanx of the second ray. However, other aspects of gelada manual morphology have not been examined in detail. In particular, opposition between the first and second digits involves movement at the carpometacarpal joint surfaces. An assessment of the morphological characteristics of the base of the first metacarpal (Mc1) and second metacarpal (Mc2) could indicate important functional differences between geladas and baboons, despite their many gross skeletal similarities as seen in Figure 4.1.

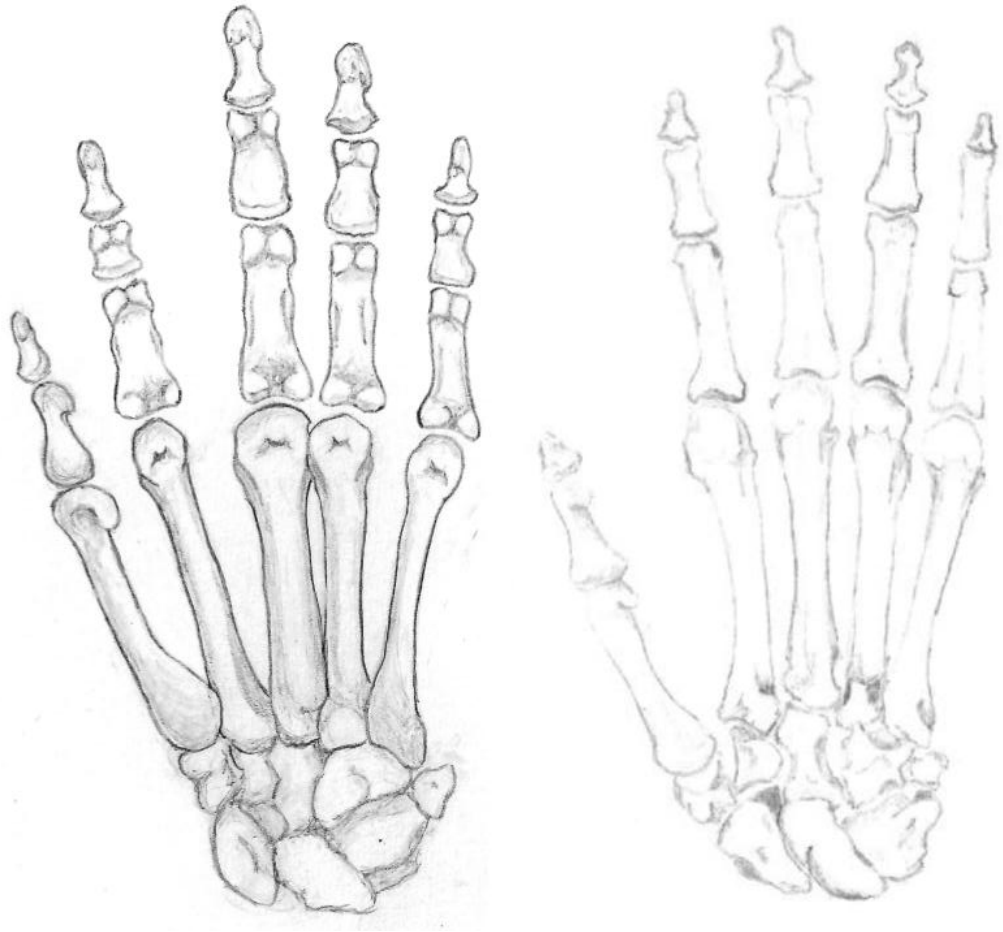

Left hand, *Theropithecus gelada*
Palmar view

Left hand, *Papio cynocephalus*
Palmar view

Figure 4.1
Side-by-side of the palmar view of the left hand of *Theropithecus gelada* and *Papio cynocephalus,* hand-drawn by the author from gelada museum specimen detailed in chapter 3 of this study and from baboon images featured in Swindler and Wood (1973).

Previous work focusing on hominins and extant ape taxa has demonstrated that metacarpal joint surface anatomy can reflect habitual force patterns through the hands, the range of motion, and degree of stability at the carpometacarpal joints (e.g. Rose, 1992; Niewoehner, 2000, 2005; Marzke et al, 2010; Marchi et al., 2017). Behavioral patterns and precision gripping abilities of extant and extinct primate taxa have been inferred based on the metacarpal joint surface anatomy, particularly of Mc1. While extant apes feature prominently as comparative

taxa in previous studies, geladas and baboons are largely absent. Additionally, Mc2 proximal articular surface morphology and its role in fine object manipulation and precision gripping has not been assessed for these taxa. The relative neglect of the proximal joint surface of Mc2 could be due to its complex morphology, though it should be thoroughly examined, especially considering the emphasis placed on digit proportions for opposability that include ray 2 (e.g. Napier and Napier, 1967).

The goal of this study was to quantify the morphology of the Mc1 and Mc2 proximal articular surfaces of geladas and baboons using 3D geometric morphometrics. I examine the null hypothesis that there are no differences between geladas and baboons in the morphology of the proximal articular surfaces at the trapezium-Mc1 and trapezoid-Mc2 joints because of similar locomotor patterns of terrestrial quadrupedalism. Alternatively, differences in shape of the Mc1 and Mc2 articular surfaces between geladas and baboons are expected if there are significant functional differences related to precision gripping between these two primate groups. For Mc1, forceful precision gripping is facilitated by high dorsopalmar curvature creating a stable carpometacarpal joint. High dorsopalmar curvature at the base of the Mc1 is expected in primates that habitually and forcefully grip objects between the thumb and forefinger. For the Mc2, high demands on the carpometacarpal joints during locomotion could necessitate high joint stability whereas forceful precision gripping requires greater mobility, especially in flexion and extension. High radioulnar curvature and deep wedging is expected in primates that have high digitigrade locomotor demands whereas high dorsopalmar curvature is

expected for primates with relatively lower locomotor demands and higher demand for precision gripping.

Materials and methods

Both the gelada (*Theropithecus gelada*) and baboon (*Papio* spp.) samples used in this study are part of collections curated at the American Museum of Natural History (AMNH) in New York, NY. Of the gelada specimens in the AMNH collections, four adult individuals had relatively complete manual elements and were suitable for computed tomography (CT) scanning. Additionally, nine adult baboons had relatively complete manual elements and were suitable for CT scanning. In the majority of specimens, all elements from the left hand were present and complete. For this reason, the left metacarpals were selected for analyses. The right hand was substituted for two individuals, one gelada and one baboon, which had substantially more data represented from the right than the left. These two right hand specimens were mirrored for analysis. All primate skeletal elements were scanned with high resolution x-ray computed tomography by engineer Justin Gladman in Durham, NC using a Nikon XTH 225 ST model microCT scanner. This work was performed at the Duke University Shared Materials Instrumentation Facility (SMIF), a member of the North Carolina Research Triangle Nanotechnology Network (RTNN), which is supported by the National Science Foundation (Grant ECCS-1542015) as part of the National Nanotechnology Coordinated Infrastructure (NNCI). Due to scan errors including low resolution and software compatibility issues across multiple platforms, three baboons were omitted from further analyses after scanning. All

available catalog data for the ten individuals included in geometric morphometric analyses are listed in Table 4.1.

Genus species	Catalog number	Sex	Age class	Provenience	Side	PCA #
Theropithecus gelada	M-19006	Male	Adult	ZOO	Left	1
Theropithecus gelada	M-60568	Male	Adult	ZOO	Right	7
Theropithecus gelada	M-200763	Male	Adult	No data	Left	2
Theropithecus gelada	M-234038	No data	Adult	No data	Left	4
Papio sp.	M-35120	Male	Adult	No data	Left	5
Papio sp.	M-81688	No data	Adult	No data	Left	8
Papio anubis	M-52688	Female	Adult	Democratic Republic of the Congo	Left	6
Papio anubis	M-82092	No data	Adult	Kenya – Rift Valley	Left	9
Papio anubis	M-82097	No data	Adult	Kenya – Rift Valley	Left	10
Papio hamadryas	M-200847	Male	Adult	"Africa"	Right	3

Table 4.1
Catalogue details available from the AMNH Individual specimens included in this analyses and corresponding number for PCA plots.

MicroCT scanning produced a series of TIFF (tagged image file format) stacks for each scan session containing multiple specimens. I used the following software packages: The FIJI distribution of ImageJ (Schindelin et al., 2012), Invesalius 3.1 (Amorim et al., 2011; de Moraes et al., 2011; Amorim et al., 2015), and MeshLab (Cignoni et al., 2008; Ranzuglia et al., 2012; Pietroni et al., 2010). For partial or disjointed scans, I used FIJI to stitch together partial TIFF stacks to produce complete scans of an individual's entire articulated hand. I constructed surface meshes of each specimen with InVesalius 3.1 and exported the surface mesh for the first and second metacarpals as separate PLY (polygon file format) files. The quality of each mesh varied depending on the condition of the original TIFF files. Some files required additional manual cleaning using the eraser function in InVesalius. The most common need for manual

image cleaning resulted from dried soft tissue in the scans, manual cleaning was also necessary for isolation of skeletal elements.

The mesh for each metacarpal was individually loaded into MeshLab for additional processing and trimming. For poor quality meshes, I filled breaks in the surface using the “Close holes” function and smoothed the surface with the “Laplacian smooth (surface preserve)” function to produce a continuous surface on the proximal articular face that was anatomically accurate and compatible with geometric morphometric analyses. I additionally isolated the proximal articular surface of each metacarpal, where the first metacarpal articulates with the trapezium and where the second metacarpal articulates with the trapezoid, by removing all other faces and vertices of the mesh. Due to the complexity of the base and proximal articular surface of the second metacarpal and the limits of available software, analyses are limited to the joint surface that articulates with the trapezoid.

The meshes of the isolated joint surfaces of each metacarpal were then loaded into R version 3.6.1 (R Core Team, 2016) using the Geometric Morphometric Analyses of 2D/3D Landmark Data package version 3.2.1 known as geomorph (Collyer and Adams, 2018; Adams et al., 2019; Adler et al., 2019; Collyer and Adams, 2019). The geomorph package contains procedures for digitizing fixed landmarks and sliding semi-landmarks upon imported meshes. The first step in the process is building a template, which contains all relevant fixed landmarks using a single specimen that can be applied to the remaining specimens. From that point, sliding surface semi-landmarks are approximated relative to the fixed landmarks. Because of the high scan

quality and complete proximal articular surfaces, I digitized gelada specimen M-238034 first and used it as the template for digitizing the remaining specimens for analyses of both the first and second metacarpals. It is possible that selecting a different specimen for the initial template would have yielded different results, though the digitization and semi-landmark approximation methods in the geomorph package are designed to limit this potential issue (Adams et al., 2019). After identifying the fixed landmarks on all specimens, 50 sliding surface semi-landmarks were calculated and added to the point clouds characterizing the proximal articular surface of each metacarpal included in this study. Eight fixed landmarks were selected on the proximal articular surface of both the first and second metacarpal to fully characterized the joint surfaces of interest without reducing the computational efficiency or repeatability across multiple specimens. Introducing additional fixed landmarks and sliding semi-landmarks could reveal additional shape details, but would also substantially slow computational speeds.

Landmark selection

For the first metacarpal, I selected eight fixed landmarks on the proximal articular surface of each specimen where it articulates with the trapezoid. Landmarks were modeled after those used by Marchi and colleagues (2017) and were selected to best characterize the shape of the proximal surface, specifically the outer edges of the trapezoid-Mc1 joint surface. Landmarks 1 and 2 are direct analogues to March et al.'s (2017) volar C1 and dorsal C1, respectively. Additionally, every fixed landmark needed to be repeatable and present on all samples. All fixed landmarks used in this study were identified as follows and visually depicted in Figure 4.2:

Landmark 1 – the most proximal point on the palmar edge

Landmark 2 – the most proximal point on the dorsal edge

Landmark 3 and 4 – the two most radial points along the radial edge

Landmark 5 – the most ulnar point between landmarks 3 and 4 along the radial edge

Landmark 6 and 7 – the two most ulnar points along the ulnar edge

Landmark 8 – the most radial point between landmarks 6 and 7 along the ulnar edge

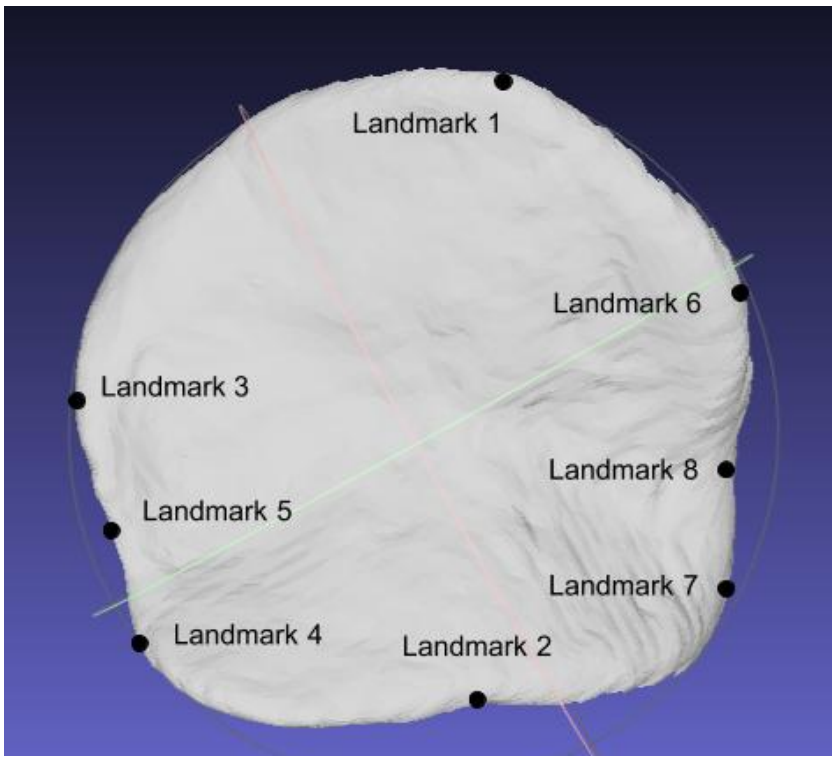

Figure 4.2
Proximal surface of the base of Mc1 where it articulates with the trapezium for gelada specimen M-234038 indicating the placement of landmarks 1 through 8 on the articular surface. Landmarks in this image are visual approximations of the actual points selected for analysis.

For the second metacarpal, I selected eight fixed landmarks on the proximal articular surface with the trapezoid for each specimen. These were chosen based on the same criteria as the first metacarpal. These landmarks best characterize the joint surface in question and are repeatable

across the all specimens. The fixed landmarks used in this study are identified as follows and visually depicted in Figure 4.3:

Landmark 1 – the most palmar point on the palmar edge

Landmark 2 – the palmar extreme of the groove formed by the crest of the trapezoid approximately bisecting the articular surface

Landmark 3 – the point at the dorso-lateral extreme

Landmark 4 – the dorsal extreme of the groove formed by the crest of the trapezoid approximately bisecting the articular surface

Landmark 5 – the point at the dorso-medial extreme

Landmark 6 – the most dorsal point of the semicircular notch in the middle of the medial edge

Landmark 7 – the most palmar point of the semicircular notch in the middle of the medial edge

Landmark 8 – the most lateral point along the medial edge between landmarks 6 and 7

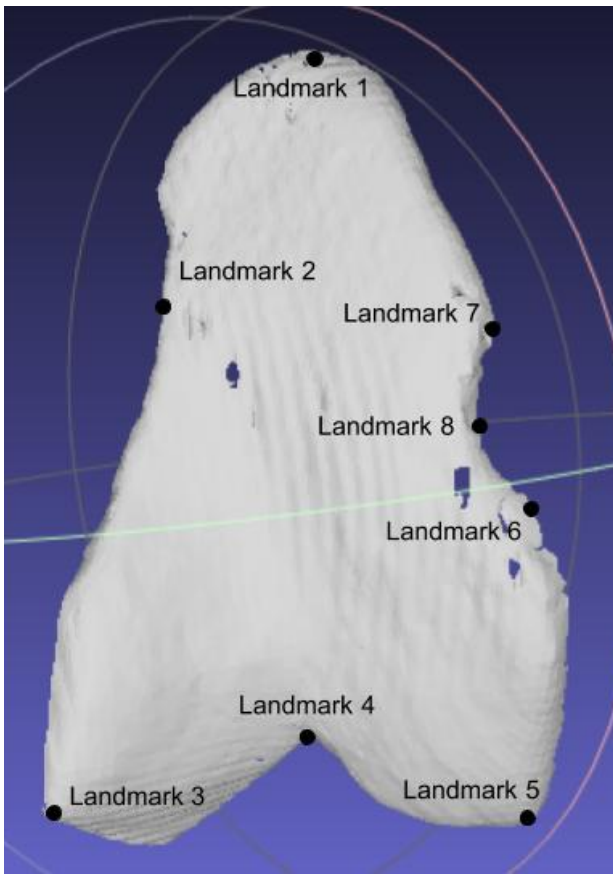

Figure 4.3
Proximal surface of the base of Mc2 where it articulates with trapezoid the for gelada specimen M-234038 indicating the placement of landmarks 1 through 8 on the articular surface. Landmarks in this image are visual approximations of the actual points selected for analysis.

For two specimens, one gelada individual and one baboon individual, only the right hand was available. To include these samples in the analyses, I reflected the 58 3D coordinates across the y-axis by changing the sign of the value for each x coordinate value. There are no known functional differences between the right and left hands of the geladas and baboons from which I collected this sample and the mirrored images of the right metacarpals sufficiently approximate the left metacarpals for my analyses.

Procrustes alignment

Generalized Procrustes analysis (GPA) is a method to statistically compare shape information between multiple objects without the potential confounding variables of orientation and size. Procrustes superimposition must be performed prior to further geometric morphometric analyses to position the point clouds of each specimen in the same component space and accurately compare shape data. The specimens are scaled, transposed, and rotated to align to the computed average of all specimens.

Principal components analysis

Principal components analysis (PCA) provides an effective means of assessing the primary ways in which shape varies across my sample. As there are many variables that account for shape across the surface of any one articular surface and I selected 58 3D points to describe my sample, PCA reduces the dimension of this feature space in which the samples exist to only a few theoretical shapes. Principal component 1 (PC 1) describes the greatest variation in the sample while minimizing error - the point coordinates produced through Procrustes alignment for each sample are projected onto the feature space along PC 1 to maximize the difference between all samples and to minimize distance from the original coordinates. Principal component 2 (PC 2) describes the second greatest amount of variation in the data while being orthogonal to PC 1. At the positive and negative extremes of each principal component score are the warped Procrustes mean shape point clouds describing the shape variation explained by each PC score. These do not represent the actual shapes of any surfaces in my sample and their polarity is arbitrary.

Statistical tests

To test the statistical significance of PC 1 and PC 2 for distinguishing between geladas and baboons in my sample, I performed a Mann-Whitney U test on the principal component scores for each specimen at PC 1 and again and PC 2. The sample sizes included here are very small, resulting in very low statistical power and limited assessment of normality. Additionally, there is no way to guarantee that the collected sample represents a random sample, though it does represent the entire available gelada sample from the AMNH. Given these limitations, any results of U tests should be used to frame further inquiries with larger datasets. The null hypothesis for these U tests is that the distributions of PC scores for geladas and baboons are equal. The alternative hypothesis for each test is that the distributions are not equal.

R code used in digitization, generalized Procrustes alignment, and the principal components analyses is included in the appendix.

Results

First metacarpal

In the principal components analysis for Mc1, PC 1 explains 42.9% of the variation between specimens and PC 2 explains 28.0% of the variation. Principal components 3 through 10 are not morphologically informative and are not included in these results. The two-tailed Mann Whitney U test to compare principal components scores between geladas and baboons yielded a significant result for PC 1 (p = 0.038) only. The null hypothesis for PC 1 was rejected, indicating that the distribution for geladas and baboons is not the same in the component space for PC 1.

The results for PC 2 were not statistically significant (p = 0.171) and the null hypothesis for PC 2 was not rejected. This indicates that there is no significant difference between the distribution of PC 2 scores between geladas and baboons within the sampled populations. Geladas are indicated by red dots labeled 1, 2, 4, and 7 (Figure 4.4).

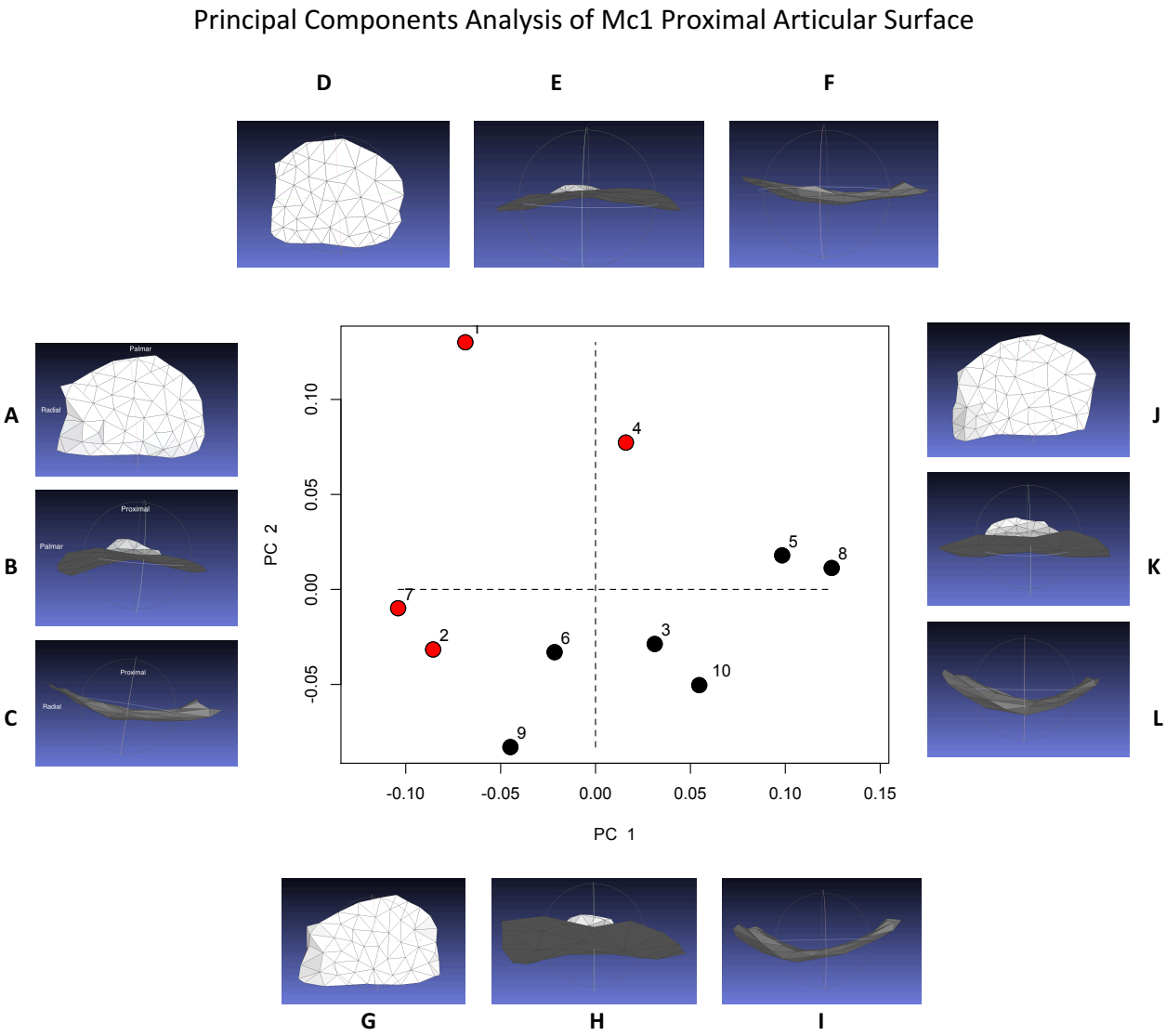

Figure 4.4

PCA of the base of the first metacarpal where it articulates with the trapezium. Red dots 1, 2, 4, and 7 are gelada individuals, falling closer to the negative side of PC 1 and positive side of PC 2. Baboon samples are indicated by the black dots 3, 5, 6, 8, 9, and 10. Baboons group closer to the positive side of PC1 and the negative side of PC2. Images A, B, and C represent the theoretical shape at the negative extreme of PC 1. Images J, K, and L represent the theoretical shape at the positive extreme of PC 1. Images D, E, and F represent the theoretical shape at the positive extreme of PC 2. Images G, H, and I represent the theoretical shape at the negative extreme of PC 2. A, D, G, and J are the proximal view with the palmar aspect oriented toward the top of the page and the radial aspect to the left. B, E, H, and K are the ulnar view with the proximal aspect oriented toward the top of the page and the palmar aspect to the left. C, F, I, and L are the palmar view with the proximal aspect oriented toward the top of the page and the radial aspect to the left.

The shape representing PC 1 is most informative for distinguishing between geladas and baboons in this sample. Geladas are primarily in the negative side of PC 1 with only one individual (M-238034) falling on the positive side of PC 1, though still very close to 0. It is interesting to note that this gelada is the only individual for whom sex data is unavailable. The baboon distribution is more widespread with the majority occupying the positive side of PC 1. The two specimens on the negative side of PC 1 (M-52688 and M-820982) are closer to 0 than the geladas on the negative side of PC 1.

The negative side of PC 1 is radioulnarly flatter compared to the convex curvature of the positive side of PC 1. The positive side of PC 1 is characterized by radial and ulnar edges that are positioned further distally to the midline than on the negative side of PC 1. Additionally, the negative side of PC 1 shows greater concavity in the dorsopalmar direction compared to the positive side of PC 1, though this is relatively slight on the palmar side. There is more pronounced extension at the dorsal edge of the articular facet compared to the positive side of PC 1, indicating the position of the volar beak. The volar beak is most pronounced at the radial side of the dorsal edge of the Mc1 proximal articular facet on the negative side of PC 1.

Though statistically not significant for distinguishing between geladas and baboons, PC 2 does represent shape variation between the positive and negative sides. Half of the geladas fall on the positive side of PC 2 whereas the other half are on the negative side, quite close to 0. Baboons are more consistent, with 2/3 of the sample falling on the negative side and the remaining 1/3 very close to 0 on the positive side of PC 2.

The positive side of PC 2 is characterized by similar measures of radioulnar breadth and dorsopalmar height, making the articular surface quite square. Additionally, the positive side of PC 2 is quite flat in both the radioulnar and dorsopalmar directions. A slight convex curvature along the radioulnar axis and slight concave curvature along the dorsopalmar axis are still present. In contrast to the positive side, the negative side of PC 2 is much more rectangular, possessing greater radioulnar breadth than dorsopalmar height. The negative side of PC 2 exhibits a similar degree of dorsopalmar concave curvature as is present on the positive side of PC 2. The greatest difference in curvature between the two sides of PC 2 is along the radioulnar axis. Where the positive side of PC 2 is only very slightly curved in the convex direction, the negative side of PC 2 shows substantially greater convex curvature along the radioulnar axis. There are also some shape differences along the palmar border of the articular facet between the positive and negative sides of PC 2. The maximum dorsopalmar height of the positive side of PC 2 occurs at the approximate radioulnar midpoint, narrowing more sharply along the radial side and maintaining greater height along the ulnar side. Conversely, the maximum dorsopalmar height on the negative side of PC 2 is to the radial side with opposite trends in decreasing height to what is present on the positive side of PC 2. The dorsopalmar height decreases more on the ulnar side than the radial side, though the angle at which it decreases is approximately equal from the dorsopalmar maximum.

Both geladas and baboons show low dorsopalmar curvature suggesting limited stability, especially when resisting axial forces, though geladas might have greater stability in this

direction than baboons. Geladas and baboons also both show relatively low radioulnar curvature which could limit abduction range. This signal is complicated in this sample and differences between geladas and baboons are contradictory across PC 1 and PC 2. The rectangular shape of the baboon Mc1 could indicate increased stability in resisting radially shifted loads during abduction. While Mc1 base morphology in geladas and baboons is relatively similar, there are differences in stability and range of motion between these two groups. Further details are explored in the discussion.

Second metacarpal

In the principal components analysis for Mc2, PC 1 explains 53.0% of the variation between specimens and PC 2 explains 16.1% of the variation. Principal components 3 through 10 are not morphologically informative and are not included in these results. The two-tailed Mann Whiney U test to compare principal components scores between geladas and baboons yielded a significant result for PC 1 (p = 0.0095) only. The null hypothesis for PC 1 was rejected, indicating that the distribution for geladas and baboons is not the same in the component space for PC 1. The results for PC 2 were not statistically significant (p = 0.257) and the null hypothesis for PC 2 is not rejected. This indicates that there is no statistical difference between the distributions of PC 2 scores for geladas and baboons within the sampled populations. Geladas are again indicated by red dots labeled 1, 2, 4, and 7 (Figure 4.5).

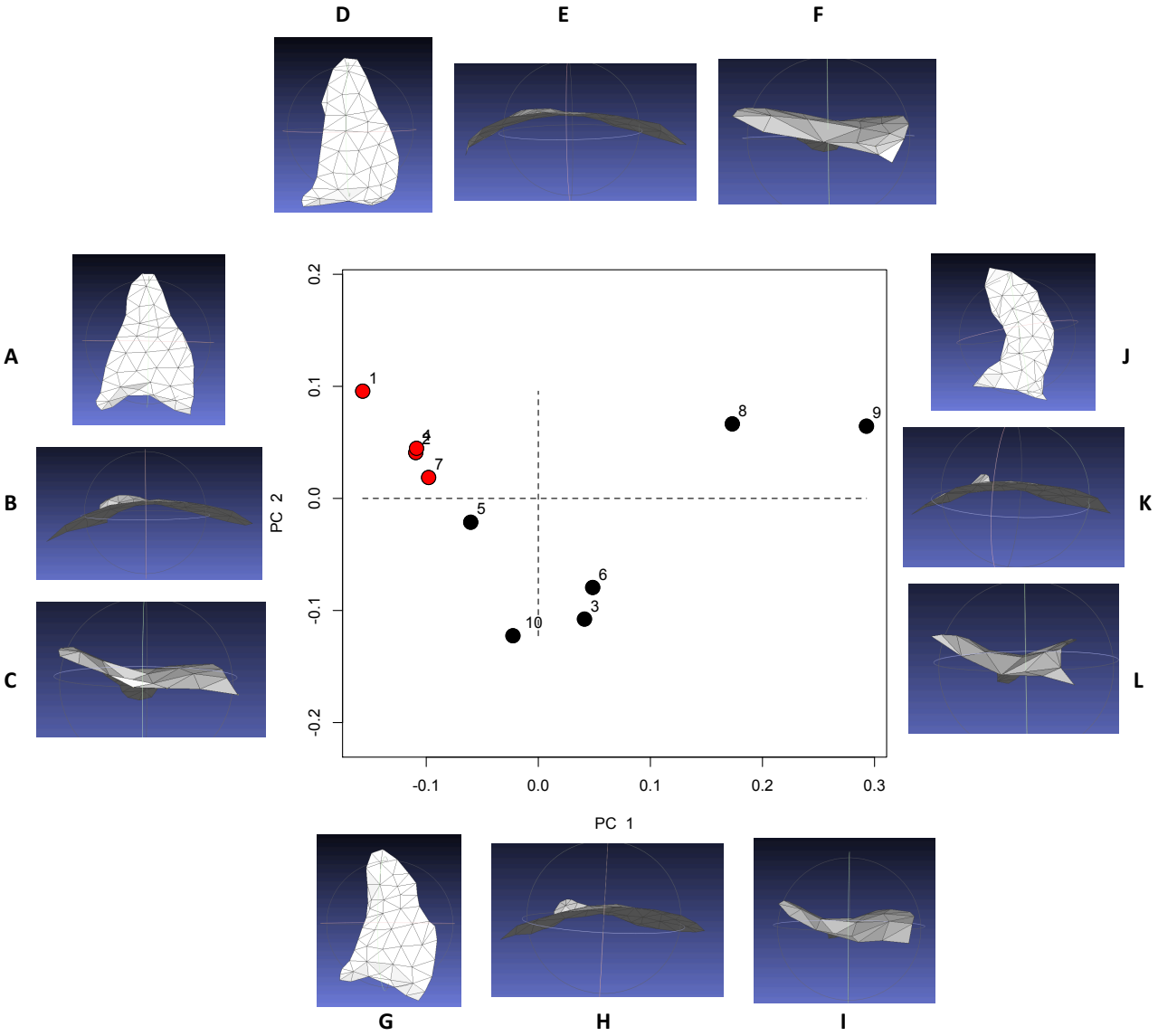

Figure 4.5

PCA of the base of the second metacarpal where it articulates with the trapezoid. Red dots 1, 2, 4, and 7 are gelada individuals, falling closer to the negative side of PC1 and positive side of PC2. Baboon samples are indicated by the black dots 3, 5, 6, 8, 9, and 10. Baboons group closer to the positive side of PC1 and the negative side of PC2. Images A, B, and C represent the theoretical shape at the negative extreme of PC 1. Images J, K, and L represent the theoretical shape at the positive extreme of PC 1. Images D, E, and F represent the theoretical shape at the positive extreme of PC 2. Images G, H, and I represent the theoretical shape at the negative extreme of PC 2. A, D, G, and J are the proximal view with the palmar aspect oriented toward the top of the page and the radial aspect to the left. B, E, H, and K are the ulnar view with the proximal aspect oriented toward the top of the page and the dorsal aspect to the left. C, F, I, and L are the dorsal view with the proximal aspect oriented toward the top of the page and the radial aspect to the left.

PC 1 is most informative for distinguishing between geladas and baboons in this sample. Geladas form a compact group on the negative side of PC 1, whereas baboons are more spread out along PC 1 showing greater shape variation in the feature space. Baboons form a large group that is oriented more on the positive side of PC 1 than geladas and there is no overlap between the baboon and gelada groups. Two baboons fall on the negative side of PC 1 (M-81688 and M-82092) while the remaining four are on the positive side of PC 1.

The positive side of PC 1 is narrower in the radioulnar dimension than the negative side of PC 1, though they are very similar in dorsopalmar dimension. Additionally, the positive side shows a greater proximal extension of the dorso-radial point creating a deeper depression for articulation with the crest of the distal surface of the trapezoid than what is present on the negative side of PC 1. Curvature in the dorsopalmar direction is greater in for the negative side of PC 1, though the difference is very small. The dorsal edge of the articular surface is quite flat for the positive side of PC 1. In contrast, the negative side of PC 1 has a clear indent that extends in the palmar direction at the approximate radioulnar midpoint. The radial and ulnar edges of the negative side of PC 1 are quite straight compared to the positive side of PC 1. The radial edge of positive PC 1 is concave and the ulnar edge is convex, giving the articular surface a crescent appearance that is not present on the negative side of PC 1 with the palmar tip shifted radially. The ulnar side of positive PC 1 also shows a clear, though shallow, semicircular notch at the approximate dorsopalmar midpoint which is absent from negative PC 1.

Though PC 2 is not statistically significant for differentiating between geladas and baboons, it is important to understand any shape variation along this axis to make functional comparisons. Geladas again form a compact group with baboons being more dispersed throughout the feature space. Geladas are all located on the positive side of PC 2 with baboons overlapping with the gelada range and being split across both sides of PC 2. Two baboons fall on the positive side of PC 2 (M-816880 and M-82092) and the other four form a compact group on the negative side of PC 2. Interestingly, these are the same two specimens that depart from the rest of the baboon group along PC 1. It is possible that there is a demographic explanation for this disjointed grouping in baboons, but none is immediately apparent. This could also be an indication of the true variation in baboon morphology and would more clearly represent a single group with the inclusion of more specimens in the sample.

The shape differences between the positive and negative sides of PC 2 are less pronounced that those apparent in PC 1. Along PC 2, both sides have approximately equal radioulnar breadth and dorsopalmar height. The negative side of PC 2 displays a deeper depression for the articulation with the crest of the trapezoid compared to the much flatter articular surface on the positive side of PC 2, especially at the dorsal edge. This is again caused by the proximal projection of the dorso-radial point on the negative side of PC 2. The positive side of PC 2 there is greater dorsopalmar convexity than the moderate convex curvature on the negative side of PC 2. The semicircular notch on the ulnar edge is apparent, though subtle, on the negative side of PC 2 but is absent from the positive side. Additionally, the dorsal edge of negative PC 2 has an indent projecting palmarly at the approximate radioulnar midpoint. This ident is much

smaller and ulnarly oriented on the positive side of PC 2. Across the entire PC 2 feature space, the indent is shallower than the extreme of the negative side of PC 1. Both positive and negative PC 2 have a concave curvature along the radial edge, however the palmar tip of positive PC 2 bends toward the radioulnar midpoint creating a soft "S" with the convex curvature subtler than the convex curvature. The ulnar edge is very similar for positive and negative sides of PC 2 showing soft convex curvature.

Geladas have a shallower depression for the crest of the trapezoid than baboons, suggesting geladas have less passive stability at the trapezoid-Mc2 articulation. High stability at this joint is important for maintaining digitigrade hand postures. In the dorsopalmar direction, geladas exhibit greater curvature than baboons possibly indicating greater flexion-extension range than baboons. Limitations to this range of motion might be important during high-speed running when baboons shift from digitigrade to palmigrade postures. These functional differences are explored in greater detail in the discussion.

Discussion

These analyses have demonstrated that there are many broad similarities between geladas and baboons in proximal articular surface morphology across Mc1 and Mc2, though there are some important characteristics to acknowledge. At the Mc1-trapezium articulation, both geladas and baboons exhibit relatively low stability. This is likely indicative of a higher involvement of this carpometacarpal joint in manipulative tasks than locomotor activities, given their primarily digitigrade locomotion. Some slight differences in stability between geladas and baboons could related to thumb position and object size during manipulation, though this signal is complicated

in this sample. For the Mc2-trapezoid articulation, baboons exhibit greater passive stability and less flexion-extension range than geladas. This may be related to differences in locomotion between the two taxa. Greater stability at this carpometacarpal joint could be beneficial for efficient propulsion during high speed running for baboons.

First metacarpal

Marzke and colleagues (2010) conducted 3D analyses of curvature of the proximal articular surface of the first metacarpal in extant hominoids, *Papio*, and some fossil hominins. Their results showed that *Papio* exhibits a significant lack of curvature in both the dorsopalmar and radioulnar directions compared to the other extant species included in the study. Greater dorsopalmar curvature creates a long volar (palmar) beak while lower dorsopalmar curvature is associated with a reduced volar beak. A long, projecting volar beak helps to stabilize the trapezio-metacarpal joint, especially in resisting dorsal subluxation of the Mc1 frequently caused by strong axial forces on a flexed thumb. In my sample, neither the baboons nor the geladas exhibited very pronounced projections of the volar beak as compared to extant apes featured in Marzke et al. (2010), however there is greater dorsopalmar curvature especially at the palmar edge of the articular surface on the negative side of PC 1 comparted to the positive side of PC 1. Geladas clumped closer to the positive side of PC 1 than baboons did as a group. This difference in dorsopalmar curvature between geladas and baboons could indicate that geladas have a more stable trapezio-metacarpal joint than baboons.

Additionally, the greater dorsopalmar curvature which characterizes the negative side of PC 1 has been observed and is exaggerated in gorillas (Marzke et al., 2010; Marchi et al., 2017). It has similarly been interpreted as a favorable trait for stability in the trapezio-metacarpal joint. Stability in this joint for gorillas could be an adaptation to forceful pulling and ripping of vegetation during foraging (Marzke, 2005). A comparison that includes *Theropithecus* with extant apes and *Papio* would help determine the degree of morphological similarity in dorsopalmar curvature of the proximal articular surface of Mc1 in geladas and gorillas. It is possible that the greater dorsopalmar curvature of geladas and associated higher stability compared to baboons indicates a similar difference behaviorally, especially regarding pulling of plant material prior to feeding. Geladas also process vegetation manually by plucking grasses between the thumb and forefinger, however the precise mechanics of gorilla pulling behaviors and gelada manual foraging need to be further explored to fully understand the involvement of the trapezio-metacarpal joint in either activity.

Also because geladas fall mainly on the negative side of PC 1, the proximal articular surface of Mc1 in geladas is generally less curved in the radioulnar direction than what is present in baboons according to that aspect of the feature space. Conversely, PC 2 suggested no differences in dorsopalmar curvature from the positive to negative sides, but does indicate greater radioulnar curvature on the negative side of the component space. The grouping of geladas along PC 2 could be split in half with two individuals on the far positive extreme and two on the negative side very close to 0. The high positive PC 2 score for half of the geladas and the associated lack of radioulnar curvature seemingly contradicts the shape variation explained

by PC 1, suggesting that geladas possess relatively greater curvature in the radioulnar direction than baboons. It is possible that the gelada sample represents two meaningful demographic groups, though no clear divisions are immediately apparent given the available data. It is also possible, and perhaps more likely, that the gelada distribution in this feature space and seeming divide is reflective of a very small sample and additional specimens would mitigate any contradictory shape variation across PC 1 and PC 2.

Rose (1992) examined the trapeziometacarpal joint mobility, stability, and strength across several primate groups and found that the cercopithecines sampled (including *Papio* but not *Theropithecus*) differed most from humans in abduction-adduction range and least in flexion-extension capabilities. Combined with the morphological assessments of Marzke et al. (2010) and Marchi et al. (2017), the general lack curvature observed in humans and *Papio* relative to non-human apes allows for a high degree of flexion and extension. More specifically, the low degree of radioulnar curvature observed for *Papio* (Marzke et al. 2010) could limit abduction range essential for the manipulation of large objects and opposition of the thumb. In this sample, the complexity of radioulnar curvature across PC 1 and PC 2 makes the differentiation between this metric for geladas and baboons very difficult. Of potentially greater importance to abduction-adduction range as it relates to the opposition of the thumb to the fingers is the radial extension of the Mc1 joint surface. The negative side of PC 2, where most baboons group in this study, shows a more rectangular joint surface with greater radioulnar breadth than the positive side. In precision grasping, the abduction of the thumb results in a radially shifted load across the trapeziometacarpal joint surface (Rose, 1992; Marzke et al., 2010). The greater

radioulnar extension of the Mc1 proximal articular surface along PC 2 could indicate that baboons have a more stable trapeziometacarpal joint compared to geladas when resisting a radially shifted load as in abduction. This study examined the joint surfaces in isolation so the position of the joint surface relative to the diaphysis is unknown for the theoretical warpgrids produced via PCA.

Second metacarpal

The morphology of the proximal articular surface of the second metacarpal has received relatively less attention in anthropological literature than the Mc1. This is a complex articular surface with many facets and articulations with the trapezium, trapezoid, capitate, and Mc3. In this study, analyses have been limited to the trapezoid – Mc2 articulation for clarity. In humans, this joint is characterized by a high degree of stability in all axes limiting frequent injury or dislocation (El-shewwany et al., 2001; Rincón Cardozo et al., 2016; Dhammi et al., 2000; Lewis, 1973). In addition to the unique joint surface geometry, there are strong ligamentous attachments that restrict radioulnar deviation, pronation-supination, and to a slightly lesser degree flexion-extension in humans (El-shewwany et al., 2001; Nakamura et al., 2001). Previous functional assessments in anthropological literature of the trapezoid-Mc2 joint have focused on apes and the contribution of carpal morphology to joint function to assess the fossil record (e.g., Tocheri et al., 2003; 2005).

The shape variation associated with the gelada grouping for Mc2 is more congruent across PC 1 and PC 2 than what was present for Mc1. Generally, geladas are characterized by a flattened

depression for the crest of the trapezoid, greater dorsopalmar curvature, slightly greater radioulnar breadth, and the lack of an apparent notch on the ulnar edge compared to baboons. Baboons more consistently trended toward the sides of the component space associated with a more pronounced depression for the crest of the trapezoid, reduced dorsopalmar curvature and radioulnar breadth, and a clear semicircular notch on the ulnar edge. The only inconsistent morphological variation was in the indent along the dorsal edge. Along PC 1, geladas are characterized by a significant indent at the radioulnar midpoint of the dorsal edge, contrary to PC 2.

The deep wedging of the Mc2 on the distal surface of the trapezoid characterizes African apes and, along with several ligaments, stabilizes the second carpometacarpal joint (Marzke et al., 1983). For digitigrade species, the close configuration of the carpal bones, especially at the Mc2 base, could limit the necessity for muscular stabilization and allow for a more passive maintenance of digitigrade hand posture (Tuttle, 1969 as cited by Patel, 2010; though see Preuschoft, 1937). In my sample, baboons exhibited a deeper depression for the crest of the trapezoid than geladas. This greater degree of interlocking between these bones could be responsible for greater passive stability through the wrist in digitigrade postures than what is present in geladas. Though the locomotor regimes of baboons and geladas are very similar, the unique feeding ecology of geladas results in some important differences in hand posture during locomotion between the two groups. While foraging, geladas sit back on their ischial callosities and fatty pads to shuffle along the ground freeing their hands to collect grasses (Jolly, 1970; Pocock, 1925; Wrangham, 1980). It is possible that the frequency of digitigrade postures is

higher in baboons, necessitating greater passive stability at the trazepoid-Mc2 joint than is necessary for geladas.

Another distinguishing morphological difference between geladas and baboons in my sample is dorsopalmar curvature. Geladas exhibit greater dorsopalmar convexity than baboons, though the range of variation present for the included baboons is high in this characteristic. It is possible that the relatively flatter joint surface for baboons limits the range of flexion and extension. During high speed running, habitually digitigrade baboons adopt palmigrade postures (Patel, 2010; Patel and Wunderlich, 2010), requiring extension at the wrist. A limited range of motion in baboons compared to geladas could prevent hyper extension and create a more efficient lever during push off at high speeds.

By including additional articular facets to characterize the morphology of the Mc2 base, further analyses can be conducted of the range of motion for pronation and supination as well. In humans, the transverse orientation of the articular facets for the trapezium and capitate on the base of Mc2 could distribute high loads through the trapezoid and allow for pronation of the Mc2 (Tocheri et al., 2003; 2005). The relative orientation of the joint surfaces is approximated in the feature space and cannot be truly known based on the PCA projections. Examination of the entire base of Mc2, the capitate, and the trapezium is necessary to confidently assess the orientation of the trapezoid-Mc2 facet relative to the transverse plane. Without these additional facets, it is unclear how the morphology of the trapezoid-Mc2 joint impacts pronation.

The apparent differences in radioulnar breadth and the presence of the semicircular notch along the ulnar edge are slight. Marzke (1983) found that the appearance of the semicircular notch which indicates a separation of the Mc2-Mc3 facet into two halves is variable within primate species. Any functional differences are unknown at this time and could be evaluated with additional sampling. Geladas are absent from much of the previous literature and it is possible that a greater proportion of geladas than baboons possess the single facet condition.

This study is limited by the small sample and the availability of gelada skeletal material in museum collections. Additional analyses with larger samples will help to substantiate these findings and more fully characterize differences in morphology, especially relative to Mc 2. Several species of baboons are included in the sample and treated as one group throughout these analyses. There are behavioral and morphological differences between these species (e.g. Chapter 5 of this study). Future analyses would benefit from an examination of species level differences rather than only genus level distinctions, again, bolstered by larger sample sizes. Likewise, the inclusion of previously examined taxa, such as apes, would further our understanding of the scale of anatomical differences observed and the associated inferred functional differences. Within the current sample, the interpretation of the degree of stability at trapezium-Mc1 joint is limited because the relative position of the diaphyses was not included. Using the same CT scans, this information could be included. The associated carpals are also available for the sampled individuals. Because the degree of joint surface congruence varies between and within individuals (reviewed in Marzke et al., 2010), assessing the

associated trapezium and trapezoid articular facets (e.g., Tocheri et al., 2003, 2005) could enhance our understanding of differences in function at the carpometacarpal joints for these taxa.

Conclusions

Manual differences between geladas and baboons have historically been characterized almost exclusively by digit proportions. To further elucidate morphological and associated functional differences in the hands of these closely related primate groups, a detailed analysis of the first and second metacarpal bases is essential. Though many similarities exist, the primary differences are as follows:

Mc1

1. Geladas and baboons differ in Mc1 in the degree of dorsopalmar curvature with geladas exhibiting a greater degree and baboons a lesser degree. This curvature is associated with greater joint stability and could be associated with forceful pulling of vegetation.
2. Radioulnar curvature of Mc1 needs more attention and more samples. This is important for understanding any potential differences in flexion and extension capabilities between geladas and baboons.
3. Radioulnar breadth of the Mc1 joint surface could be informative for understanding abduction and associated opposition. Assessment of the proximal articular surface relative to the diaphysis of Mc1 is necessary to understand if the greater radioulnar

breadth associated more with baboons than geladas in this sample is the result of radial extension (rather than ulnar extension or equal radial and ulnar extension).

Mc2

1. Baboons show a higher degree of interlocking at the trapezoid-Mc2 joint reflected by the deep depression for the crest of the Mc2 than what is present in geladas. This pattern could be linked to variations in locomotor regime between the two groups, with baboons more frequently adopting digitigrade postures throughout the day or palmigrade postures at high speeds than geladas.
2. Geladas exhibit greater dorsopalmar curvature than baboons though the range of variation is high across the baboon sample. This difference in curvature could indicate differences in flexion-extension with geladas possessing greater mobility. Further analyses are necessary to substantiate this claim.

Works Cited

Adams, D.C., Collyer, M., Kaliontzopoulou, A., & Sherratt, E. (2016). Geomorph: Software for geometric morphometric analyses. R package version 3.1.0. https://cran.r-project.org/package=geomorph.

Adler, D., Nenadic, O., & Zucchini, W. (2003). Rgl: A r-library for 3d visualization with opengl. In *Proceedings of the 35th Symposium of the Interface: Computing Science and Statistics, Salt Lake City* (35), 1-11.

Amorim, P. H., de Moraes, T. F., Azevedo, F. D. S., & da Silva, J. V. (2011). InVesalius: Software livre de imagens médicas. *Centro de Tecnologia da Informação Renato Archer-CTI, campinas/SP–2011-CSBC2011*.

Amorim, P., Moraes, T., Silva, J., & Pedrini, H. (2015). InVesalius: an interactive rendering framework for health care support. In *International symposium on visual computing* (pp. 45-54). Springer, Cham.

Callieri, M., Dellepiane, M., Ranzuglia, G., Cignoni, P., & Scopigno, R. (2009). Meshlab as a Complete Open Tool for the Integration of Photos and Colour with High Resolution 3D Geometry Data. In *Archaeology in the Digital Era Volume II, e-Papers from the 40th Conference on Computer Applications and Quantitative Methods in Archaeology, Southampton, 26-30 March 2012* (pp. 406-16).

Cardozo, D.F.R., Plata, G.V., Casas, J.A.C., & Rodríguez, N.S. (2016). Acute Dislocation of the Metacarpal-Trapezoid Joint. *Clinics in orthopedic surgery*, *8*(2), 223-227.

Cignoni, P., Callieri, M., Corsini, M., Dellepiane, M., Ganovelli, F., & Ranzuglia, G. (2008, July). Meshlab: an open-source mesh processing tool. In *Eurographics Italian chapter conference* (Vol. 2008, pp. 129-136).

Collyer, M. L., & Adams, D.C. (2018). RRPP: An r package for fitting linear models to high-dimensional data using residual randomization. *Methods in Ecology and Evolution*, *9*(7), 1772-1779.

Collyer, M. L., & Adams, D.C. (2019). RRPP: Linear model evaluation with randomized residuals in a permutation procedure. R package version 0.4.0. https://cran.r-project.org/web/packages/RRPP

de Moraes, T.F., Amorim, P.H., Azevedo, F.S., & da Silva, J.V. (2011). InVesalius—An open-source imaging application. *Comput Vis Med Image Process*, 405.

Dhammi, I.K., Jain, A.K., & Arora, A. (2001). Isolated dislocation of the second metacarpal at both ends. *Journal of orthopaedic trauma*, *15*(2), 143-145.

Dunbar, R.I.M. (1983). Theropithecines and hominids: Contrasting solutions to the same ecological problem. *Journal of Human Evolution*, *12*(7), 647-658.

Dunbar, R.I.M. (1988). *Primate social systems.* Ithaca, New York. Cornell University Press.

El-shennawy, M., Nakamura, K., Patterson, R.M., & Viegas, S.F. (2001). Three-dimensional kinematic analysis of the second through fifth carpometacarpal joints. *The Journal of hand surgery*, *26*(6), 1030-1035.

Fashing, P.J., Nguyen, N., Venkataraman, V.V., & Kerby, J.T. (2014). Gelada feeding ecology in an intact ecosystem at Guassa, Ethiopia: variability over time and implications for theropith and hominin dietary evolution. *American Journal of Physical Anthropology*, *155*(1), 1-16.

Jolly, C.J. (1970). The seed-eaters: a new model of hominid differentiation based on a baboon analogy. In *Primate Evolution and Human Origins* (pp. 323-332). Routledge.

Lewis, H.H. (1973). Dislocation of the Second Metacarpal: Report of a Case. *Clinical Orthopaedics and Related Research (1976-2007)*, *93*, 253-255.

Marchi, D., Proctor, D.J., Huston, E., Nicholas, C.L., & Fischer, F. (2017). Morphological correlates of the first metacarpal proximal articular surface with manipulative capabilities in apes, humans and South African early hominins. *Comptes Rendus Palevol*, *16*(5-6), 645-654.

Marzke, M.W. (1983). Joint functions and grips of the Australopithecus afarensis hand, with special reference to the region of the capitate. *Journal of Human Evolution*, *12*(2), 197-211.

Marzke, M.W. (2005). Who made stone tools. *Stone knapping: the necessary conditions for a uniquely hominin behaviour. Cambridge: McDonald Institute for Archaeological Research*, 243-256.

Marzke, M.W., Tocheri, M.W., Steinberg, B., Femiani, J.D., Reece, S.P., Linscheid, R.L., ... & Marzke, R.F. (2010). Comparative 3D quantitative analyses of trapeziometacarpal joint surface curvatures among living catarrhines and fossil hominins. *American Journal of Physical Anthropology: The Official Publication of the American Association of Physical Anthropologists*, *141*(1), 38-51.

Nakamura, K., Patterson, R.M., & Viegas, S.F. (2001). The ligament and skeletal anatomy of the second through fifth carpometacarpal joints and adjacent structures. *The Journal of hand surgery*, *26*(6), 1016-1029.

Niewoehner, W.A. (2000). *The functional anatomy of Late Pleistocene and recent human carpometacarpal and metacarpophalangeal articulations*. (Doctoral dissertation) University of New Mexico, New Mexico.

Niewoehner, W.A. (2005). A geometric morphometric analysis of Late Pleistocene human metacarpal 1 base shape. In *Modern morphometrics in physical anthropology* (pp. 285-298). Springer, Boston, MA.

Patel, B.A. (2010). Functional morphology of cercopithecoid primate metacarpals. *Journal of human evolution*, *58*(4), 320-337.

Patel, B.A., & Wunderlich, R.E. (2010). Dynamic pressure patterns in the hands of olive baboons (*Papio anubis*) during terrestrial locomotion: implications for cercopithecoid primate hand morphology. *The Anatomical Record: Advances in Integrative Anatomy and Evolutionary Biology*, *293*(4), 710-718.

Pietroni, N., Tarini, M., & Cignoni, P. (2009). Almost isometric mesh parameterization through abstract domains. *IEEE Transactions on Visualization and Computer Graphics*, *16*(4), 621-635.

Pocock, R.I. (1925). 57. The External Characters of the Catarrhine Monkeys and Apes. In *Proceedings of the Zoological Society of London* (Vol. 95, No. 4, pp. 1479-1579). Oxford, UK: Blackwell Publishing Ltd.

Preuschoft, H. (1973). Body posture and locomotion in some East African Miocene Dryopithecinae. In Day, M. (ed) *Human evolution*, 13-46.

R Core Team (2019). R: A language and environment for statistical computing. R Foundation for Statistical Computing, Vienna, Austria. URL https://www.R-project.org/.

Rose, M.D. (1992). Kinematics of the trapezium-1st metacarpal joint in extant anthropoids and Miocene hominoids. *Journal of Human Evolution*, *22*(4-5), 255-266.

Schindelin, J., Arganda-Carreras, I., Frise, E., Kaynig, V., Longair, M., Pietzsch, T., ... & Tinevez, J. Y. (2012). Fiji: an open-source platform for biological-image analysis. *Nature methods*, *9*(7), 676-682.

Tocheri, M.W., Marzke, M.W., Liu, D., Bae, M., Jones, G.P., Williams, R.C., & Razdan, A. (2003). Functional capabilities of modern and fossil hominid hands: Three-dimensional analysis of trapezia. *American Journal of Physical Anthropology: The Official Publication of the American Association of Physical Anthropologists*, *122*(2), 101-112.

Tocheri, M.W., Razdan, A., Williams, R.C., & Marzke, M.W. (2005). A 3D quantitative comparison of trapezium and trapezoid relative articular and nonarticular surface areas in modern humans and great apes. *Journal of Human Evolution*, *49*(5), 570-586.

Tuttle, R.H. (1969). Terrestrial trends in the hands of the Anthropoidea. A preliminary report. *Proceedings Second International Congress of Primatology*, (2), 192-200.

Wrangham, R.W. (1980). Bipedal locomotion as a feeding adaptation in gelada baboons, and its implications for hominid evolution. *Journal of Human Evolution*, *9*(4), 329-331.

Appendix 4.1

R code for all analyses

```
> library(geomorph)
Loading required package: RRPP
Loading required package: rgl
```

```
> setwd("/Users/sarahedlund/Desktop/Scans/GM_files")
> MC1.list <- list.files(pattern=".nts")
> MC1.list
 [1] "AMNH19006MC1gel.nts"
 [2] "AMNH200763MC1gel.nts"
 [3] "AMNH200847MC1-reflectedbab.nts"
 [4] "AMNH238034MC1gel.nts"
 [5] "AMNH35120MC1bab.nts"
 [6] "AMNH52688MC1bab.nts"
 [7] "AMNH60568MC1-reflectedgel.nts"
 [8] "AMNH81688MC1bab.nts"
 [9] "AMNH82092MC1bab.nts"
[10] "AMNH82097MC1bab.nts"
> MC1all <- readmulti.nts(MC1.list)
> x <- 9:58
> plotTangentSpace
function (A, axis1 = 1, axis2 = 2, warpgrids = TRUE, mesh = NULL,
    label = NULL, groups = NULL, legend = FALSE, ...)
> grp <- factor(c(1,1,0,1,0,0,1,0,0,0))
> GPAall <- gpagen(MC1all, surfaces = x)
  |============================================================| 100%
> GPAall

Call:
gpagen(A = MC1all, surfaces = x)

Generalized Procrustes Analysis
with Partial Procrustes Superimposition

8 fixed landmarks
50 semilandmarks (sliders)
3-dimensional landmarks
6 GPA iterations to converge
Minimized Bending Energy used


Consensus (mean) Configuration

           X           Y           Z
1   0.018785398  0.146415906 -2.484311e-02
2  -0.006705457 -0.116310907 -3.919001e-02
3   0.168717995  0.001349595  2.851012e-02
4   0.154244297 -0.088617931  2.049371e-02
5   0.158904415 -0.048459431  2.888115e-02
6  -0.149700213  0.072826008  2.089034e-02
7  -0.168031187 -0.065309870  3.342409e-02
8  -0.150350828 -0.002360867  3.770566e-02
9   0.013599321 -0.002782509 -1.060367e-02
10  0.161904188  0.002499427  2.503905e-02
11 -0.145633118  0.047126051  2.202920e-02
12  0.073810421  0.005069982 -1.635542e-03
13  0.111227608 -0.111299985 -4.222670e-03
14 -0.042238506 -0.038467551 -1.407687e-02
```

```
15 -0.044879459  0.134590578 -1.752909e-02
16  0.066942717 -0.120550226 -2.345052e-02
17 -0.159505007 -0.034055186  3.993627e-02
18 -0.098332314  0.033561276  3.229073e-03
19 -0.145564950  0.010780288  3.171231e-02
20  0.058098175  0.145561601 -1.429898e-02
21 -0.099611734 -0.073163705 -1.025583e-02
22  0.041047632  0.036696667 -9.004109e-03
23  0.122801708  0.099614057  9.586723e-03
24  0.147383494  0.071710328  2.191751e-02
25  0.041656527  0.108200539 -2.080287e-02
26  0.161345764  0.036954806  2.970839e-02
27 -0.057484132 -0.071739212 -2.061618e-02
28  0.045596283 -0.090889636 -2.367974e-02
29  0.109392825  0.039818245  4.551384e-03
30 -0.055501173  0.053485419 -9.133959e-03
31  0.001161586  0.086693457 -1.972041e-02
32  0.082152278 -0.038634975 -5.099551e-05
33 -0.005773006  0.044760816 -1.498465e-02
34 -0.085717177  0.074003389 -5.837632e-03
35  0.011291648  0.144279944 -2.484569e-02
36 -0.080912295 -0.107305204 -2.386921e-02
37 -0.123126689 -0.008525977  1.538639e-02
38 -0.092258940  0.108293368 -6.119175e-03
39  0.094721359 -0.075834150 -3.153908e-03
40 -0.028226737 -0.111711117 -3.636898e-02
41 -0.055323376  0.018910921 -4.639091e-03
42 -0.044016309  0.097073941 -1.653393e-02
43  0.135755283 -0.055695452  1.768199e-02
44 -0.025694420  0.001113902 -1.040924e-02
45 -0.129856831 -0.098775589 -1.559492e-03
46  0.034570620 -0.041074244 -1.311845e-02
47  0.072925206  0.072230993 -1.046659e-02
48  0.117724826 -0.010377423  1.308882e-02
49 -0.132092512  0.081232950  6.714976e-03
50  0.017685227 -0.118080528 -3.552353e-02
51  0.090736150  0.121745356 -2.380092e-03
52 -0.005882794 -0.067808050 -2.469998e-02
53 -0.160929895 -0.078050942  2.426083e-02
54 -0.099865719 -0.037940338  2.605988e-03
55 -0.133689371 -0.057593591  1.140613e-02
56  0.153972432 -0.028161385  2.455552e-02
57  0.144953422 -0.093031867  1.374836e-02
58 -0.081482256 -0.008034368  1.413107e-03
> PCA.MC1all <- plotTangentSpace(GPAall$coords, label = TRUE, groups = grp)
> PCA.MC1all

PC Summary

Importance of first k=9 (out of 10) components:
                            PC1     PC2     PC3     PC4     PC5
Standard deviation      0.07796 0.06305 0.03699 0.0302  0.02531
Proportion of Variance 0.42854 0.28034 0.09648 0.0643  0.04516
```

```
Cumulative Proportion  0.42854     0.70889           0.80536           0.8697           0.91482
                              PC6       PC7               PC8               PC9
Standard deviation     0.02469     0.01907           0.01249           0.008851
Proportion of Variance 0.04299     0.02566           0.01100           0.005520
Cumulative Proportion  0.95782     0.98347           0.99448           1.000000
> PCA.MC1$pc.scores
                                PC1                PC2                PC3
AMNH19006MC1gel          -0.06859151  0.130079972 -0.01058853
AMNH200763MC1gel         -0.08557077 -0.031609048 -0.02379028
AMNH200847MC1-reflectedbab  0.03118514 -0.028715623 -0.03191406
AMNH238034MC1gel          0.01600505  0.077303163  0.03434349
AMNH35120MC1bab           0.09832940  0.017931467  0.05836957
AMNH52688MC1bab          -0.02157638 -0.033025652  0.01622117
AMNH60568MC1-reflectedgel  -0.10402293 -0.009891385 -0.01259530
AMNH81688MC1bab           0.12443900  0.011276628 -0.06907169
AMNH82092MC1bab          -0.04484902 -0.082971035  0.02566535
AMNH82097MC1bab           0.05465201 -0.050378488  0.01336027
                               PC4                PC5
AMNH19006MC1gel          -0.034401966  0.0007756525
AMNH200763MC1gel         -0.009685837 -0.0071369342
AMNH200847MC1-reflectedbab  0.011346927 -0.0077764445
AMNH238034MC1gel          0.064162959 -0.0195510755
AMNH35120MC1bab          -0.037767055  0.0037739889
AMNH52688MC1bab           0.024086957  0.0634427151
AMNH60568MC1-reflectedgel  -0.003728034  0.0039968666
AMNH81688MC1bab           0.006462425  0.0001063829
AMNH82092MC1bab           0.004109269 -0.0347215640
AMNH82097MC1bab          -0.024585645 -0.0029095878
                               PC6                PC7
AMNH19006MC1gel           0.0256041762 -0.0116473781
AMNH200763MC1gel         -0.0288308829  0.0007140259
AMNH200847MC1-reflectedbab -0.0229554713 -0.0415536791
AMNH238034MC1gel         -0.0106566083  0.0083492077
AMNH35120MC1bab          -0.0199348050 -0.0036022235
AMNH52688MC1bab           0.0166631152 -0.0062604523
AMNH60568MC1-reflectedgel  -0.0211859696  0.0257519430
AMNH81688MC1bab           0.0183211824  0.0168089846
AMNH82092MC1bab           0.0435884570 -0.0060848279
AMNH82097MC1bab          -0.0006131938  0.0175243998
                               PC8                PC9
AMNH19006MC1gel           0.0034514704  0.003587463
AMNH200763MC1gel         -0.0241341954  0.008625814
AMNH200847MC1-reflectedbab  0.0131493365 -0.001637517
AMNH238034MC1gel         -0.0002722758  0.003981860
AMNH35120MC1bab          -0.0089902413 -0.009474211
AMNH52688MC1bab          -0.0028498549  0.001253409
AMNH60568MC1-reflectedgel   0.0146158124 -0.013159741
AMNH81688MC1bab          -0.0075704744 -0.004786438
AMNH82092MC1bab          -0.0036398885 -0.005250102
AMNH82097MC1bab           0.0162403109  0.016859466

> MC2.list = list.files(pattern = "*.nts")
> MC2.list
```

```
 [1] "AMNH19006MC2gel.nts"
 [2] "AMNH200763MC2gel.nts"
 [3] "AMNH200847MC2-reflectedbab.nts"
 [4] "AMNH238034MC2gel.nts"
 [5] "AMNH35120MC2bab.nts"
 [6] "AMNH52688MC2bab.nts"
 [7] "AMNH60568MC2-reflectedgel.nts"
 [8] "AMNH81688MC2bab.nts"
 [9] "AMNH82092MC2bab.nts"
[10] "AMNH82097MC2newbab.nts"
> MC2.all = readmulti.nts(MC2.list)
> x <- 9:58
> grpMC2 <- factor (c(1, 1, 0, 1, 0, 0, 1, 0, 0, 0))
> GPA_MC2 <- gpagen(MC2.all, surfaces = x)
  |=========================================================| 100%
> GPA_MC2

Call:
gpagen(A = MC2.all, surfaces = x)



Generalized Procrustes Analysis
with Partial Procrustes Superimposition

8 fixed landmarks
50 semilandmarks (sliders)
3-dimensional landmarks
6 GPA iterations to converge
Minimized Bending Energy used

Consensus (mean) Configuration

           X                Y               Z
1  -0.237000396 -0.015587506 -0.0418965905
2  -0.097194198 -0.068606641 -0.0167447063
3   0.129517717 -0.121064551  0.0091018512
4   0.133116236  0.009904076 -0.0392377860
5   0.161470222  0.065021985 -0.0457653495
6  -0.019184866  0.101504500  0.0220767567
7  -0.089184957  0.076552009  0.0163281736
8  -0.060280924  0.081205673  0.0191147925
9   0.035741665  0.035386797  0.0124310130
10 -0.018080740  0.057018419  0.0255036831
11 -0.081604093 -0.015361471  0.0051579518
12  0.099916308  0.099251522  0.0020646003
13  0.026844253  0.076829340  0.0209386658
14 -0.126593812 -0.024620010 -0.0051681822
15  0.049225131 -0.006863202  0.0048661110
16 -0.072952893 -0.059416568 -0.0055168919
17  0.082444901 -0.044701753  0.0057943799
18  0.146675495  0.029961955 -0.0375288988
19  0.159540745  0.066766842 -0.0429377801
```

```
20  0.130333686 -0.088769351 -0.0048532485
21 -0.043555085 -0.065166428  0.0020551522
22 -0.221586662 -0.034577099 -0.0375540287
23  0.121021171  0.062598561 -0.0097327025
24  0.156325084  0.047081273 -0.0383013652
25 -0.003071428 -0.034006713  0.0103003654
26  0.103461202 -0.082032230  0.0137876933
27  0.075442166 -0.093194489  0.0248602410
28 -0.187365090 -0.057193132 -0.0343283352
29 -0.012507373 -0.070592334  0.0110490985
30 -0.071354230  0.075718843  0.0211108091
31  0.081785269  0.060043218  0.0061083236
32 -0.099846987 -0.056038901 -0.0121850552
33 -0.004373530  0.009804553  0.0134141576
34 -0.136097460  0.012211399  0.0049104416
35  0.060257785  0.103641670  0.0160008858
36  0.041676531 -0.050003382  0.0146890771
37 -0.144569841 -0.061876140 -0.0249866789
38  0.123701409 -0.118397179  0.0149803701
39  0.120347118  0.001091901 -0.0249326909
40  0.123614084 -0.032798490 -0.0212222511
41  0.093567028 -0.112191478  0.0266615596
42  0.135044712  0.083820988 -0.0159153764
43 -0.174925682  0.027408347 -0.0008350043
44  0.014440840  0.106836863  0.0222107742
45  0.131644588  0.025247714 -0.0284461336
46 -0.076683249  0.031346615  0.0189915751
47 -0.220647060 -0.001884656 -0.0307085489
48 -0.115355346  0.054201817  0.0149322182
49  0.021257691 -0.076319224  0.0204245476
50 -0.028638479  0.092324549  0.0223799360
51  0.084681588  0.023417118 -0.0041618758
52 -0.048975326  0.031882454  0.0212424035
53 -0.084894231  0.073128665  0.0194160159
54 -0.046540287 -0.016230948  0.0082871718
55  0.049953573 -0.082248535  0.0231005683
56 -0.098177728  0.024078664  0.0142806805
57  0.107043154 -0.117264506  0.0237953518
58 -0.184277005 -0.015776514 -0.0159068186
> PCA.MC2 = plotTangentSpace(GPA_MC2$coords, label = TRUE, groups = grpMC2, verbose = TRUE)
> PCA.MC2

PC Summary

Importance of first k=9 (out of 10) components:
                            PC1     PC2     PC3     PC4     PC5
Standard deviation     0.1421  0.07827 0.05769 0.05417 0.04986
Proportion of Variance 0.5299  0.16073 0.08731 0.07699 0.06522
Cumulative Proportion  0.5299  0.69067 0.77797 0.85497 0.92019
                            PC6     PC7     PC8     PC9
Standard deviation     0.03123 0.03054 0.02659 0.02065
Proportion of Variance 0.02559 0.02447 0.01855 0.01119
Cumulative Proportion  0.94579 0.97026 0.98881 1.00000
```

```
> PCA.MC2$pc.scores
                                        PC1         PC2         PC3
AMNH19006MC2gel           -0.15670034  0.09571695 -0.126769019
AMNH200763MC2gel          -0.10935009  0.04092137  0.050420525
AMNH200847MC2-reflectedbab  0.04117463 -0.10767764 -0.051105562
AMNH238034MC2gel          -0.10866884  0.04467406  0.069600136
AMNH35120MC2bab           -0.06032665 -0.02124860 -0.011200918
AMNH52688MC2bab            0.04851409 -0.07945820  0.006485815
AMNH60568MC2-reflectedgel  -0.09788183  0.01866879  0.056878110
AMNH81688MC2bab            0.17307014  0.06649908  0.018599786
AMNH82092MC2bab            0.29281559  0.06446899 -0.011469153
AMNH82097MC2newbab         -0.02264671 -0.12256479 -0.001439720
                                        PC4         PC5         PC6
AMNH19006MC2gel           -0.007782167  0.01539225 -0.010119134
AMNH200763MC2gel           0.076896940 -0.01995898 -0.018181385
AMNH200847MC2-reflectedbab  0.085089089 -0.04316161 -0.007487083
AMNH238034MC2gel           0.015449926  0.08655612  0.001057448
AMNH35120MC2bab           -0.077709199 -0.02159962  0.043950441
AMNH52688MC2bab           -0.070730556  0.02421376 -0.067484140
AMNH60568MC2-reflectedgel  -0.020458841 -0.07572409  0.008242712
AMNH81688MC2bab           -0.029442307 -0.04729273 -0.005302924
AMNH82092MC2bab            0.024886745  0.03662935  0.018234170
AMNH82097MC2newbab         0.003800370  0.04494554  0.037089896
                                        PC7          PC8                 PC9
AMNH19006MC2gel           0.011189156  0.0087259127  0.006438864
AMNH200763MC2gel          -0.041911743 -0.0179737572  0.026261606
AMNH200847MC2-reflectedbab  0.001829149 -0.0003447794 -0.029650371
AMNH238034MC2gel           0.005895291  0.0113834176 -0.032110672
AMNH35120MC2bab           -0.040545177 -0.0311985808 -0.013767930
AMNH52688MC2bab            0.001722459 -0.0137704246  0.005073547
AMNH60568MC2-reflectedgel   0.060978132 -0.0061888570  0.004023073
AMNH81688MC2bab           -0.025879710  0.0519349933 -0.003877072
AMNH82092MC2bab            0.019840484 -0.0323754499  0.007772382
AMNH82097MC2newbab         0.006881957  0.0298075255  0.029836573
```

Chapter 5
Manual proportions and grooming in primates

Abstract

Allogrooming, the grooming of another individual, plays an important social and utilitarian role in primate societies. Associations between grooming investment and group size, body size, dispersal patterns, and social relationships have been investigated in previous literature highlighting the complex nature of primate allogrooming. Much of the grooming process relies on pad to pad precision gripping between the distal ends of the first and second rays, whether it is for removal of ectoparasites and debris or pulling hair aside. The role of manual morphology has been largely absent from primate grooming studies. One aspect of primate hand anatomy, the Opposability Index, is presented here as it relates to primate grooming investment for apes and several Cercopithecoid species. There is a strong positive correlation between opposability index and grooming investment (as represented by percent of daily activity budget) for the taxa included here. These data suggest that there is an important link between primate grooming and opposability. It is possible that high opposability is an exaptation originally under positive selection for other manipulative tasks that is now used for grooming. Primates with low opposability may be constrained by locomotor demands, limiting the utility of their manual morphology for grooming activity.

Introduction

While many kinds of mammals have social grooming, several branches of primates are distinctive in grooming using prehensile hands. All primate hands are prehensile to some degree, meaning they can grasp objects using the digits of one hand. However, primates vary in

the amount to which the thumb can move independent of the other rays. This variation in thumb mobility strongly impacts hand function.

Grooming within primate taxa serves both hygienic and social functions. Dunbar's (2010) review of primate grooming argued that the most important function of grooming is to reinforce social bonds, which is especially important for anthropoid primates (though grooming is practiced extensively by prosimian primates as well). Dunbar's argument for the importance of bonding in monkeys and apes relates strongly to the purported cognitive demands of their complex within-sex relationships. Social grooming seems to help facilitate and reinforce these bonds by creating "a psychopharmacological environment that enhances commitment" (p. 260 Dunbar, 2010). Maintaining complex anthropoid primate relationships may be achieved through frequent grooming and, according to Dunbar's social brain hypothesis (Dunbar, 1998), the complex human brain evolved to keep track of these relationships, especially considering their importance for individual survival. The importance of grooming is further emphasized by reviewing the daily activity budgets for primates. Almost 20% of the daily activity of some species is occupied by grooming, whether that is autogrooming (self-grooming) or allogrooming (social grooming or grooming of another individual) (reviewed by Dunbar, 2010).

Geladas devote a large percentage of their daily activity budget to grooming (Iwamoto and Dunbar, 1983). The species grooms for 17% of the day, on average. An extreme case of a very large group showed 20% of the daily activity budget being consumed by grooming activities (data from Lehmann et al., 2007 as cited in Dunbar, 2010). Another unique gelada characteristic

is their particularly large and variable group sizes. Gelada herds can number in the hundreds, often exceeding the group size of other primate species (Dunbar, 1980; 1988; Ohsawa and Dunbar, 1984; Iwamoto, 1993). Some researchers have more broadly linked these two aspects of primate behavior, citing the importance of grooming for social cohesion (Dunbar, 1991; Lehmann et al., 2007). Essentially, the greater the number of relationships to be maintained, the greater the amount of time spent grooming. Lehmann et al. (2007) assessed grooming behavior as a function of group size, phylogenetic proximity, dispersal patterns, and sex ratios. They found that grooming time is strongly positively correlated with group size and that dispersal patterns and sex ratios also impacted grooming investment.

Napier and Napier (1967) organized primates into three groups based on the opposability of the thumb. One group included primates with non-opposable thumbs, including tarsiers and marmosets. A second group was characterized by pseudo-opposable thumbs, including prosimians and New World monkeys except for marmosets. The third group consisted of primates that possess truly opposable thumbs, including Old World monkeys, apes, and humans. The "thumbless" *Ateles* and *Colobus* species were excluded from the classification entirely. Napier and Napier (1967) identified the opposability index as a measure of the functional effectiveness of opposition in primate genera. This index is a simple ratio of the length of the first ray (total length of metacarpal plus phalanges that comprise the thumb) to the length of the second ray (total length of metacarpal plus phalanges of the index finger). Greater opposability index values are assumed to reflect morphology that allows for easy pad to pad precision gripping between the distal ends of the first and second rays. Second only to

humans, geladas (*Theropithecus gelada*) have the greatest opposability index of extant primate species, suggesting that precision gripping is essential to daily activities (Etter, 1973).

Other intrinsic hand proportions (the length of one manual ray compared to the length of another manual ray) have been previously assessed (e.g., Liu et al., 2016; Almécija et al., 2015; Jouffroy et al., 1991). Almécija and colleagues (2015) found that there is heterogeneity of thumb to fourth ray ratios among apes. This ratio does not seem to be strongly influenced by phylogenetic proximity showing instead that closely related species do not resemble each other more than expected due to Brownian motion (randomness). Their findings suggest that intrinsic hand proportions provide information about function and possible selective pressures rather than exclusively shared evolutionary history. Similar conclusions regarding metacarpal length ratios were put forth by Jouffroy et al. (1991) linking unique manual proportions to functional differences in locomotion or manipulation, however Liu et al. (2016) noted that manipulative capabilities of primate hands and manual proportions do not always provide a straightforward link between form and function. Nevertheless, intrinsic hand proportions warrant greater functional consideration especially concerning the especially high opposability index of geladas.

Morphologically, one of the most frequently cited traits unique to geladas is in their hands (Napier and Napier, 1967; Jolly, 1970; Etter, 1973; Dunbar, 1983; Elton, 2006; Patel and Maiolino, 2016). They possess relatively long thumbs and shortened second digits, setting their hands apart from other African monkeys in their intrinsic hand proportions. Gelada manual proportions allow for efficient tip to tip precision grasping between the thumb and forefinger,

often used during feeding to manipulate tender grasses or seeds. Being the only extant group of primates that subsist primarily on grasses, the most commonly cited explanation for this hand morphology has been for their specialized feeding ecology. While this unique morphology is almost always explained by their graminivorous diet and specialized manual grazing, we can look for alternative explanations in other manipulative activities. For example, geladas also use the tip to tip precision grasping during grooming to remove external parasites or dirt and debris from the skin and fur of a group member.

Considering some of the unique characteristics of geladas together – very high opposability index, large group sizes, and substantial percentage of daily activity devoted to grooming – we must question whether there is a link between the morphological and behavioral traits in addition to the demonstrated correlation between grooming time and group size. While the opposability index is informative regarding pad to pad precision gripping, grooming consists of multiple actions. Pushing fur and gentle combing with the fingertips does not require a great deal of manual dexterity for primates. To reveal the skin and any potential external parasites or debris, the fur must be gripped and pulled back, typically with the thumb or thenar region and side of the second digit. To perform the hygienic function of grooming (remove small ticks, lice, eggs, dirt, grass, or other materials between hairs), some degree of fine object manipulation is necessary, though the exact grips that are used are only well known for some taxa (macaques: Macfarlane and Graziano, 2009). Further supporting the importance of pad to pad precision gripping and grooming are the especially low rates of grooming performed by primate taxa with reduced or vestigial thumbs. Gibbons and some colobines fall into this category and are

therefore unable to perform pad to pad precision gripping using the thumb and second ray. Additionally, support for a potential link between grooming behaviors and manual morphology is found in some observational studies of colobines. Asian colobines tend to have lower levels of louse infestation than African colobines (Kuhn, 1968 as cited in Hutchins and Barash, 1976), potentially due to the reduced thumb in African genera and less effective grooming postures (Hutchins and Barash, 1976).

An examination of a potential correlation between grooming investment and hand morphology might help us understand selective pressures throughout primate evolution on the form of the hand. This study investigates the null hypothesis that there is no correlation between opposability index and grooming investment, suggesting that primates groom in a wide variety of ways that are not limited to pad-to-pad precision grasping. Alternatively, if small object manipulation, especially using pad-to-pad precision gripping, is an essential component to grooming behaviors, grooming investment and opposability index are expected to be correlated. This analysis will inform further studies on primate manual morphology and grooming postures, especially expansion upon behavioral data cataloguing the grips use throughout grooming bouts (as seen in part in Macfarlane and Graziano, 2009).

Materials

Per Napier and Napier (1967), true opposability is only present within the catarrhine primates, including Old World monkeys, apes, and humans. Despite the prehensile abilities of capuchins, studies examining the carpal and metacarpal morphology of these primates with “pseudo-

opposability" have supported Napier and Napier's (1967) original functional classifications (Roqueline, 2014). For this reason and to align with common primate models for understanding hominin evolution, I have only included Old World monkeys and apes in my analysis. Data are further limited to taxa for which both grooming activity and opposability indices (or relevant raw data with which to calculate indices) are available. This led to twelve species being included from ten genera (Table 5.1). From these taxa, we can evaluate general trends in the relationship between grooming time investment and opposability for primates with true opposability. While this sample pulls from several catarrhine groups, it is biased in that there is a higher representation of hominids relative to hylobatids among the apes. Likewise there are several more papionins included here than other Old World monkeys. Tribe Cercopithecini is represented by two species within the Cercopithecinae but Subfamily Colobinae is absent from the sample. Given these biases, these data might best be used to evaluate grooming and opposability among hominids and papionins more specifically. Phylogenetic analyses have been included to mitigate the impact of potential autocorrelation of closely related taxa. Future work would benefit from a more inclusive sample, regardless of opposability category.

Opposability indices

Jouffroy and colleagues (1991) compiled digital ray length ratios across several primate genera. Ray lengths were defined by the combined lengths of metacarpals and all phalanges for a given ray. Jouffroy et al. (1991) calculated all ratios relative to the longest digit, ray 3 for all genera. From these ratios, I calculated the opposability index for each genus as defined by Napier and Napier (1967), the sum of the lengths of metacarpal 1, proximal phalanx 1, and distal phalanx 1

divided by the sum of the lengths of metacarpal 2, proximal phalanx 2, intermediate phalanx 2, and distal phalanx 2 X 100. Unfortunately, Jouffroy et al.'s (1991) data have their limitations. The values are only listed across genus, while many the genera include multiple species. Species within diverse genera may have different social structures, group sizes, and data on grooming may be difficult to compare among these. In the case of genera *Gorilla, Hylobates,* and *Colobus,* the opposability indices presented by Jouffroy et al. (1991) were matched with one species for which suitable grooming data were most abundant and available. For *Pan*, genus level measurements from Jouffroy et al. (1991) were included in weighted averages with my own calculations of known species. Other opposability indices were provided by Etter (1973), calculations unique to this study and associated data collection, and a weighted average of the available sources. I did not consider subspecies level distinctions in these calculations. Figure 5.1, modified for clarity from Napier and Napier's (1967) original definition, indicates the points of measurement for calculating opposability indices. Data not previously published were generated from primate skeletal materials curated at the American Museum of Natural History in New York (AMNH), the Cleveland Museum of Natural History in Ohio (CMNH), the National Museum of Natural History in Washington, D.C. (NMNH), and the Digital Morphology Museum at the Kyoto University Primate Research Institute (KUPRI). Opposability indices (weighted averages across all samples), number of individuals, and sources for the included taxa are listed in Table 5.1.

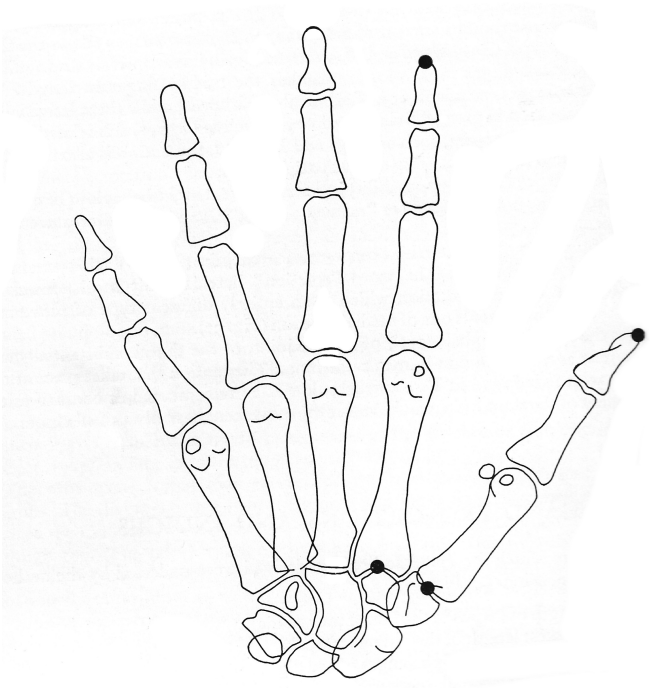

Figure 5.1
Palmar view of a primate right hand. Black dots indicate the points at which length measurements of rays 1 and 2 should be taken.

Primate taxa	**N**	**Opp. Index**	**Source**
Colobus sp.	10	26.1	Jouffroy et al., 1991
*Chlorocebus aethiops**	12	49.2	Etter, 1973
Erythrocebus patas	9	52.8	Etter, 1973
Gorilla sp.	6	49.2	Jouffroy et al., 1991
Hylobates sp.	8	46.5	Jouffroy et al., 1991
Macaca fuscata	2	53.6	this study**
Macaca mulatta	15	53.2	Etter, 1973
Pan troglodytes	26	44.4	Jouffroy et al., 1991 and this study**
Papio cynocephalus	10	53.4	Etter, 1973 and this study**
Papio hamadryas	16	59.1	Etter, 1973
Papio ursinus	1	54.7	this study**
Pongo sp.	9	38.8	Jouffroy et al., 1991
Symphalangus syndactylus	5	45.4	Jouffroy et al., 1991 and this study**
Theropithecus gelada	8	70.7	Etter, 1973 and this study**

Table 5.1
Opposability index for each primate taxon. N = number of individuals (combined total for weighted averages including data from this study and other sources); **Cercopithecus aethiops* in Etter, 1973; **measurements of all included elements and source specimens are included in the appendix

Grooming time

Data were gathered from the literature on the percentage of daily activity budget devoted to grooming for these fourteen primate taxa. For taxa with multiple study populations within a single publication, grooming frequency data are a weighted mean of grooming time across all included populations. Data were drawn from original publications when possible as well as Dunbar (1991), Lehmann et al. (2007), and Grueter et al. (2013). For several taxa, data from these three comparative studies are the same. One notable discrepancy between these sources is in the grooming data for *Theropithecus gelada*. Dunbar (1991), Lehmann et al. (2007), and Grueter et al. (2013) acquired grooming time data from Iwamoto and Dunbar (1983), however the percentage of daily grooming budget listed was different; Lehmann et al. (2007) indicated 17.4% as the grooming percentage of the daily budget for geladas – and Grueter et al. (2013) used the data from Lehmann et al. (2007), whereas Dunbar (1991) indicated a grooming percentage of daily budget as 18.3 for geladas. My calculations of a simple average across the three study populations listed in Iwamoto and Dunbar (1983) align with Dunbar (1991). In their original study, Iwamoto and Dunbar (1983) indicated a "Socializing" percentage of the daily activity budget but did specify a breakdown within that category which likely includes grooming and other social activities like playing that could artificially increase the calculation of grooming noted in Dunbar (1991). Because of the uncertainty regarding the Lehman et al. (2007) value derived from Iwamoto and Dunbar (1983), I am using the 18.3% value also used in Dunbar (1991). A complete list of primate taxa, total number of study populations, weighted average of percentage of daily budget devoted to grooming, and sources are included in Table 5.2. Further breakdown of individual study populations and sources can be found in the appendices.

Primate taxa	N	Grooming %	Source
Colobus guereza	3	6.17	Oates, 1997 as cited by Grueter et al., 2013; Fashing, 2001
Chlorocebus aethiops	10	7.39	Baldellou and Adan, 1997; 1998 and Lee, 1982 as cited by Lehmann et al., 2007; Isbell and Young, 1993 as cited by Grueter et al., 2013
Erythrocebus patas	4	6.8	Nakagawa, 1989 and Chism, 2002 as cited by Grueter et al., 2013; Ashagrie, 2015
Gorilla beringei	7	2.49	Karisoke, long term records, 2008 as cited by Grueter et al., 2013
Hylobates lar	7	3.11	Ellefson, 1974, Gittins and Raemaekers, 1980, and Bartlett, 1999 as cited by Grueter et al., 2013
Macaca fuscata	11	11.16	Agetsuma, 1995, Maruhashi, 1981, and Wada and Tokida, 1981 as cited by Grueter et al., 2013; Seth and Seth, 1986
Macaca mulatta	2	10.8	Teas et al., 1980 as cited by Lehmann et al., 2007; Marriott, 1988 as cited by Grueter et al., 2013
Pan troglodytes	4	8.88	Wrangham, 1977 and Huffman, 1990 as cited by Grueter et al., 2013; Boesch and Boesch-Achermann, 2000
Papio cynocephalus	3	5.7	Schino et al., 1988 as cited by Dunbar, 1991
Papio hamadryas	1	13.5	Nagel, 1973 as cited by Grueter et al., 2013
Papio ursinus	8	12.75	Schino et al., 1988 as cited by Dunbar, 1991; Barrett et al., 1999 as cited by Grueter et al., 2013; Hill et al., 2003; Gaynor, 1994
Pongo pygmaeus	1	0.01	Wich et al., 2009 as cited by Grueter et al., 2013; Mackinnon, 1974
Symphalangus syndactylus	4	8.33	Chivers, 1974 and Gittins and Raemaekers, 1980 as cited by Grueter et al., 2013
Theropithecus gelada	3	18.3	Iwamoto and Dunbar, 1983

Table 5.2
Grooming time per primate taxon, listed alphabetically. N = number of populations

Phylogeny

The phylogeny used in this study was downloaded from 10k Trees Website (Version 3, http://10ktrees.fas.harvard.edu/). This phylogenetic tree is a consensus chronometric tree of the extant anthropoid taxa of interest to this study. The 10k Trees Website infers phylogenetic trees based on samples from a Bayesian phylogenetic analysis of genetic data available in GenBank. The 10k Trees Website specifies phylogenetic data for some taxa to the subspecies designation. For *Pan troglodytes* data on opposability and grooming investment, *Pan troglodytes verus* was selected as the representative subspecies on the tree. The resultant consensus phylogenetic tree of included species is found in Figure 5.2. The 10k Trees Website also provides branch length estimates to quantify the phylogenetic tree information during statistical analyses. The NEXUS output and relevant branch lengths are included in Figure 5.3.

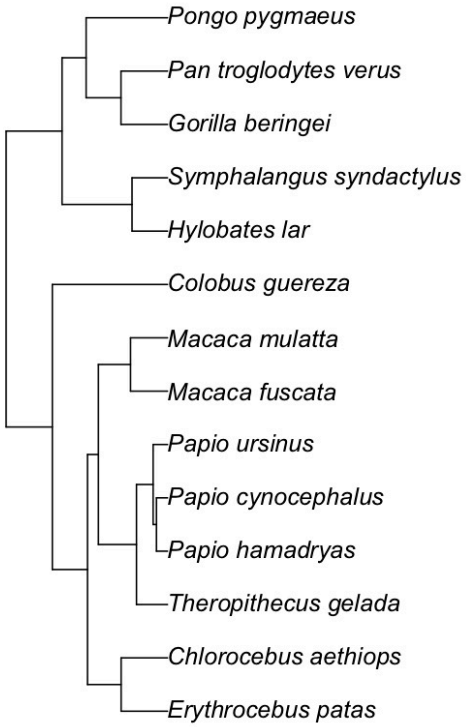

Figure 5.2. Consensus phylogenetic tree. Image generated in R using TreeTools package (R Core Team, 2013; Smith, 2019) from data acquired through 10k Trees Website (Arnold et al., 2010).

```
#NEXUS
[created by the 10kTree Website - http://10kTrees.fas.harvard.edu]
BEGIN TREES;
translate
1 Chlorocebus_aethiops,
2 Erythrocebus_patas,
3 Gorilla_beringei,
4 Hylobates_lar,
5 Pan_troglodytes_verus,
6 Pongo_pygmaeus,
7 Symphalangus_syndactylus,
8 Macaca_fuscata,
9 Macaca_mulatta,
10 Papio_cynocephalus,
11 Papio_hamadryas,
12 Papio_ursinus,
13 Theropithecus_gelada,
14 Colobus_guereza;
tree consensus_14species = ((((2:8.627245,1:8.627244):6.247934,
((13:5.769164,((11:2.058446,10:2.058446):0.619816,12:2.678262):
3.090901):7.083362,(8:6.877996,9:6.877995):5.974530):2.022653):
6.535196,14:21.410374):8.589626,((4:6.598361,7:6.598362):13.007584,
((3:8.652233,5:8.652233):6.480222,6:15.132455):4.473491):10.394055);
END;
```

Figure 5.3. NEXUS output of consensus phylogenetic tree for twelve primate taxa of interest generated by 10k Trees Website (Arnold et al., 2010). Branch length values are listed at the bottom following the number associated with each taxon.

Methods

Correlation

Pearson correlation coefficient (Pearson's *r*) assesses if there is a linear correlation between two variables; in this case between opposability index and the percentage of daily activity devoted to grooming for a given primate taxa. The calculation of Pearson's *r* assumes that each trait is sampled from a normally distributed population, despite the sample consisting of single observations of several species. To test this assumption of normality, Shapiro Wilk tests provide statistical rigor and must be conducted prior to calculating Pearson's *r*. Shapiro Wilk tests for each variable were not significant, indicating that the data do not violate the assumption of normality (opposability index; W = 0.9365, $p = 0.3747$ and grooming data; W = 0.9868, $p = 0.9973$). Additionally, a simple correlation assumes phylogenetic independence of all continuous data.

Phylogenetic Generalized Least Squares

Based on the sample of morphological and behavioral data from the primate taxa in this study, it is important to account for the possibility of phylogenetic non-independence in the correlation. Phylogenetic generalized least squares (PGLS) models incorporate the phylogenetic distance between taxa in the model to calculate expected covariance within the data (Symonds and Blomberg, 2014). This covariance is then incorporated to the calculations of correlation. There are several methods for modeling evolution within PGLS, Brownian motion and the Ornstein-Uhlenbeck process, both of which have been popular models for the evolution of quantitative traits (Blomberg et al., 2020). Brownian motion assumes random changes in trait values, modeling the evolution of these traits as the sum of many small random forces (though not exclusively by genetic drift). This is characterized as a random walk in which change in traits is equally likely in any direction. Another variation on Brownian motion is the Ornstein-Uhlenbeck (OU) model in which traits are under stabilizing selection and subject to genetic drift. Change in traits in the OU model are more likely to occur toward an optimum. Both correlation methods were incorporated to distinct PGLS tests to account for potential phylogenetic non-independence within the sample. Phylogenetic independent contrasts is another method used to consider the potential impact of phylogeny when evaluating correlations, though PGLS offers traditional least squares statistical methods for further analyses (Garland and Ives, 2000). This utility of PGLS has made it popular for phylogenetic analyses in the past decade. PGLS has previously been used to assess the potential autorcorrelation of related taxa for studies of primate grooming, manual morphology, and

locomotion (e.g Lehmann et al., 2007; Nelson et al., 2011; Rein, 2011; and Machnicki et al., 2016).

All tests were conducted in R using the ape, phytools, TreeTools, nlme, and geiger packages (R Core Team, 2019; Paradis and Schliep, 2018; Revell, 2012; Smith, 2019; Pinheiro et al., 2019; Pennell et al., 2019). Relevant R code can be found in the appendix.

Results

Pearson correlation coefficient

There is a strong positive correlation between opposability index and grooming time in this study ($r = 0.695$, $p = 0.0058$). We reject the null hypothesis that there is no correlation between grooming investment and opposability index.

PGLS

The statistically significant ($\alpha = 0.05$) positive correlation is still present when phylogeny is considered through PGLS models. The first PGLS model assumed Brownian motion as the mode of evolution for the traits within the given phylogeny. Under the Brownian motion PGLS model, the correlation is moderate and positive (correlation = 0.408, $p = 0.024$). The scatterplot of raw data with the Brownian motion model regression line (y-intercept = -11.62, slope = 0.408) is found in Figure 5.4. The second PGLS model assumes an Ornstein-Uhlenbeck process of evolution including stabilizing selection. Again, this model considers the phylogenetic proximity of sample primate taxa in the correlation calculation. Under the OU PGLS model, the correlation

is also moderate and positive (correlation = 0.332, p = 0.0058). The scatterplot of the raw data with the OU model regression line (y-intercept = -8.29, slope = 0.332) is found in Figure 5.5.

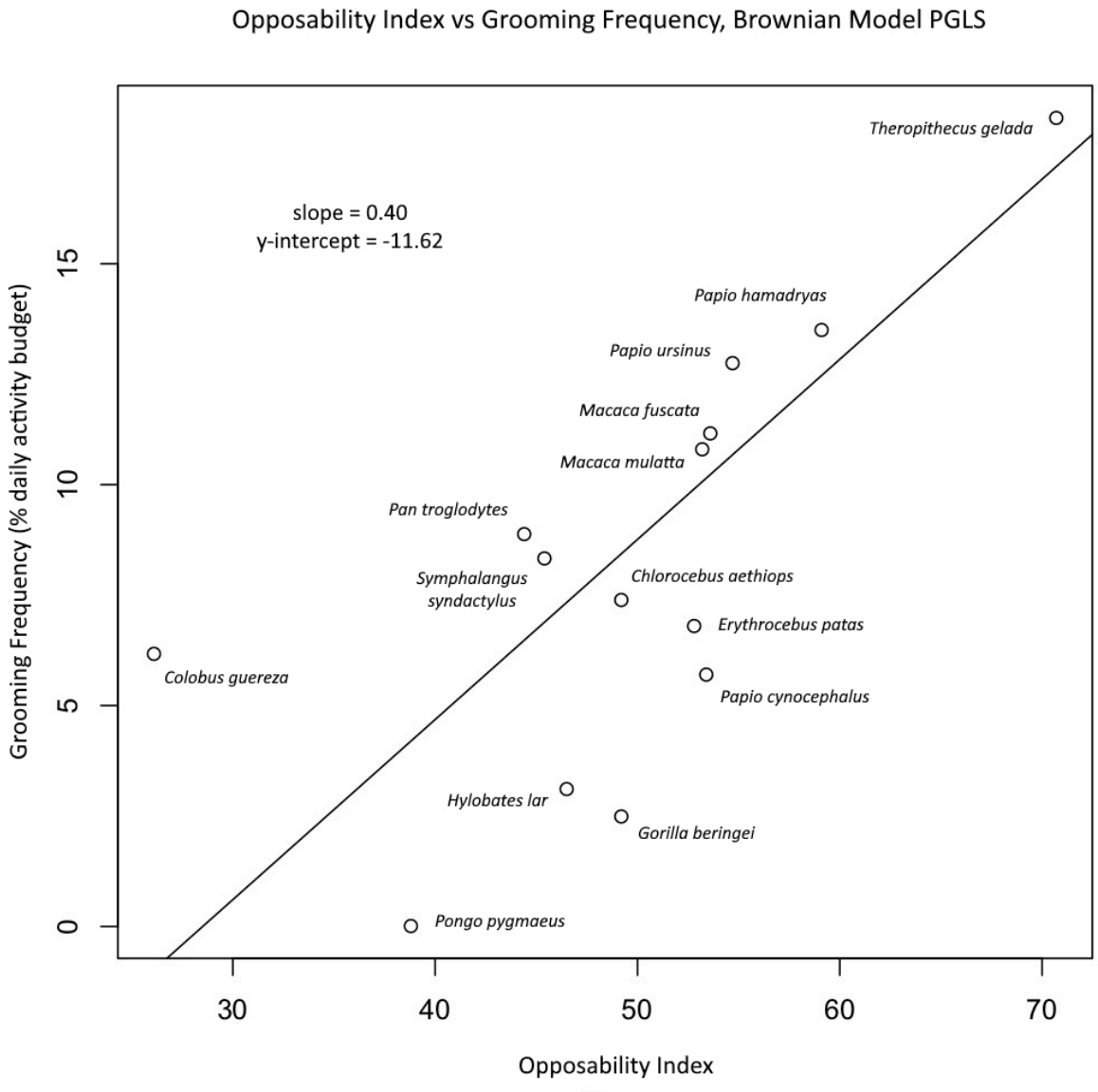

Figure 5.4
Plot of opposability index vs. grooming frequency including the regression line for the model assuming Brownian motion as the mode of evolution.

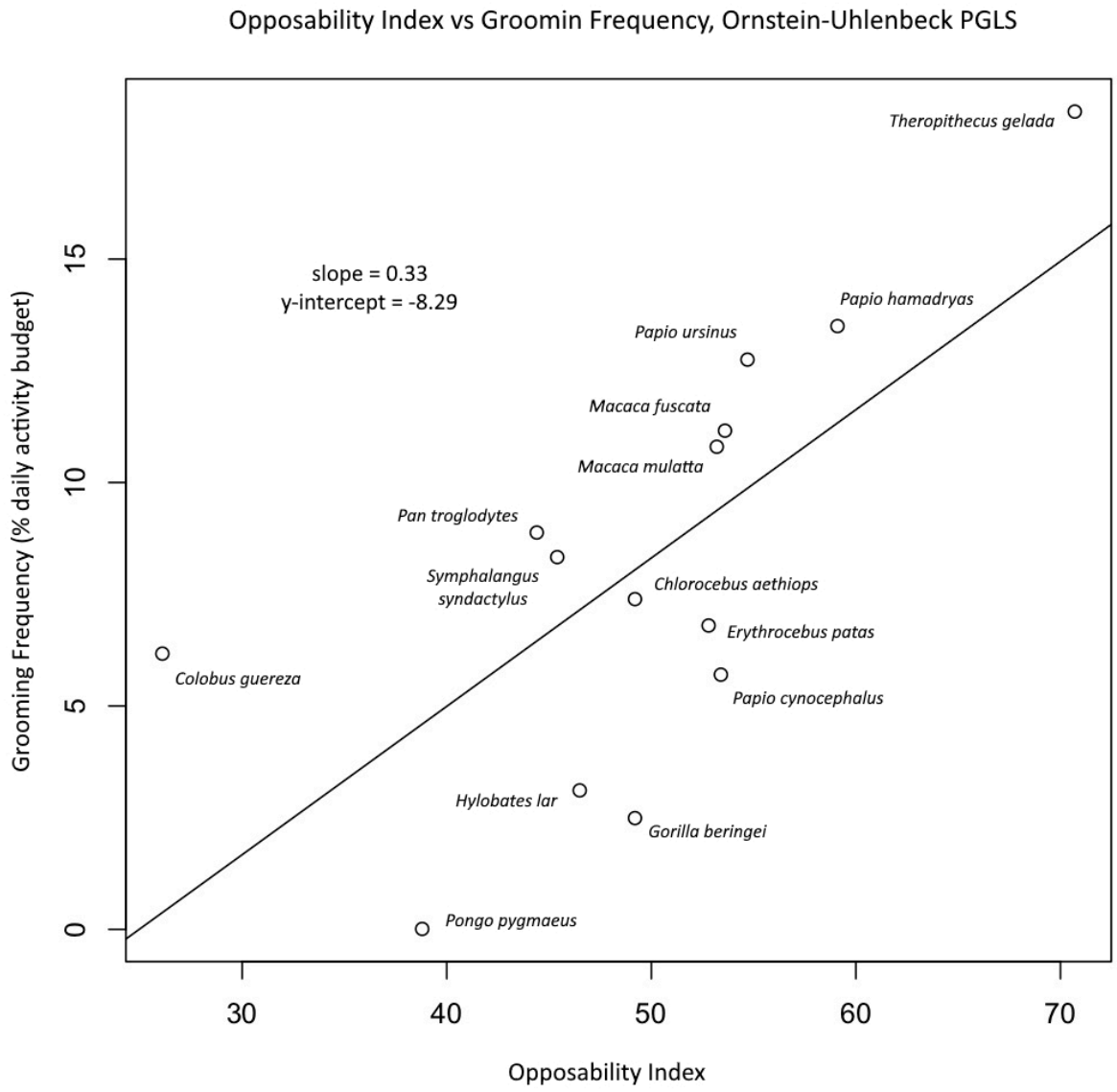

Figure 5.5
Plot of opposability index vs. grooming frequency including the regression line for the model assuming the Ornstein-Uhlenbeck process as the mode of evolution.

Though phylogeny did not eliminate or alter the direction of the correlation, it did reduce the strength of the correlation. Another important thing to note is that primate taxa do fall in phylogenetically meaningful groupings on the scatter plot (Figure 5.6). Tribe Papionini (*Papio* spp., *Theropithecus gelada,* and *Macaca* spp. in this sample) scored generally high in both

opposability and grooming investment, apes scored low in these traits on average, and Tribe Cercopithecini (*Chlorocebus aethiops* and *Erythrocebus patas* in this sample) had intermediate scores for both traits of concern to this study. *Colobus guereza*, the sole representative from subfamily Colobinae, is separate from the other taxonomic groups, scoring very low on opposability index and intermediate in grooming investment.

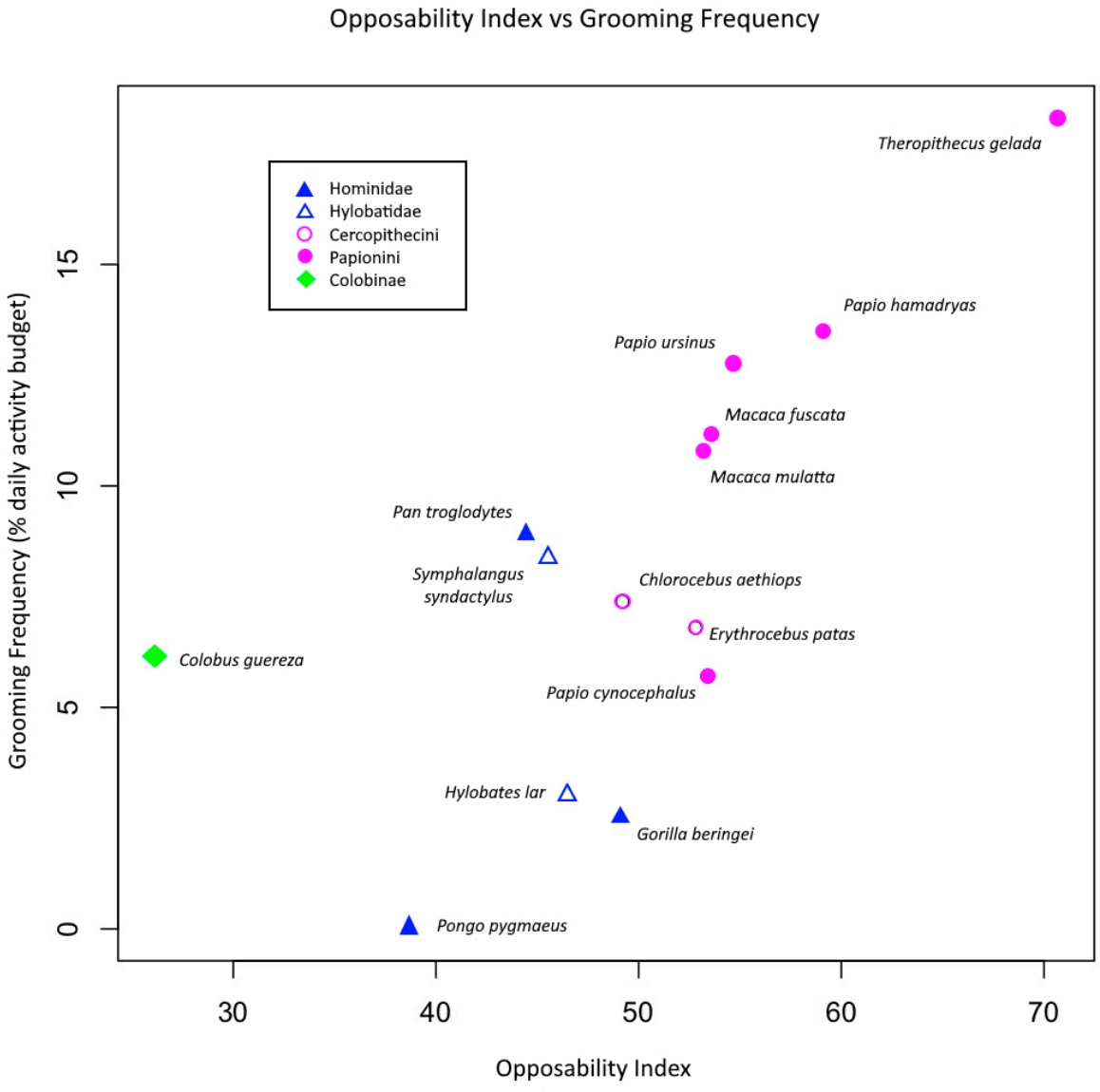

Figure 5.6
Plot of opposability index vs grooming frequency with primate groups identified by color and shape markers.

Discussion

For the ape and Old World monkeys included in this study, there is a positive relationship between opposability index and grooming when accounting for phylogenetic proximity. For species with high opposability indices, we see higher rates of grooming in their daily activity budget. Similarly, in species with short first rays and long second rays, grooming time investment tends to be low. It is possible that there is a functional relationship between pad to pad precision gripping between the first and second rays and grooming efficiency, though this needs to be investigated more thoroughly. If the function of grooming is primarily hygienic, we would expect high grooming efficiency (as identified by high opposability) to lead to low grooming time investment. Likewise, if reduced opposability leads to grooming inefficiency, we might expect primates with reduced opposability to invest more time in grooming activities. In contrast to this expectation, Dunbar (2010) noted that primate species with vestigial thumbs and therefore low opposability indices perform allogrooming at particularly low rates, though this does not seem to negatively impact their fitness.

It is also possible that pad to pad precision gripping is a poor indicator of grooming efficiency and a closer examination of the grooming process is necessary to evaluate any link between manual dexterity and grooming efficiency. Specifically, grooming involves many hand postures in addition to pad to pad precision gripping and the literature that includes frequencies of grooming does not specify hand postures nor does it further break down grooming activity frequencies by a given hand posture. The correlation identified in this study suggests that there

is a relationship between hand morphology and grooming activity, but a more detailed investigation of the exact hand postures and the frequency at which they are used during grooming would further clarify this relationship.

This study was limited to primate species for which "true opposability" (Napier and Napier, 1967) is possible – apes and Old World monkeys – but grooming takes place in most primate taxa. A high opposability index might help facilitate efficient removal of dirt, ectoparasites, and debris from the fur, but it is not necessary to all grooming efforts. For example, primates that lack thumbs and primate taxa without true opposability still groom and some have other physical adaptations to facilitate grooming (e.g. toothcombs and toilet claws). Considering these adaptations, grooming efficiency could have been important for fitness throughout primate evolution.

In addition to morphological differences, the primary function of allogroming might not be shared in catarrhines and platyrrhines. Dunbar (1991) asserted that there is a different relationship between grooming time and group size in catarrhines and platyrrhines. Catarrhines show a positive relationship – grooming time increases with group size. For platyrrhines, body size correlates much more with grooming time than group size. This distinction might suggest that grooming for hygiene is more important than grooming to maintain social cohesion in platyrrhines. Citing Whiten and Byrne (1988), Dunbar additionally states that catarrhines are the only primate group who "make extensive use of complex social strategies such as coalition formation and deception" (p. 127). Despite these presumed differences in platyrrhine behavior,

there is important diversity in grooming investment and social grooming outcomes to be examined in New World taxa.

Studies of platyrrhine species have suggested that allogrooming has important social implications similar to those of some catarrhines. For example, despite low grooming frequency in a population of free ranging spider monkeys (*Ateles geoffroyi*), grooming was the most frequent affinitive behavior observed (Ahumada, 1992). Additionally, a study of a captive population of the same species demonstrated grooming was an important predictor of reciprocal food sharing and strong affiliative relationships between individuals, emphasizing the social importance of grooming for this platyrrhine species despite low grooming frequency (Pastor-Nieto, 2001). Also, studies of mantled howler monkeys (*Alouatta palliata*) and red howler monkeys (*Alouatta seniculus*) have indicated that social grooming can be a good indicator of dominance relationships and might be more complicated in platyrrhines than a primarily hygienic explanation would allow (Jones, 1979; Sánchez-Villagra et al., 1997). Allogrooming in tufted capuchin monkeys (*Cebus apella*) is also related to dominance structure and, importantly, to coalition formation (di Bitetti, 1997).

It is important to note that closely related taxa are in similar places along the regression line and within the scatterplots. Given this placement, there might be other factors (be they locomotor, behavioral, or developmental) that closely related species share that could co-vary with opposability index and/or grooming investment. Previous studies have indicated that social grooming is not correlated with body size but group size, dispersal patterns, and sex

ratios all impact grooming investment (Dunbar, 1991; Lehmann, 2007). These previous studies accounted for phylogeny, but it is possible that other factors that have yet to be considered have a strong phylogenetic signal related to grooming investment or opposability index. Additionally, while it is possible that there was positive selection for a high opposability index in some primates for increased grooming efficiency, it is also possible that the high opposability index and the associated pad to pad precision gripping capabilities used in grooming represent an exaptation. Opposability might have been positively selected in response to other manipulative tasks and was co-opted for grooming in these primate taxa. The results of this study support further investigation of the relationship between precision gripping between the first and second rays and social grooming in primate taxa.

Another possible explanation for these data is that primate grooming is a function of grooming ease, meaning that primates who can groom easily by pad-to-pad precision grasping do so at high rates simply because it is easy. When grooming via pad to pad precision gripping poses a functional challenge (like for those primates with reduced or absent thumbs) the time devoted to the activity reduces, perhaps to the minimum required to maintain appropriate hygiene (Dunbar, 2010). In humans, there is support for the tendency to prefer the low hanging fruit or the path of least resistance. Human participants in a recent study (Hagura et al., 2017) showed a clear bias in favor of the easier option, even shifting their perception of what they observed in response to subtle physical obstacles. For primates with high opposability, the path of least resistance in social activity may be grooming. Rather than grooming serving as an evolutionary

constraint on hand morphology, perhaps it is high opposability that actively facilitates high grooming investment.

An important additional consideration is the fact that the intrinsic hand proportions of apes are highly derived, likely due to their specific locomotor regimes and a variety of distinct evolutionary processes (Almécija et al., 2015). Papionins display intrinsic hand proportions more like those of other monkeys than apes. The particularly high rates of grooming in papionins could represent the upper extreme of relatively high rates of grooming among monkeys in contrast to the low rates of grooming of apes. The observed signal could represent a reduction in grooming efforts along the ape lineage, perhaps substituted for other modes of social communication rather than an increase among the papionins. Even within this framework, papionins (especially gelada) groom at very high rates relative to other monkeys. I suggest that the pattern observed in this study is evidence of a mixed signal. There are limitations imposed by locomotion on ape hand anatomy, and therefore grooming ability, that result in relatively low grooming investment among apes. Additionally, the very high grooming rates of papionins are facilitated (or driven) by high opposability whether it is for hygienic, thermoregulatory, or social purposes.

Works Cited

Agetsuma, N. (1995). Foraging strategies of Yakushima macaques (*Macaca fuscata yakui*). *International Journal of Primatology*, *16*(4), 595-609.

Ahumada, J.A. (1992). Grooming behavior of spider monkeys (*Ateles geoffroyi*) on Barro Colorado Island, Panama. *International journal of primatology*, *13*(1), 33-49.

Almécija, S., Smaers, J.B., & Jungers, W.L. (2015). The evolution of human and ape hand proportions. *Nature communications*, *6*(1), 1-11.

Amorim, P. H., de Moraes, T. F., Azevedo, F. D. S., & da Silva, J. V. (2011). InVesalius: Software livre de imagens médicas. *Centro de Tecnologia da Informação Renato Archer-CTI, campinas/SP–2011-CSBC2011*.

Amorim, P., Moraes, T., Silva, J., & Pedrini, H. (2015). InVesalius: an interactive rendering framework for health care support. In *International symposium on visual computing* (pp. 45-54). Springer, Cham.

Arnold, C., Matthews, L.J., & Nunn, C.L. (2010). The 10kTrees Website: A New Online Resource for Primate Phylogeny. Evolutionary Anthropology 19:114-118.

Ashagrie, M. (2015). *Behavioral Ecology of the Patas Monkey (Erythrocebus patas) and Conservation Challenges in Alatish National Park, Northwest Ethiopia* (Doctoral dissertation, Addis Ababa University).

Aversi-Ferreira, R.A., Maior, R.S., Aziz, A., Ziermann, J.M., Nishijo, H., Tomaz, C., Tavares, M.C., & Aversi-Ferreira, T.A. (2014). Anatomical analysis of thumb opponency movement in the capuchin monkey (*Sapajus* sp). *PloS one*, *9*(2).

Baldellou, M., & Adan, A.N.A. (1997). Time, gender, and seasonality in vervet activity: A chronobiological approach. *Primates*, *38*(1), 31-43.

Baldellou, M., & Adan, A.N.A. (1998). Diurnal and seasonal variations in vervet monkeys' activity. *Psychological reports*, *83*(2), 675-685.

Barrett, L., Henzi, S.P., Weingrill, T., Lycett, J.E., & Hill, R.A. (1999). Market forces predict grooming reciprocity in female baboons. *Proceedings of the Royal Society of London. Series B: Biological Sciences*, *266*(1420), 665-670.

Bartlett, T.Q. (1999). Feeding and ranging behavior of the white-handed gibbon (Hylobates lar) in Khao Yai National Park, Thailand. *Washington University, PhD thesis*.

Blomberg, S.P., Rathnayake, S.I., & Moreau, C.M. (2020). Beyond Brownian motion and the Ornstein-Uhlenbeck process: Stochastic diffusion models for the evolution of quantitative characters. *The American Naturalist*, *195*(2), 000-000.

Boesch, C., & Boesch-Achermann, H. (2000). *The chimpanzees of the Taï Forest: Behavioural ecology and evolution*. Oxford University Press, USA.

Chism, J., & Rogers, W. (2004). Grooming and social cohesion in patas monkeys and other guenons. In *The guenons: Diversity and adaptation in African monkeys* (pp. 233-244). Springer, Boston, MA.

Chivers, D.J. (1974). The siamang in Malaya. A field study of a primate in tropical rain forest.

de Moraes, T.F., Amorim, P.H., Azevedo, F.S., & da Silva, J.V. (2011). InVesalius—An open-source imaging application. *Comput Vis Med Image Process*, 405.

di Bitetti, M.S. (1997). Evidence for an important social role of allogrooming in a platyrrhine primate. *Animal behaviour*, *54*(1), 199-211.

Dunbar, R.I.M. (1980). Demographic and life history variables of a population of gelada baboons (Theropithecus gelada). *The Journal of Animal Ecology*, 485-506.

Dunbar, R.I.M. (1983). Theropithecines and hominids: Contrasting solutions to the same ecological problem. *Journal of Human Evolution*, *12*(7), 647-658.

Dunbar, R.I.M. (1988). *Primate social systems.* Ithaca, New York. Cornell University Press.

Dunbar, R.I.M. (1991). Functional significance of social grooming in primates. *Folia primatologica*, *57*(3), 121-131.

Dunbar, R.I.M. (1998). The social brain hypothesis. *Evolutionary Anthropology: Issues, News, and Reviews: Issues, News, and Reviews*, *6*(5), 178-190.

Dunbar, R.I.M. (2010). The social role of touch in humans and primates: behavioural function and neurobiological mechanisms. *Neuroscience & Biobehavioral Reviews*, *34*(2), 260-268.

Ellefson, J.O. (1974). A natural history of white-handed gibbons in the Malayan peninsula. *Gibbon and siamang*, *3*, 1-136.

Elton, S. (2006). Forty years on and still going strong: the use of hominin-cercopithecid comparisons in palaeoanthropology. *Journal of the Royal Anthropological Institute*, *12*(1), 19-38.

Etter, H.F. (1973). Terrestrial adaptations in the hands of Cercopithecinae. *Folia Primatologica*, *20*(5-6), 331-350.

Fashing, P.J. (2001). Activity and ranging patterns of guerezas in the Kakamega Forest: intergroup variation and implications for intragroup feeding competition. *International Journal of Primatology*, *22*(4), 549-577.

Garland, Jr, T., & Ives, A.R. (2000). Using the past to predict the present: confidence intervals for regression equations in phylogenetic comparative methods. *The American Naturalist*, *155*(3), 346-364.

Gaynor, D. (1994). Foraging and feeding behaviour of chacma baboons in a woodland habitat. *Durban: University of Natal*, *PhD thesis.*

Gittins, S.P., & Raemaekers, J.J. (1980). Siamang, lar and agile gibbons. In *Malayan forest primates* (pp. 63-106). Springer, Boston, MA.

Goodall, J. (1965). Chimpanzees of the Gombe stream reserve. In DeVore, I. (ed): *Primate behavior: Field studies of monkeys and apes*, 425-473.

Grueter, C.C., Bissonnette, A., Isler, K., & van Schaik, C.P. (2013). Grooming and group cohesion in primates: implications for the evolution of language. *Evolution and Human Behavior*, *34*(1), 61-68.

Hagura, N., Haggard, P., & Diedrichsen, J. (2017). Perceptual decisions are biased by the cost to act. *Elife*, *6*, e18422.

Harcourt, A.H., & Fossey, D. (1977). Feeding ecology of free-ranging mountain gorilla (Gorilla gorilla beringei). In Clutton-Brock, T.H. (ed): *Primate Ecology*, London, Academic Press, 415-447.

Hill, R.A., Barrett, L., Gaynor, D., Weingrill, T., Dixon, P., Payne, H., & Henzi, S.P. (2003). Day length, latitude and behavioural (in) flexibility in baboons (*Papio cynocephalus ursinus*). *Behavioral Ecology and Sociobiology*, *53*(5), 278-286.

Huffman, M.A. (1990). Some socio-behavioral manifestations of old age. In *The Chimpanzees of the Mahale Mountains: Sexual and Life History Strategies* (pp. 237-255). University of Tokyo Press, Tokyo.

Hutchins, M., & Barash, D.P. (1976). Grooming in primates: implications for its utilitarian function. *Primates*, *17*(2), 145-150.

Isbell, L.A., & Young, T.P. (1993). Social and ecological influences on activity budgets of vervet monkeys, and their implications for group living. *Behavioral ecology and sociobiology*, *32*(6), 377-385.

Iwamoto, T. (1993). The ecology of *Theropithecus gelada*. In *Theropithecus: The rise and fall of a primate genus* (pp. 441-452). Cambridge University Press.

Iwamoto, T., & Dunbar, R.I.M. (1983). Thermoregulation, habitat quality and the behavioural ecology of gelada baboons. *The Journal of animal ecology*, 357-366.

Jolly, C.J. (1970). The seed-eaters: a new model of hominid differentiation based on a baboon analogy. In *Primate Evolution and Human Origins* (pp. 323-332). Routledge.

Jones, C.B. (1979). Grooming in the mantled howler monkey, *Alouatta palliata* Gray. *Primates*, *20*(2), 289-292.

Jouffroy, F.K., Godinot, M., & Nakano, Y. (1993). Biometrical characteristics of primate hands. In *Hands of primates* (pp. 133-171). Springer, Vienna.

Kuhn, H.J. (1968). Parasites and the phylogeny of the catarrhine primates. *Taxonomy and phylogeny of Old World Primates with references to the origin of Man*, 187-195.

Lee, P.C. (1982). *Ecological and social influences on development of vervet monkeys (Cercopithecus aethiops). University of Cambridge, Doctoral dissertation*.

Lehmann, J., Korstjens, A.H., & Dunbar, R.I.M. (2007). Group size, grooming and social cohesion in primates. *Animal Behaviour*, *74*(6), 1617-1629.

Liu, M.J., Xiong, C.H., & Hu, D. (2016). Assessing the manipulative potentials of monkeys, apes and humans from hand proportions: implications for hand evolution. *Proceedings of the Royal Society B: Biological Sciences*, *283*(1843), 20161923.

Macfarlane, N.B., & Graziano, M.S. (2009). Diversity of grip in *Macaca mulatta*. *Experimental brain research*, *197*(3), 255-268.

Machnicki, A.L., Spurlock, L.B., Strier, K.B., Reno, P.L., & Lovejoy, C.O. (2016). First steps of bipedality in hominids: evidence from the atelid and proconsulid pelvis. *PeerJ*, *4*, e1521.

MacKinnon, J. (1974). The behaviour and ecology of wild orang-utans (*Pongo pygmaeus*). *Animal behaviour*, *22*(1), 3-74.

Marriott, B.M. (1988). Time budgets of rhesus monkeys (*Macaca mulatta*) in a forest habitat in Nepal and on Cayo Santiago. *Ecology and behavior of food-enhanced primate groups*, *11*, 125-149.

Maruhashi, T. (1981). Activity patterns of a troop of Japanese monkeys (*Macaca fuscata yakui*) on Yakushima Island, Japan. *Primates*, *22*(1), 1-14.

Nagel, U. (1973). A comparison of anubis baboons, hamadryas baboons and their hybrids at a species border in Ethiopia. *Folia primatologica*, *19*(2-3), 104-165.

Nakagawa, N. (1989). Activity budget and diet of patas monkeys in Kala Maloue National Park, Cameroon: a preliminary report. *Primates*, *30*(1), 27-34.

Napier, J.R. & Napier, P.H. (1967): A handbook of living Primates. Academic Press, London.

Nelson, E., Rolian, C., Cashmore, L., & Shultz, S. (2011). Digit ratios predict polygyny in early apes, Ardipithecus, Neanderthals and early modern humans but not in Australopithecus. *Proceedings of the Royal Society B: Biological Sciences*, *278*(1711), 1556-1563.

Oates, J.F. (1977). The guereza and its food. In *Primate Ecology: Studies of Feeding and Ranging Behaviour in Lemurs, Monkeys, and Apes* (pp. 275-321). Academic Press, New York.

Ohsawa, H., & Dunbar, R.I.M. (1984). Variations in the demographic structure and dynamics of gelada baboon populations. *Behavioral Ecology and Sociobiology*, *15*(3), 231-240.

Paradis, E. & Schliep, K. (2018). ape 5.0: an environment for modern phylogenetics and evolutionary analyses in R. Bioinformatics 35: 526-528.

Pastor-Nieto, R. (2001). Grooming, kinship, and co-feeding in captive spider monkeys (Ateles geoffroyi). *Zoo Biology: Published in affiliation with the American Zoo and Aquarium Association*, *20*(4), 293-303.

Patel, B.A., & Maiolino, S.A. (2016). Morphological diversity in the digital rays of primate hands. In *The evolution of the primate hand* (pp. 55-100). Springer, New York, NY.

Pennell, M.W., Eastman, J.M., Slater, G.J., Brown, J.W., Uyeda, J.C., FitzJohn, R.G., Alfaro, M.E., & Harmon, L.J. 2014. geiger v2.0: an expanded suite of methods for fitting macroevolutionary models to phylogenetic trees. Bioinformatics 30:2216-2218.

Pinheiro, J., Bates, D., DebRoy, S., Sarkar, D., R Core Team (2019). _nlme: Linear and Nonlinear Mixed Effects Models_. R package version 3.1-140, <URL: https://CRAN.R-project.org/package=nlme>.

R Core Team (2019). R: A language and environment for statistical computing. R Foundation for Statistical Computing, Vienna, Austria. URL https://www.R-project.org/.

Rein, T.R. (2011). The correspondence between proximal phalanx morphology and locomotion: implications for inferring the locomotor behavior of fossil catarrhines. *American journal of physical anthropology*, *146*(3), 435-445.

Revell, L. J. (2012) phytools: An R package for phylogenetic comparative biology (and other things). Methods Ecol. Evol. 3 217-223. doi:10.1111/j.2041-210X.2011.00169.x

Sánchez-Villagra, M.R., Pope, T.R., & Salas, V. (1998). Relation of intergroup variation in allogrooming to group social structure and ectoparasite loads in red howlers (*Alouatta seniculus*). *International Journal of Primatology*, *19*(3), 473-491.

Schino, G., Scucchi, S., Maestripieri, D., & Turillazzi, P.G. (1988). Allogrooming as a tension-reduction mechanism: a behavioral approach. *American journal of primatology*, *16*(1), 43-50.

Seth, P.K., & Seth, S. (1985). Ecology and Feeding behaviour of the free ranging rhesus monkeys in India. *Indian Anthropologist*, *15*(1), 51-62.

Smith, M.R. (2019). *TreeTools: create, modify and analyse phylogenetic trees*. doi: 10.5281/zenodo.3522725, R package version 0.1.4.

Symonds, M.R., & Blomberg, S.P. (2014). A primer on phylogenetic generalised least squares. In *Modern phylogenetic comparative methods and their application in evolutionary biology* (pp. 105-130). Springer, Berlin, Heidelberg.

Teas, J., Richie, T., Taylor, H., & Southwick, C.H. (1980). Population patterns and behavioural ecology of rhesus monkeys (*Macaca mulatta*) in Nepal. In Lindburg D.G. (ed): *The Macaques*. New York, Van Nostrand Reinhold, 247-262.

Wada, K., & Tokida, E. (1981). Habitat utilization by wintering Japanese monkeys (*Macaca fuscata fuscata*) in the Shiga Heights. *Primates*, *22*(3), 330-348.

Whiten, A., & Byrne, R.W. (1988). Tactical deception in primates. *Behavioral and brain sciences*, *11*(2), 233-244.

Wich, S.A., Setia, T.M., & van Schaik, C.P. (Eds.). (2010). *Orangutans: geographic variation in behavioral ecology and conservation*. OUP Oxford.

Wrangham, R.W. (1977). Behavior of feeding chimpanzees in the Gombe National Park, Tanzania. In Clutton-Brock, T.H. (ed): *Primate Ecology*, London, Academic Press, 503-538.

Appendix 5.1

Genus, species, specimen number, sex, linear measurements for opposability index calculations in millimeters, and resulting opposability indices. Each linear measurement value represents the proximo-distal length of the element to the nearest tenth of a millimeter, as measured using digital calipers. Opposability index is calculated as the sum of the lengths of the elements of ray 1 (metacarpal, proximal phalanx, and distal phalanx) divided by the sum of the lengths of the elements of ray 2 (metacarpal, proximal phalanx, intermediate phalanx, and distal phalanx)

and the resulting ratio does not have units. These data were gathered from skeletal material curated at the American Museum of Natural History in New York (AMNH), the Cleveland Museum of Natural History in Ohio (CMNH), and the National Museum of Natural History in Washington, D.C (NMNH). Data for *Macaca fuscata* do not include linear measurements as they were gathered from electronic CT data made available through the Digital Morphology Museum at the Kyoto University Primate Research Institute (KUPRI). Only opposability index is presented in this table for *Macaca fuscata* for that reason. Invesalius 3.1 (Amorim et al., 2011; de Moraes et al., 2011; Amorim et al., 2015) was used to create 3D renderings and collect the opposability indices for the two KUPRI specimens.

Primate taxa	**Specimen #**	**Sex**	**Mc1 (mm)**	**PP1 (mm)**	**DP1 (mm)**	**Mc2 (mm)**	**PP2 (mm)**	**IP2 (mm)**	**DP2 (mm)**	**Opp. Index**
Macaca fuscata	KUPRI Mff963	F	N/A	N/A	N/A	N/A	N/A	N/A	N/A	53.7
Macaca fuscata	KUPRI 10052	N/A	N/A	N/A	N/A	N/A	N/A	N/A	N/A	53.4
Papio cynocephalus	NMNH-313783	N/A	28.6	15.1	8.1	45.0	21.9	12.9	7.8	59.1
Papio cynocephalus	NMNH-452509	M	34.2	17.2	10.3	56.0	30.1	18.6	11.8	53.0
Papio hamadryas	CMNH- HTB 890	M	30.6	13.7	9.2	45.8	26.2	16.8	10.7	53.8
Papio hamadryas	CMNH- HTB 900	M	32.6	17.1	9.7	50.6	24.5	14.7	11.8	58.5
Papio hamadryas	CMNH- HTB 1027	F	24.5	12.1	7.6	40.1	19.3	11.0	8.2	56.2
Papio hamadryas	CMNH- HTB 2097	M	30.9	15.9	9.5	50.2	24.2	14.0	9.2	57.7
Papio ursinus	NMNH-20860	F	36.2	17.4	9.3	58.3	27.6	16.6	12.4	54.7
Pan troglodytes	NMNH-176227	M	35.8	20.1	16.2	82.5	46.2	29.2	15.4	41.6
Pan troglodytes	NMNH-176230	N/A	42.1	26.8	18.6	98.2	53.8	34.1	17.6	43.0
Pan troglodytes	CMNH- HTB 1718	M	43.1	27.2	18.7	99.5	51.4	30.0	16.6	45.1
Pan troglodytes	CMNH- HTB 1719	F	38.1	23.6	17.5	82.1	46.8	28.9	16.3	45.5
Pan troglodytes	CMNH- HTB 1721	F	40.6	24.3	17.7	89.1	52.5	36.7	19.8	41.7
Pan troglodytes	CMNH- HTB 1880	F	40.4	26.5	20.4	96.5	51.4	31.3	17.4	44.4
Pan troglodytes	CMNH- HTB 1882	M	40.6	20.8	19.6	90.0	51.6	37.3	19.2	40.9
Pan troglodytes	CMNH- HTB 1993	F	38.9	25.6	18.2	89.3	52.6	33.6	18.6	42.6
Pan troglodytes	CMNH- HTB 2746	M	34.5	21.3	16.4	84.6	50.2	30.9	16.2	39.6
Pan troglodytes	CMNH- HTB 2747	M	43.1	26.0	17.0	89.1	45.8	29.0	17.4	47.5
Pan troglodytes	CMNH- HTB 2771	F	38.5	22.5	16.5	87.7	53.3	34.5	17.1	40.2
Pan troglodytes	CMNH- HTB 1713	F	37.4	20.1	15.1	84.4	49.6	32.7	16.5	39.6

Symphalangus syndactylus	NMNH-395514	M	35.1	19.3	11.3	66.4	41.4	24.2	11.9	45.7
Symphalangus syndactylus	NMNH-143759	F	34.0	21.8	11.2	66.1	41.5	25.2	11.6	46.4
Theropithecus gelada	NMNH-305107	M	36.6	18.6	8.6	44.6	20.4	10.7	10.0	74.4
Theropithecus gelada	AMNH-201008	M	36.9	14.1	9.3	48.1	17.8	7.6	10.2	72.0
Theropithecus gelada	CMNH-HTB0892	F	30.8	11.6	7.5	40.2	14.8	6.9	8.7	70.7

Appendix 5.2

Primate taxa, number of populations, grooming frequency (as represented by a percentage of daily activity budget), and source publication(s).

Primate taxa	**N**	**Grooming %**	**Source(s)**
Colobus guereza	1	5.6	Fashing, 2001
Colobus guereza	1	6.7	Fashing, 2001
Colobus guereza	1	6.2	Oates, 1997 as cited by Grueter et al., 2013
Chlorocebus aethiops	2	8.6	Isbell and Young, 1993 as cited by Grueter et al., 2013
Chlorocebus aethiops	4	5.0	Isbell and Young, 1993 as cited by Grueter et al., 2013
Chlorocebus aethiops	4	9.17	Baldellou and Adan, 1997; 1998 and Lee, 1982 as cited by Lehmann et al., 2007
Erythrocebus patas	1	1.0	Nakagawa, 1989 as cited by Grueter et al., 2013
Erythrocebus patas	1	9.5	Chism, 2002 as cited by Grueter et al., 2013
Erythrocebus patas	1	3.1	Chism, 2002 as cited by Grueter et al., 2013
Erythrocebus patas	1	13.6	Ashagrie, 2015
Gorilla beringei	1	3.22	Karisoke, long term records, 2008 as cited by Grueter et al., 2013
Gorilla beringei	1	0.02	Karisoke, long term records, 2008 as cited by Grueter et al., 2013
Gorilla beringei	1	3.54	Karisoke, long term records, 2008 as cited by Grueter et al., 2013
Gorilla beringei	1	2.32	Karisoke, long term records, 2008 as cited by Grueter et al., 2013
Gorilla beringei	1	2.29	Karisoke, long term records, 2008 as cited by Grueter et al., 2013
Gorilla beringei	1	2.65	Karisoke, long term records, 2008 as cited by Grueter et al., 2013
Gorilla beringei	1	3.38	Karisoke, long term records, 2008 as cited by Grueter et al., 2013
Hylobates lar	1	6.0	Bartlett, 1999 as cited by Grueter et al., 2013
Hylobates lar	1	7.2	Bartlett, 1999 as cited by Grueter et al., 2013
Hylobates lar	1	3.0	Gittins and Raemaekers, 1980 as cited by Grueter et al., 2013
Hylobates lar	4	1.4	Ellefson, 1974
Macaca fuscata	1	18.9	Agetsuma, 1995 as cited by Grueter et al., 2013

Macaca fuscata	1	27.9	Maruhashi, 1981 as cited by Grueter et al., 2013
Macaca fuscata	1	7.2	Wada and Tokida, 1981 as cited by Grueter et al., 2013
Macaca fuscata	8	8.6	Seth and Seth, 1986
Macaca mulatta	1	6.6	Marriott, 1988 as cited by Grueter et al., 2013
Macaca mulatta	1	15.0	Teas et al., 1980 as cited by Lehmann et al., 2007
Pan troglodytes	2	6.2	Wrangham, 1977 as cited by Grueter et al., 2013
Pan troglodytes	1	9.0	Boesch and Boesch-Achermann, 2000
Pan troglodytes	1	14.1	Huffman, 1990 as cited by Grueter et al., 2013
Papio cynocephalus	3	5.7	Schino et al., 1988 as cited by Dunbar, 1991
Papio hamadryas	1	13.5	Nagel, 1973 as cited by Grueter et al., 2013
Papio ursinus	2	11.9	Schino et al., 1988 as cited by Dunbar, 1991
Papio ursinus	1	15.1	Hill et al., 2003
Papio ursinus	1	8.0	Barrett et al., 1999 as cited by Grueter et al., 2013
Papio ursinus	1	12.0	Barrett et al., 1999 as cited by Grueter et al., 2013
Papio ursinus	1	14.0	Barrett et al., 1999 as cited by Grueter et al., 2013
Papio ursinus	1	17.0	Barrett et al., 1999 as cited by Grueter et al., 2013
Papio ursinus	1	12.1	Gaynor, 1994
Pongo pygmaeus	unknown	0.0	Mackinnon, 1974
Pongo pygmaeus	1	0.01	Wich et al., 2009 as cited by Grueter et al., 2013
Symphalangus syndactylus	1	5.3	Chivers, 1974 as cited by Dunbar, 1991
Symphalangus syndactylus	1	12.0	Chivers, 1974 as cited by Grueter et al., 2013
Symphalangus syndactylus	1	15.0	Chivers, 1974 as cited by Grueter et al., 2013
Symphalangus syndactylus	1	1.0	Gittins and Raemaekers, 1980 as cited by Grueter et al., 2013
Theropithecus gelada	3	18.3	Iwamoto and Dunbar, 1983

Appendix 5.3

R code

```
> library(ape)
> library(phytools)
> library(nlme)
> library(geiger)
> setwd("/Users/sarahedlund/Desktop/")
> ConsensusTree <- "consensusTree_Primates_Full.nex"
> ConsensusTreePhy <- read.nexus(ConsensusTree)
> plot(ConsensusTreePhy)
> PrimateData <- read.csv("Primates_data.csv")
> plot(PrimateData[, c("Opp.index", "Grooming")])
> groom <- PrimateData[, "Grooming"]
> oppind <- PrimateData[, "Opp.index"]
> names(groom) <- names(oppind) <- rownames(PrimateData)
> pglsModel <- gls(Grooming ~ Opp.index, correlation = corBrownian(phy = ConsensusTreePhy), data =
PrimateData, method = "ML")
> summary(pglsModel)
Generalized least squares fit by maximum likelihood
  Model: Grooming ~ Opp.index
```

```
 Data: PrimateData
     AIC      BIC    logLik
 88.5849   90.50208   -41.29245

Correlation Structure: corBrownian
 Formula: ~1
 Parameter estimate(s):
numeric(0)

Coefficients:
               Value Std.Error   t-value p-value
(Intercept) -11.621897  8.021341 -1.448872   0.173
Opp.index     0.407639  0.157881  2.581933   0.024

 Correlation:
         (Intr)
Opp.index -0.885

Standardized residuals:
       Min             Q1            Med             Q3            Max
-0.8951591   -0.5894089    0.1255978    0.2047075    1.0771726

Residual standard error: 6.640089
Degrees of freedom: 14 total; 12 residual
> plot(groom ~oppind)
> abline(a = coef(pglsModel)[1], b = coef(pglsModel)[2])
> pglsModelOU <- gls(Grooming ~ Opp.index, correlation = corMartins(1, phy = ConsensuTreePhy), data =
PrimateData, method = "ML")
> summary(pglsModelOU)
Generalized least squares fit by maximum likelihood
  Model: Grooming ~ Opp.index
  Data: PrimateData
     AIC      BIC    logLik
  81.64851   84.20474   -36.82425

Correlation Structure: corMartins
 Formula: ~1
 Parameter estimate(s):
alpha
   4.712538

Coefficients:
               Value Std.Error   t-value p-value
(Intercept) -8.288623  5.031539 -1.647334  0.1254
Opp.index    0.331991  0.099156  3.348157  0.0058

 Correlation:
         (Intr)
Opp.index -0.981

Standardized residuals:
      Min        Q1       Med        Q3       Max
-1.6543210 -1.0169192  0.4426598  0.7037293  1.7252981
```

```
Residual standard error 3.358066
Degrees of freedom: 14 total; 12 residual
> plot(groom ~ oppind)
> abline(a = coef(pglsModelOU)[1], b = coef(pglsModelOU)[2])
> plot(groom ~oppind)
> shapiro.test(groom)

        Shapiro-Wilk normality test

data:  groom
W = 0.98682, p-value = 0.9973

> shapiro.test(oppind)

        Shapiro-Wilk normality test

data:  oppind
W = 0.93645, p-value = 0.3747

> cor.test(oppind, groom, method=c("pearson"))

        Pearson's product-moment correlation

data:  oppind and groom
t = 3.3482, df = 12, p-value = 0.0058
alternative hypothesis: true correlation is not equal to 0
95 percent confidence interval:
 0.2604173 0.8953877
sample estimates:
     cor
0.6949712
```

Chapter 6
Conclusion

This dissertation examined the manual skeletal morphology of *Theropithecus gelada,* both in isolation and compared to that of baboons, and evaluated grooming as a potential explanatory behavior for primate intrinsic hand proportions. Throughout these studies, it has become clear that an updated interpretation of the seed-eaters model that continues to make use of geladas as an inferential model is still useful for interpreting the human evolutionary path (Jolly, 1970).

The high opposability index and broad similarities to other terrestrial digitigrade primates ae the most well-known aspects of gelada hand morphology. The foraging ecology of geladas was of interest in this study because of its uniqueness among extant primates and the pad-to-pad precision grip employed during manual grazing that is facilitated by their high opposability index. The manipulative abilities of geladas could be explained largely by plucking motions used to collect small food objects like grasses and rhizomes, but other functions had not been previously explored.

A comparison between geladas and baboons is foundational to the seed-eaters model of hominin evolution and especially appropriate for studies of manual functional morphology. In the first analytical chapter, I described the skeletal elements of the gelada hand. Paying special attention to the proximal articular surfaces of metacarpals 1 and 2, I compared the morphology of gelada and baboon hands using 3D geometric morphometric shape analyses in the subsequent chapter. I continued with an investigation of potential links between intrinsic hand proportions and grooming investment in primates.

An important result of this dissertation is a catalogue of detailed descriptions of the manual skeletal elements of extant *Theropithecus gelada*. These were previously absent from published literature, though essential for comparative work with fossil *Theropithecus* and related fossil taxa, especially when recovered material is incomplete (Jablonski et al., 2002; Guthrie, 2011). Additionally, they provide comparative data for further analyses with extant species. My analyses verified the known character of intrinsic hand proportions of geladas, showing a relatively long ray 1 and relatively short ray 2 exemplified by a particularly short intermediate phalanx 2. These results also indicated that, aside from the opposability index, the phalanges of geladas are quite similar to baboons and other terrestrial digitigrade monkeys. Most marked qualitative differences were observed in the metacarpals, which were the focus of chapter 4.

Chapter 4 used 3D geometric morphometrics to examine the morphology of the proximal articular surfaces of metacarpals 1 and 2 in geladas and baboons. Considering the manipulative behaviors of geladas and their habitual use of the pad-to-pad precision grip, the proximal joint surface of the first metacarpal is significant for understanding manipulative capabilities in these primates. The morphology of the second metacarpal was largely absent from previous analyses despite its functional importance for precision gripping. There are differences between geladas and baboons related to foraging ecology, grooming investment, and habitat that make an assessment of the functional differences of the first and second rays in geladas and baboons important. 3D geometric morphometric analyses and principal components analyses (PCA) showed that there are significant shape differences in the proximal articular surfaces of the first

and second metacarpals of geladas and baboons in addition to highlighting many broad similarities between these two groups. The observed differences are primarily related to joint stability. At the first metacarpal-trapezium joint, geladas exhibit morphology reflective of greater stability for resisting axial loads compared to baboons, though both show relatively low stability compared to apes (Marzke et al., 2010; Marchi et al., 2017). High stability in this joint in gorillas has previously been explained as an adaptation for forcefully pulling vegetation (Marzke, 2005). Geladas exhibit less passive stability and greater flexion-extension range relative to baboons at the second metacarpal-trapezoid joint. These subtle differences likely indicate differences in manipulation and locomotion between these two taxa, perhaps due to habitat and/or dietary differences. Geladas subsist extensively on grasses on the highland plateaus of Ethiopia, whereas baboons (as a diverse group of species) are more varied in habitat and diet (Iwamoto, 1993). Additional behavioral differences between geladas and baboons could also explain these differences in hand morphology.

Grooming investment is another area in which variation exists between geladas and baboons. Allogrooming is important for primate societies and is performed at varying rates between taxa (Dunbar, 1991; Lehmann et al., 2007). Chapter 5 provided an assessment of a link between grooming investment and hand morphology, specifically the opposability index. In some primates, effective removal of debris and separation of the fur requires pad-to-pad precision gripping, though several hand postures are used throughout the grooming process. Primate grooming is complex, not only in its execution, but also in its social and utilitarian function within primate groups.

Adding to our understanding of primate grooming, chapter 5 demonstrated a positive correlation between grooming time investment and opposability index for several ape and Old World monkey taxa. Though the exact postures used throughout all grooming bouts were unavailable for this study, these results do indicate that there is an important link between grooming and opposability that deserves additional attention. In particular, future analyses would benefit from the inclusion of platyrrhine taxa and a more detailed examination of the mechanics of grooming in the hand. This future work could give us insight into the selective pressures that resulted in high opposability for some taxa. High opposability could represent an exaptation that was originally under positive selection for other tasks, like food manipulation or extraction.

Understanding geladas and the evolution of their hand morphology can help us decipher important aspects of the hominin fossil record. This dissertation adds to our knowledge of gelada manual skeletal anatomy and provides several avenues of future research which will be valuable for a modern interpretation of the seed-eaters model. Additional detailed quantitative analyses of gelada and baboon manual morphology can elucidate other functional differences between these closely related taxa upon which we can base hypotheses about the evolutionary path of humans. While no inferential model is perfect, geladas continue to offer valuable data for interpreting the hominin fossil record.

Works Cited

Dunbar, R.I.M. (1991). Functional significance of social grooming in primates. *Folia primatologica*, *57*(3), 121-131.

Guthrie, E.H. (2011). *Functional morphology of the postcranium of Theropithecus brumpti (Primates: Cercopithecidae)* (Doctoral dissertation, University of Oregon).

Iwamoto, T. (1993). The ecology of Theropithecus gelada. *Theropithecus: The rise and fall of a primate genus*, 441-452.

Jablonski, N.G., Leakey, M.G., Kiarie, C., & Antón, M. (2002). A new skeleton of Theropithecus brumpti (Primates: cercopithecidae) from Lomekwi, west turkana, Kenya. *Journal of Human Evolution*, *43*(6), 887-923.

Jolly, C.J. (1970). The seed-eaters: a new model of hominid differentiation based on a baboon analogy. In *Primate Evolution and Human Origins* (pp. 323-332). Routledge.

Lehmann, J., Korstjens, A.H., & Dunbar, R.I.M. (2007). Group size, grooming and social cohesion in primates. *Animal Behaviour*, *74*(6), 1617-1629.

Marchi, D., Proctor, D.J., Huston, E., Nicholas, C.L., & Fischer, F. (2017). Morphological correlates of the first metacarpal proximal articular surface with manipulative capabilities in apes, humans and South African early hominins. *Comptes Rendus Palevol*, *16*(5-6), 645-654.

Marzke, M.W. (2005). Who made stone tools. *Stone knapping: the necessary conditions for a uniquely hominin behaviour. Cambridge: McDonald Institute for Archaeological Research*, 243-256.

Marzke, M.W., Tocheri, M.W., Steinberg, B., Femiani, J.D., Reece, S.P., Linscheid, R.L., ... & Marzke, R.F. (2010). Comparative 3D quantitative analyses of trapeziometacarpal joint surface curvatures among living catarrhines and fossil hominins. *American Journal of Physical Anthropology: The Official Publication of the American Association of Physical Anthropologists*, *141*(1), 38-51.